Appendix

List of Publications and Presentations

Patents filed from thesis

1. Mittal A., **Italiya K. S.**, Mazumdar S., Chitkara D. Orally active nanoformulation of lysofylline and composition thereof. (Indian Patent Application filed on 05 **Feb 2019**; Application no. 201911004346; Complete specifications)
2. Mittal A., **Italiya K. S.**, Mazumdar S., Chitkara D. Surfactant-free, Self-assembling micelles of fatty acid conjugated to hydrophilic drug and method for preparing the same. (Indian Patent Application filed on 13 **Dec 2017;** 201711044842; Complete specifications)- Published

Research publications from thesis

1. **Italiya, K. S.,** Basak, M., Mazumdar, S., Sahel, D.K., Shrivastava, R., Chitkara, D. and Mittal, A. Scalable Self-Assembling Micellar System for Enhanced Oral Bioavailability and Efficacy of Lisofylline for Treatment of Type-I Diabetes. *Molecular Pharmaceutics*, 16 (12), 4954-4967 (**2019**)

2. **Italiya, K. S.**, Mazumdar, S., Sharma, S., Mahato, R. I., Chitkara, D., and Mittal, A. Self-assembling lisofylline-fatty acid conjugate for effective treatment of diabetes mellitus. *Nanomedicine: Nanotechnology, Biology and Medicine*, 15 (1), 175-187 (**2019**)

3. **Italiya, K. S**., Sharma, S., Kothari, I., Chitkara, D., and Mittal, A. Simultaneous estimation of lisofylline and pentoxifylline in rat plasma by high performance liquid chromatography-photodiode array detector and its application to pharmacokinetics in rat. *Journal of Chromatography B*, 1061, 49-56 (**2017**)

4. **Italiya, K. S.**, Singh A. K., Chitkara D., and Mittal, A. Nanoparticulate tablet dosage form of lisofylline-linoleic acid conjugate for type 1 diabetes: In-vitro and In-situ Single-Pass Intestinal Perfusion (SPIP) studies in rat. (*Under Review***)**

List of Paper Presentations

1. **Italiya, K. S.**, Mazumdar, S., Sharma, S., Mahato, R. I., Chitkara, D., and Mittal, A. Self-assembling lisofylline-fatty acid conjugate for effective treatment of diabetes mellitus. International conference AAPS 2019 PharmSci360 held at San antonio, Texas, USA, 03-06 November, (**2019)** (Received ***AAPS 2019 Best Abstract Award***)

2. **Italiya, K. S.**, Mazumdar, S., Sharma, S., Mahato, R. I., Chitkara, D. Self-assembling nanoformulation of lisofylline-linoleic acid conjugate for effective treatment of type-I diabetes. 2nd National Biomedical Research Competition (NBRCom-2019), PGIMER Chandigarh, India, 17 November, (**2019)** (Received ***Best Poster Presentation Award in Innovative Idea & Patents category***)

3. **Italiya, K. S.,** Sharma, S., Kothari I., Chitkara, D., Mittal, A. Development and validation of reverse-phase HPLC-PDA method for simultaneous determination of lisofylline and pentoxifylline in rat plasma and its application to pharmacokinetics in rat. The Ramanbhai Foundation 8th International Symposium on Current Trends in Healthcare, Advances in New Drug Discovery & Development, Ahmedabad, India, 02-04 February, (**2017)**

List of other Publications

1. Shukla A., **Italiya, K.S.**, Sahel D.K., Gaikwad A.B., Mittal A., and Chitkara D. Single Step Salting-Out Extraction of Temozolomide from Plasma and its Application in Pharmacokinetic Studies. *Chromatographia*. (**2020)**. (Communicated)

2. Agarwal D.S., Mazumdar S., **Italiya K.S**., Chitkara D., and Sakhuja R. Bile acid Appended Triazolyl Aryl Ketones: Design, Synthesis, in vitro Anticancer activity and Pharmacokinetics in rats. *Bioorganic chemistry*. (**2020**). (Communicated)

3. Kothari, I. R., Mazumdar, S., Sharma, S., **Italiya, K. S.**, Mittal, A. and Chitkara, D. Docetaxel and alpha-lipoic acid co-loaded nanoparticles for cancer therapy. *Therapeutic Delivery*, *10*(4), 227-240 (**2019**)
4. Uppal, S., **Italiya, K. S.**, Chitkara, D. and Mittal, A. Nanoparticulate-based drug delivery systems for small molecule anti-diabetic drugs: An emerging paradigm for effective therapy. *Acta Biomaterialia*, *81*, 20-42 (**2018**)

5. Mazumdar, S., **Italiya, K. S.**, Sharma, S., Chitkara, D. and Mittal, A. Effective cellular internalization, cell cycle arrest and improved pharmacokinetics of Tamoxifen by cholesterol based lipopolymeric nanoparticles. *International Journal of Pharmaceutics*, *543*(1-2), 96-106 (**2018**)

6. Kothari, I. R., **Italiya, K. S.**, Sharma, S., Mittal, A. and Chitkara, D. A rapid and precise liquid chromatographic method for simultaneous determination of alpha lipoic acid and docetaxel in lipid-based Nanoformulations. *Journal of Chromatographic Science*, *56*(10), 888-894 (**2018**)

7. **Italiya, K. S.**, Valicherla, G. R., Gupta, C. P., Mishra, S., Riyazuddin, M., Syed, A. A., Singh, S. K., Shahi, S., Taneja, G., Wahajuddin, M. and Goel, A. Evaluation of oral pharmacokinetics, in vitro metabolism, blood partitioning and plasma protein binding of novel antidiabetic agent, S009-0629 in rats. *Drug Development Research*, *79*(4), 173-183 (**2018**)

8. Sharma, S., Mazumdar, S., **Italiya, K. S.**, Date, T., Mahato, R. I., Mittal, A. and Chitkara, D.. Cholesterol and Morpholine grafted cationic Amphiphilic copolymers for miRNA-34a delivery. *Molecular Pharmaceutics*, *15*(6), 2391-2402 (**2018**)

9. Singh, S. K., Valicherla, G. R., Joshi, P., Shahi, S., Syed, A. A., Gupta, A.P., Hossain, Z., **Italiya, K. S.**, Makadia, V., Singh, S. K. and Wahajuddin, M. Determination of permeability, plasma protein binding, blood partitioning, pharmacokinetics and tissue distribution of Withanolide A in rats: A neuroprotective steroidal lactone. *Drug Development Research*, *79*(7), 339-351 (**2018**)

10. Sharma, S., **Italiya, K. S.**, Mittal, A. and Chitkara, D. New strategies for cancer management: how can temozolomide carrier modifications improve its delivery? *Therapeutic Delivery*, 475-477 (**2017**)

11. Valicherla, G. R., Tripathi, P., Singh, S. K., Syed, A. A., Riyazuddin, M., Husain, A., Javia, D., **Italiya, K. S.**, Mishra, P. R. and Gayen, J. R. Pharmacokinetics and bioavailability assessment of Miltefosine in rats using high performance liquid chromatography tandem mass spectrometry. *Journal of Chromatography B*, *1031*, 123-130 (**2016**)

Patents filed other than thesis:

1. Chitkara D., Sahel D. K., **Italiya K. S.,** Sharma S., Shah S., Mittal, A. A drug conjugate and preparation of thereof. (Indian Patent Application filed on 07 May **2019**; Application no. 201911018304; Status: Application under review)

Biography of Dr. Anupama Mittal

Dr. Anupama Mittal is currently working as an Assistant professor in Department of Pharmacy, BITS, Pilani, Pilani campus. She received her Ph.D. degree in Pharmaceutical Sciences in 2012 from NIPER, SAS Nagar, India. She pursued her post doctorate research (2012-2014) at University of Tennessee Health Science Center (UTHSC), Tennessee, USA and University of Nebraska Medical Center (UNMC), Nebraska, USA. She has been the recipient of prestigious Young scientist award (SERB-DST) and Ranbaxy Science Scholar award (Ranbaxy Science Foundation) in Pharmaceutical Sciences. She has been involved with teaching and research for nearly last 6 years. Her areas of interest includes, nanoparticles & polymeric micelles for site-specific drug delivery, polymer/fatty acid drug conjugates for effective treatment of cancer & diabetes, stem cells and exosomes as biogenic carriers of miRNA & proteins in cancer, and growth factor and peptide based therapeutics for wound healing. She has published 28 research and review articles in peer reviewed international journals, edited 01 book (CRC press), authored 02 book chapters and filed 04 Indian/PCT patent applications. She has also received several awards for best papers presented at National/International conferences. Her lab is generously funded by several extramural research grants from SERB-DST, DST-Rajasthan, DST-Nanomission, ICMR and DBT. She has guided several M. Pharm and B. Pharm students and is currently supervising 05 Ph.D students.

Biography of Mr. Italiya Kishan Shamjibhai

Mr. Italiya Kishan S has completed his Bachelor of Pharmacy from L.M. College of Pharmacy, Gujarat Technological University, in the year of 2013 and M.S. (Pharm.) in Pharmaceutics from NIPER, Raebareli (currently in Lucknow) in 2015 with Gold medal. He worked in CSIR-CDRI, Lucknow for one year as a part of his M.S. (Pharm.) thesis. He also completed his Post Graduate Diploma in Patent Law (PGDPL) from NALSAR University, Hyderabad. He joined as Ph.D. Scholar (DST INSPIRE Fellow) in Department of Pharmacy, BITS Pilani, Pilani campus in January, 2016. His areas of interests include pharmaceutical formulations, PK-PD and pharmaceutical analysis for various therapeutic agents and designing of novel polymers as well as lipid drug conjugates. He has received various best paper awards (as author and co-author). He has published 16 research/review articles in renowned journals, filed 03 Indian patents and presented papers in National/International conferences.

Journal of Chromatography B 1061–1062 (2017) 49–56

Contents lists available at ScienceDirect

Journal of Chromatography B

journal homepage: www.elsevier.com/locate/jchromb

Simultaneous estimation of lisofylline and pentoxifylline in rat plasma by high performance liquid chromatography-photodiode array detector and its application to pharmacokinetics in rat

Kishan S. Italiya, Saurabh Sharma, Ishit Kothari, Deepak Chitkara, Anupama Mittal*

Industrial Research Laboratory (IRL), Department of Pharmacy, Birla Institute of Technology and Science (BITS-PILANI), Pilani, Rajasthan, 333031, India

ARTICLE INFO

Keywords:
Lisofylline
Pentoxifylline
Method validation
HPLC
Plasma
Pharmacokinetics

ABSTRACT

Lisofylline (LSF) is an anti-inflammatory and immunomodulatory agent with proven activity in serious infections associated with cancer chemotherapy, hyperoxia-induced acute lung injury, autoimmune disorders including type-1 diabetes (T1DM) and islet rejection after islet transplantation. It is also an active metabolite of another anti-inflammatory agent, Pentoxifylline (PTX). LSF bears immense therapeutic potential in multiple pharmacological activities and hence appropriate and accurate quantification of LSF is very important. Although a number of analytical methods for quantification of LSF and PTX have been reported for pharmacokinetics and metabolic studies, each of these have certain limitations in terms of large sample volume required, complex extraction procedure and/or use of highly sophisticated instruments like LC–MS/MS.

The aim of current study is to develop a simple reversed-phase HPLC method in rat plasma for simultaneous determination of LSF and PTX with the major objective of ensuring minimum sample volume, ease of extraction, economy of analysis, selectivity and avoiding use of instruments like LC–MS/MS to ensure a widespread application of the method.

A simple liquid-liquid extraction method using methylene chloride as extracting solvent was used for extracting LSF and PTX from rat plasma (200 µL). Samples were then evaporated, reconstituted with mobile phase and injected into HPLC coupled with photo-diode detector (PDA). LSF, PTX and 3-isobutyl 1-methyl xanthine (IBMX, internal standard) were separated on Inertsil® ODS (C18) column (250 × 4.6 mm, 5 µm) with mobile phase consisting of A-methanol B-water (50:50 v/v) run in isocratic mode at flow rate of 1 mL/min for 15 min and detection at 273 nm. The method showed linearity in the concentration range of 50–5000 ng/mL with LOD of 10 ng/mL and LLOQ of 50 ng/mL for both LSF and PTX. Weighted linear regression analysis was also performed on the calibration data. The mean absolute recoveries were found to be 80.47 ± 3.44 and 80.89 ± 3.73% for LSF and PTX respectively. The method was successfully applied for studying the pharmacokinetics of LSF and PTX after IV bolus administration at dose of 25 mg/kg in Wistar rat. In conclusion, a simple, sensitive, accurate and precise reversed-phase HPLC-UV method was established for simultaneous determination of LSF and PTX in rat plasma.

1. Introduction

Lisofylline (LSF, 1-(5-Hydroxyhexyl)-3,7-dimethylxanthine) is a modified methyl xanthine derivative (Fig. 1), having anti-inflammatory and immunomodulatory properties [1,2]. It was originally developed and tested to reduce cellular damage due to autoimmunity, hypoxia and ischemic reperfusion [3,4]. LSF has been used to overcome morbidity and mortality during serious infections associated with cancer chemotherapy and for treatment of acute lung injury after severe trauma [5,6]. LSF is also reported for its therapeutic potential in early treatment of diabetes, wherein it enhanced glucose-stimulated insulin secretion [7,8], caused reversal of insulin insensitivity by modulating oxidized free fatty acids (FFA) and glucose-induced phosphorylation of the insulin receptor [9]. The protective role of LSF in diabetes is mainly attributed to the promotion of mitochondrial metabolism in β-cells, normalizing the membrane potential of mitochondria and thus stimulating energy production [10,11]. This broad spectrum of activity suggests that LSF bears significant clinical utility in preventing both Type-1 diabetes mellitus (T1DM) and Type-2 diabetes mellitus (T2DM) [1,12]. Its therapeutic potential is further reflected by a clinical trial

* Corresponding author at: Department of Pharmacy, Birla Institute of Technology and Science (BITS), Pilani Campus, Pilani, Rajasthan, 333 031, India.
E-mail address: anupama.mittal@pilani.bits-pilani.ac.in (A. Mittal).

http://dx.doi.org/10.1016/j.jchromb.2017.06.043
Received 28 March 2017; Received in revised form 21 June 2017; Accepted 24 June 2017
Available online 29 June 2017
1570-0232/

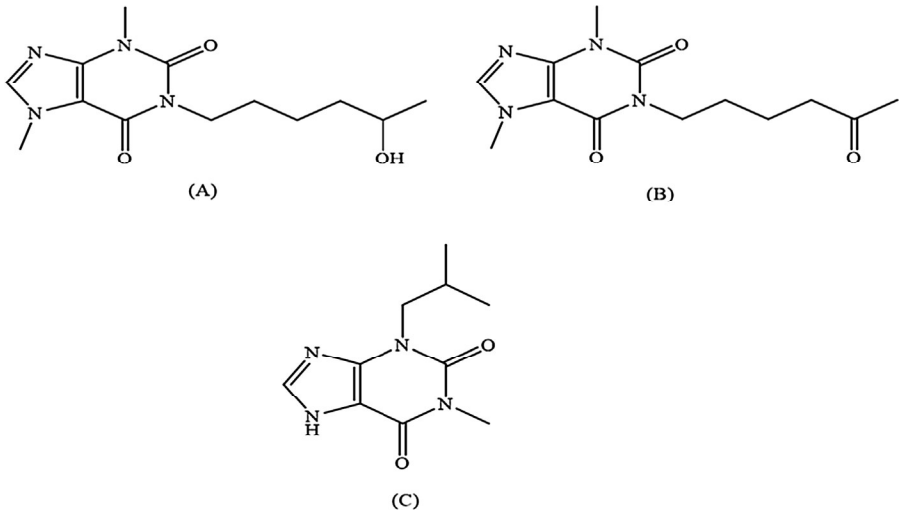

Fig. 1. Chemical structures of (A) Lisofylline, 1-(5-Hydroxyhexyl)-3,7-dimethylxanthine, (B) Pentoxifylline, 3,7-Dimethyl-1-(5-oxohexyl) xanthine and, (C) 3-Isobutyl 1-Methyl Xanthine, IBMX.

wherein, LSF is administered by continuous subcutaneous or intravenous route in subjects with T1DM to evaluate its safety, tolerability and bioavailability [13]. Apart from being administered as a drug itself, LSF is also reported to be an active metabolite of another drug, Pentoxifylline (PTX; 3,7-Dimethyl-1-(5-oxohexyl) xanthine, Fig. 1) which is clinically used as a haemorrheologic agent for the treatment of cerebrovascular and peripheral vascular disease [14]. It has also been reported that LSF and PTX undergo interconversion *in vivo* [15]. PTX has also demonstrated immunomodulatory effects in animal model of sepsis [16]. Considering the immense therapeutic potential and multiple pharmacological activities of LSF and PTX as stated above, appropriate and accurate quantification of LSF is of paramount significance.

Few methods have been reported in literature, which are based on either a complex sample preparation procedure or use of sophisticated instruments like LC–MS/MS that hinders its use in routine analysis for various applications. Chivers, et al. developed a HPLC-UV method for simultaneous quantification of LSF and PTX in plasma at a high flow rate (2 mL/min) using a sample volume of 1000 μL that required 10 mL of extracting solvent (methylene chloride) [17]. Grasela, et al. reported a HPLC-UV method requiring a multistep liquid–liquid extraction (LLE) process and high injection volume (250 μL) that may not be applicable for routine analysis [18]. A LC–MS/MS method has been reported to LSF and PTX up to 1 ng/mL however it requires a highly specific sample preparation method (lithium precipitation using Seraprep reagent) [19]. Although, use of LC–MS/MS method is a recommended procedure and significantly enhances the sensitivity of the method; it is not available in every research laboratory, requires highly trained personnel and is associated with a high running and maintenance cost. Moreover, LSF has been reported to be administered at a high dose ranging from 25 to 50 mg/kg in animals [1,20] and 1–3 mg/kg in humans [14]. Thus, the need of detecting a concentration below 50 ng/mL may not arise at all and hence HPLC based methods might also be equally useful.

The present work describes method development and its detailed validation for quantification of LSF and PTX in rat plasma within the range of 50–5000 ng/mL. The proposed method uses a simple liquid–liquid extraction (LLE) method using methylene chloride (2 mL) as an extracting solvent, and small sample volume (200 μL). 3-isobutyl 1-methyl xanthine (IBMX) was selected as internal standard (I.S) (Fig. 1). Full validation was carried out including selectivity, lower limit of quantification (LLOQ), limit of detection (LOD), precision, accuracy, carry over effect, dilution integrity and stability, using internationally accepted guidelines for bioanalytical method validation [21,22]. Stability studies were also performed to determine the stability of stock solutions and of plasma samples that were exposed to different storage conditions including repeated freeze-thaw cycles, autosampler, long term, and bench top storage. The developed method was applied to the pharmacokinetics (PK) studies of LSF and PTX (25 mg/kg, i.v.) in wistar rat.

2. Material and methods

2.1. Chemicals, reagents and experimental animals

(±) LSF (purity ≥99%, HPLC) was purchased from Cayman Chemicals Inc. (Michigan, USA). PTX and IBMX (purity ≥99%, HPLC) were obtained from Sigma Aldrich (St. Louis, MO, USA). HPLC grade solvents, acetonitrile (ACN), methanol and methylene chloride were obtained from Merck Limited (Mumbai, India). Purified water was used in our studies which refers to the Mili-Q Reference ultrapure water (Type 1, as described by ASTM®, ISO® 3696 and CLSI® norms) prepared using Milli-Q® Reference water purification system. Wistar rats (male; 8–10 weeks, 200–220 g) were procured from Central Animal Facility, BITS-PILANI (Pilani, India). Animal experiment protocol was approved by Institutional Animal Ethics Committee (IAEC), BITS-PILANI, Pilani and experiments were conducted as per CPCSEA guidelines. Rats were housed in well ventilated cages at standard laboratory conditions with regular light/dark cycles for 12 h and fed with standard normal diet *ab libitum*. All other chemicals and reagents were of analytical grade and used as obtained.

2.2. Liquid chromatographic conditions

A Shimadzu HPLC system (Kyoto, Japan) equipped with a binary pump (LC-20AD), Photo Diode Array (PDA) detector (SPD-M20A) and auto sampler (SIL-HTC, Shimadzu, Japan) were used to develop the analytical method. The HPLC system was equilibrated for approximately 40 min before beginning the sample analysis. LSF, PTX and IBMX were separated on Inertsil® ODS (C18) column (250 × 4.6 mm, 5 μm) with a mobile phase consisting of A-methanol B-water (50:50 v/v) run in isocratic mode at a flow rate of 1 mL/min and injection volume of 80 μL. Eluents were monitored at a wavelength of 273 nm. Control of hardware and data handling was performed using LCsolution software version 1.22 SP1.

2.3. Preparation of stock solutions, calibration curve standards (CS) and quality control (QC) samples

Stock solutions of LSF (1 mg/mL) and PTX (1 mg/mL) were prepared by dissolving the accurately weighed amount of each of these analytes in Milli-Q water. The stock solution (1 mg/mL) of IBMX was

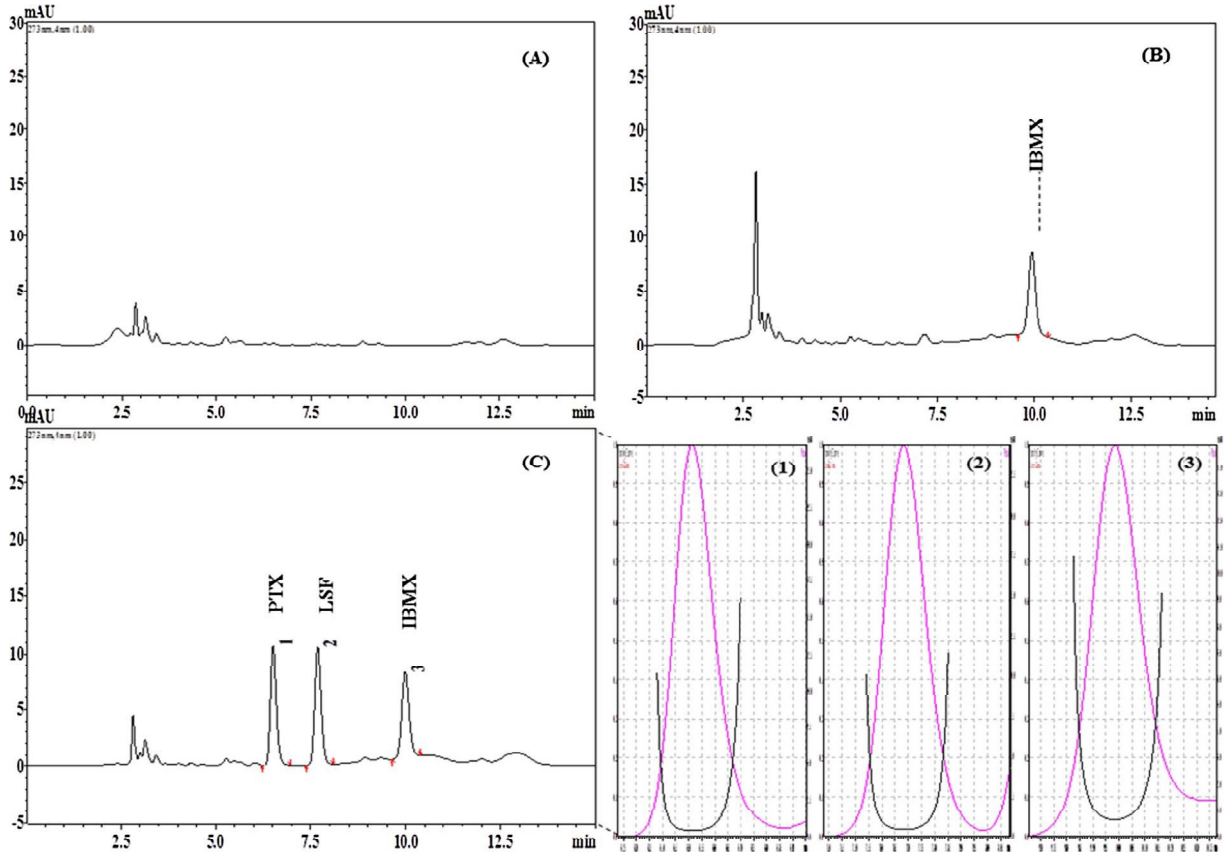

Fig. 2. Representative HPLC-PDA chromatograms obtained after extraction and analysis of (A) Blank rat plasma, (B) Zero (blank rat plasma spiked with internal standard, IS), (C) Plasma containing LSF, PTX (both 500 ng/mL) and I.S (400 ng/mL) and, (D) Peak purity curves of the analytes and I.S. (Peak purity indices have also been indicated which show peak purity for all peaks ≥0.9999).

Table 1
Precision and accuracy of back calculated concentrations of calibration standard samples of LSF and PTX in rat plasma (n = 5).

Analyte	Nominal concentration (ng/mL)	Measured concentration (Mean ± SD, ng/mL)	Precision (% CV)	Accuracy (% bias)
LSF	5000	5055.08 ± 90.93	1.80	1.10
	2500	2501.52 ± 84.89	3.39	0.06
	1000	1001.92 ± 16.82	1.68	0.19
	500	517.42 ± 07.61	1.47	3.48
	250	261.86 ± 11.37	4.34	4.74
	100	97.15 ± 07.48	7.70	−2.85
	50	49.51 ± 05.07	10.25	−0.97
PTX	5000	5013.78 ± 127.95	2.55	0.28
	2500	2506.43 ± 61.93	2.47	0.26
	1000	982.22 ± 40.55	4.13	−1.78
	500	520.14 ± 22.51	4.33	4.03
	250	253.78 ± 13.46	5.31	1.51
	100	97.26 ± 5.70	5.86	−2.74
	50	48.95 ± 3.73	7.61	−2.10

SD, standard deviation; CV, coefficient of variation.

prepared by dissolving it in ACN and to make its working solution, it was diluted (with ACN) to 2 μg/mL. Further, same volumes of LSF and PTX stock solutions (1 mg/mL) were combined and diluted with water to obtain 200 μg/mL working solution. From 200 μg/mL working solution, further dilutions of 1, 2, 5, 10, 20, 50 and 100 μg/mL were prepared by stepwise dilution using mobile phase. The concentrations of working QC standard solutions were prepared as 1.6, 6 and 60 μg/mL. CS and QC samples were prepared by spiking 190 μL of drug free rat plasma with 10 μL of corresponding working standard solutions. The final CS were prepared as 50, 100, 250, 500, 1000, 2500 and 5000 ng/mL in plasma matrix. The QC samples were prepared using a working standard solution at three concentration levels, low QC (LQC, 80 ng/mL), medium QC (MQC, 300 ng/mL) and high QC (HQC, 3000 ng/mL). All the stock and working solutions were stored in the refrigerator at −20 °C until used for analysis (The stock solutions were tested for stability under these conditions and found to be stable, as detailed in Section 3.3).

2.4. Sample preparation

A simple Liquid-liquid extraction (LLE) method was used for extracting both LSF and PTX from the rat plasma. A 200 μL aliquot of plasma sample containing LSF and PTX was transferred in 5 mL glass tube, followed by the addition of 50 μL of I.S (IBMX, 2 μg/mL) solution.

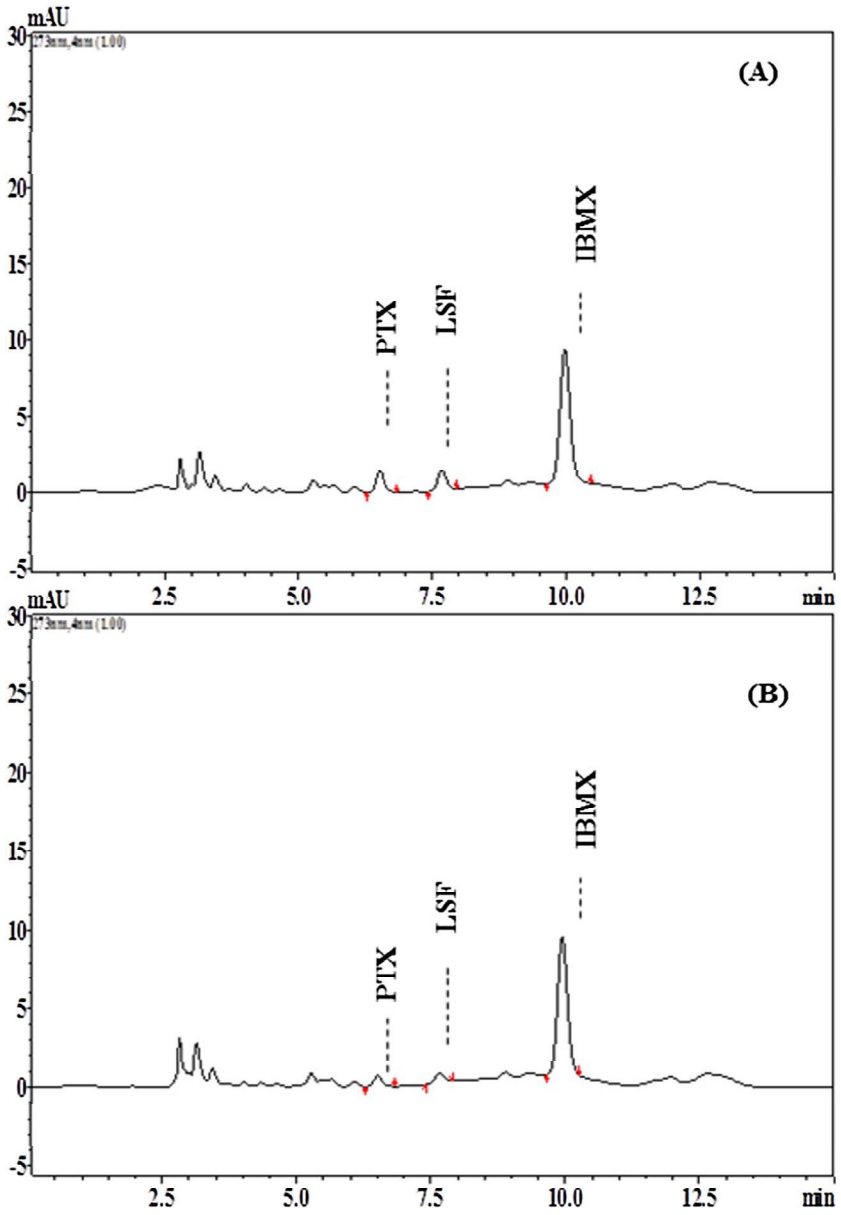

Fig. 3. Representative HPLC-PDA chromatograms at (A) LLOQ (50 ng/mL) and, (B) LOD (10 ng/mL).

Samples were vortexed for 1 min and then 2 mL of methylene chloride added as extracting solvent. The samples were vortexed for 5 min and centrifuged at 3500 rpm for 15 min at 4 °C. The lower organic layer was collected and evaporated to dryness at 40 ± 0.5 °C under a stream of nitrogen gas. The residue was reconstituted with 100 μL of mobile phase and vortexed for 30 s. Finally, 80 μL of sample was injected into HPLC for quantification.

2.5. Method validation procedures

The proposed method was validated as per internationally accepted recommendations for bioanalytical method validation [21,22].

2.5.1. Selectivity

The selectivity of the method was carried out to evaluate potential chromatographic interference from the rat plasma matrix. For this purpose, plasma samples were collected from six different randomly selected Wistar rats and analyzed as per the described chromatographic conditions.

2.5.2. Linearity and calibration curve

The calibration curves of two analytes (LSF and PTX) were prepared using seven calibration standards in a range of 50–5000 ng/mL. Five calibration curves were prepared by plotting peak area ratios (Drug/IS) on Y axis *versus* nominal plasma concentrations on X-axis. Weighted linear regression analysis was performed on calibration data. All the different weighting factors were applied to the data obtained from least-squares regression analysis and the best weighting factors were chosen according the percentage relative error (% Σ RE) [23,24].

2.5.3. Limit of detection (LOD) and lower limit of quantitation (LLOQ)

LOD and LLOQ were determined by **SIGNAL TO NOISE (S/N)** ratio method, USP using following formula,

$$S/N = 2H/h$$

where, H is the height of the peak measured from the peak apex to a baseline extrapolated over a distance ≥5 times the peak width at its half-height; and h is the difference between the largest and smallest noise values observed over a distance ≥5 times the width at the half-height of the peak. By using the S/N method, the noise around the analyte retention time was manually measured, and subsequently, the

concentration of the analyte that yielded a signal equal to certain value of noise to signal ratio is estimated.

The LOD and LLOQ obtained by S/N method were further confirmed by visual evaluation method wherein, for confirming LOD, both analytes were spiked at concentrations lower than LLOQ and LOD was selected as the minimum level at which the analytes could be reliably detected. Further, for confirming LLOQ, analyte samples (n = 6) at the concentration obtained from S/N ratio method and higher were run in HPLC and LLOQ was determined as the concentration of the analyte which showed acceptable accuracy and precision (± 20%).

2.5.4. Precision and accuracy

The intra-day and inter-day assay precision and accuracy were determined by analyzing five replicates at three different QC levels (LQC, MQC, HQC) and LLOQ. For intra-day assay precision and accuracy samples were analyzed on same day, while inter-day assay precision and accuracy were determined by analyzing samples on three consecutive days. The acceptance criteria for accuracy are within ± 15% (expressed as percentage of deviation from nominal concentration, % bias) and for precision within ± 15% (expressed as percentage deviation, % CV) except for LLOQ, where it should not exceed ± 20% for both accuracy and precision [21].

2.5.5. Recovery

The percentage recoveries of LSF and PTX through LLE were determined by comparing the detector response obtained from amount of analytes (at QC sample concentrations) added and extracted from plasma with detector response obtained from actual concentration of analytes in mobile phase. The percentage recovery of I.S was also calculated at a single concentration in of 400 ng/mL (n = 6).

2.5.6. Carry over effect and dilution integrity

Carry over effect was determined by injecting upper limit of quantification calibration standard sample (ULOQ, 5000 ng/mL) followed by blank sample. Dilution integrity was performed to assess the ability of the method to accurately quantify concentrations above 5000 ng/mL (which might be observed in routine analysis). Dilution integrity was determined by diluting 10 times the plasma (n = 6) containing 25,000 ng/mL of LSF and PTX with blank (drug free) rat plasma to obtain 2500 ng/mL concentration (within calibration range); accuracy values was calculated.

2.6. Stability studies

Stability of analytes in both aqueous solution and in plasma matrix was evaluated before (reference samples) and after subjecting to different conditions that could be encountered during regular analysis. Stock solution stability was assessed for 3 months at −20 ± 0.5 °C.

Stability of analytes in plasma was evaluated in terms of freeze–thaw stability, bench top stability, long-term stability and autosampler stability. All stability studies were conducted in three replicates at each concentration of three different QC levels (LQC, MQC and HQC). Freeze thaw stability was performed after freezing (−80 ± 10 °C for 48 h) and thawing QC samples for three consecutive cycles within 2 days. Bench top stability was analyzed at room temperature (RT) for 24 h and long term stability was evaluated after storing the samples at −80 ± 10 °C for 45 days. Replicate injections of extracted plasma samples were analyzed after 48 h to estimate auto sampler stability at 4 ± 0.5 °C.

All QC samples were extracted and quantified against fresh calibration curves and fresh QC samples. The acceptance criteria of accuracy and precision for all stability samples should be within ± 15%.

2.7. Pharmacokinetic study of LSF and PTX in wistar rats

The intravenous (i.v.) pharmacokinetics study of LSF and PTX alone were performed on wistar rats (200–220 g). LSF and PTX were separately dissolved in 0.9% w/v saline (25 mg/mL) and administered intravenously at the dose of 25 mg/kg with maximum dosing volume of 250 μL to each rat without fasting (n = 4). After i.v dosing, blood samples were collected in micro centrifuge tubes for each preset time point at 5, 15, 30, 45, 60, 120, 180, 240, 360, 480 min.

For blood sampling, rats were mildly anaesthetized and blood samples were collected from retro-orbital plexus into heparinized micro centrifuge tubes at pre-determined time interval. Blood samples were centrifuged at 5000 rpm for 10 min to obtain plasma which was subsequently stored at −80 ± 10 °C until analyzed as per developed method. LSF and PTX plasma concentration-time profiles were plotted separately. Plasma concentration-time profiles were analyzed by non-compartmental model approach using Phoenix 2.1 WinNonlin (Pharsight corporation, USA) to determine $t_{1/2}$, elimination half-life; C_0, drug concentration in plasma at t = 0; AUC_{0-t}, area under curve from zero to the last time point; $AUC_{0-\infty}$, area under curve from zero to infinity; MRT, mean residence time; CL, clearance and V_z, apparent volume of distribution.

3. Results and discussion

3.1. Method development

3.1.1. Optimization of liquid chromatographic conditions

A systematic approach was followed for the method development so as to obtain a method using suitable chromatographic conditions, along with easy and quick sample preparation technique while still ensuring an appropriate recovery, symmetry of peaks and high resolution of analytes and I.S. Considering this objective, initially liquid chromatographic conditions such as choice of mobile phase and its composition, column selection, flow rate and injection volume were optimized accordingly. Final optimization was carried out by making deliberate variation in chromatographic conditions such as flow rate, mobile

Table 2
Precision (% CV) and accuracy (% bias) of the analytes in rat plasma samples at quality control concentrations of the calibration ranges (n = 5).

Analyte	Level	Nominal Conc. (ng/mL)	Inter-day			Intra-day		
			Measured Conc. (Mean ± SD, ng/mL)	Precision (% CV)	Accuracy (% bias)	Measured Conc. (Mean ± SD, ng/mL)	Precision (% CV)	Accuracy (% bias)
LSF	LLOQ	50	49.24 ± 0.60	0.75	−1.52	49.75 ± 0.54	0.67	−0.49
	LQC	80	79.90 ± 6.57	5.92	−0.13	76.46 ± 2.38	2.21	−4.43
	MQC	300	309.74 ± 18.40	5.40	3.25	308.11 ± 14.20	4.19	2.70
	HQC	3000	3052.39 ± 68.50	2.22	1.75	3136.48 ± 119.57	3.78	4.55
PTX	LLOQ	50	48.23 ± 2.43	3.76	−3.55	49.20 ± 4.76	7.25	−1.60
	LQC	80	75.65 ± 1.16	1.26	−5.44	79.10 ± 17.97	6.34	−1.12
	MQC	300	312.67 ± 11.36	3.45	4.22	315.03 ± 17.99	5.43	5.01
	HQC	3000	3014.89 ± 31.37	1.03	0.50	3109.63 ± 158.84	5.08	3.65

Table 3
Absolute recoveries (%) of analytes in rat plasma samples from quality control concentrations of the calibration ranges.

Analyte	Level	Nominal concentration (ng/mL)	n	Recovery (%)	
				Mean ± SD	% CV
LSF	LLOQ	50	5	82.50 ± 5.62	6.82
	LQC	80	5	79.52 ± 4.05	5.10
	MQC	300	5	80.60 ± 2.51	3.12
	HQC	3000	5	80.18 ± 2.37	2.96
		Mean	20	80.47 ± 3.44	4.28
PTX	LLOQ	50	5	81.07 ± 5.08	6.27
	LQC	80	5	79.37 ± 3.63	4.57
	MQC	300	5	81.85 ± 1.49	1.83
	HQC	3000	5	81.27 ± 2.62	3.23
		Mean	20	80.89 ± 3.73	4.61

n, number of samples; SD, standard deviation; CV, coefficient of variation.
Recovery for I.S was 78.87 ± 1.84% (n = 6).

phase composition and column temperature and different system suitability parameters including retention time (t_R), peak tailing (10%), resolution (R_s), height equivalent to theoretical plate (HETP), theoretical plate number (N) were assessed (Supplementary data; Table S1). After final optimization, Inertsil® ODS column (250 × 4.6 mm, 5 μm), mobile phase including A-methanol B-water (50:50 v/v) in isocratic mode and 1 mL/min flow rate was found to be the most suitable for the quantification of LSF and PTX since it offered best peak shape and peak intensities along with selectivity and speed of analysis. Using the optimized chromatographic conditions LSF, PTX and IBMX showed retention time of 6.50, 7.67 and 9.97 min respectively with an overall run time of 15 min. A representative chromatogram for sample containing LSF, PTX and IBMX is depicted in Fig. 2.

3.1.2. Optimization of sample preparation method

The plasma sample clean-up procedure plays a vital role in the method as it directly affects sensitivity and selectivity of the method. Higher recoveries of analytes from plasma matrix can be obtained by minimizing sample preparation steps as well as appropriate selection of extraction solvent. The sample preparation technique was optimized in terms of extraction solvent type, sample volume and time required (Supplementary data; Table S2). We have tested different solvents including methylene chloride, chloroform, methanol, ACN, chloroform-methylene chloride (1:1 v/v), methylene chloride –methanol (1:0.1 v/v), methylene chloride with 0.1 M hydrochloric acid; among these different solvents, methylene chloride was selected as the extraction solvent of choice because it provides good recoveries of analytes, has a low boiling point (~40 °C) and could be easily evaporated after extraction using evaporator or simply by air drying. Although evaporation and reconstitution steps are included, sample preparation remains simple and allows high throughput analysis, while requiring only small volume of plasma for analysis (200 μL). The extraction procedure used only 2 mL of methylene chloride which is found to be sufficient to obtain recoveries (≥80%) of LSF and PTX from plasma. Finally, a simple method of extraction was optimized in which both analytes and I.S showed good resolution factor (R_s, 3.55 ± 0.07 for LSF and PTX peak), appropriate retention times (6.5, 7.67 and 9.97 min for PTX, LSF and IBMX respectively) and no interference of plasma matrix (peak purity in all cases, < 0.9999).

Table 4
Stability studies.

(a) Stock solution stability (−20 °C) for LSF and PTX.

Analyte	Peak area (Mean ± SD)[b]		% CV		% diff[a]
	Old Stock (3 months)	Fresh Stock (0 h)	Old stock	Fresh stock	
LSF	1,993,402 ± 14,174	2,003,204 ± 6775	0.71	0.34	0.49
PTX	1,925,070 ± 14,778	1,934,924 ± 8728	0.78	0.45	0.51

(b) Stability of analytes in rat plasma at three QC levels.

Stability	Nominal concentration (ng/mL)	Measured concentration (Mean ± SD, ng/mL)		Precision (% CV)		Accuracy (% bias)	
		LSF	PTX	LSF	PTX	LSF	PTX
0 h (for all)	3000	3070.13 ± 64.20	2999.66 ± 45.15	1.59	1.50	0.37	−0.01
	300	303.58 ± 5.32	308.64 ± 9.77	1.75	3.17	1.19	2.88
	80	78.08 ± 1.18	78.64 ± 2.11	2.41	2.69	−2.45	−1.69
Autosampler (48 h)	3000	2969.36 ± 19.67	2931.44 ± 39.18	0.66	1.34	−1.02	−2.28
	300	281.20 ± 6.67	277.24 ± 3.37	2.37	1.22	−6.27	−7.59
	80	78.98 ± 1.29	82.40 ± 1.38	1.63	1.68	−1.27	3.00
Bench-top (24 h, RT)	3000	2988.95 ± 99.20	2923.97 ± 93.13	3.31	3.19	−0.03	−2.53
	300	294.81 ± 7.89	283.60 ± 9.59	2.68	3.38	−1.73	−5.47
	80	75.88 ± 1.89	77.72 ± 3.83	2.49	4.93	−5.15	−2.85
Freez-thaw (–80 °C, 3 cycle)	3000	2955.69 ± 35.58	2889.35 ± 27.81	1.20	0.96	−1.48	−3.69
	300	301.34 ± 1.97	287.41 ± 1.88	0.65	0.66	0.45	−4.20
	80	78.85 ± 3.47	75.77 ± 2.71	4.41	3.58	−1.44	−5.28
Short term (4 °C,48 h)	3000	2970.80 ± 46.17	2910.85 ± 39.30	1.54	1.35	−0.97	−2.97
	300	292.04 ± 3.62	282.60 ± 2.69	1.12	0.95	−2.65	−5.80
	80	75.33 ± 2.77	78.18 ± 1.55	2.60	1.98	−5.84	−2.28
Long term (–80 °C, 45 days)	3000	2932.87 ± 67.28	2858.13 ± 45.48	2.29	1.59	−2.24	−4.73
	300	282.58 ± 14.00	275.67 ± 3.99	4.96	1.45	−5.81	−8.11
	80	73.14 ± 1.86	75.83 ± 2.44	2.54	3.22	−8.57	−5.22

[a] % difference determined by following equation: (mean test − mean control)/[(mean test + mean control)/2] × 100.
[b] Peak area obtained for dilution of stock solutions up to 50 μg/mL.

3.2. Method validation

3.2.1. Selectivity

The analysis of blank plasma samples from six different healthy rats using the developed method confirmed the absence of matrix interference at the retention time of the analytes and I.S.

Fig. 2 showed representative HPLC-PDA chromatograms obtained after extraction and analysis of blank rat plasma, blank rat plasma spiked with I.S (Zero), plasma containing LSF, PTX (both 500 ng/mL) and peak purity curves of the analytes and I.S.

3.2.2. Linearity, calibration curve, LOD, LLOQ

All the five calibration curves exhibited linearity and reproducibility in the range of 50–5000 ng/mL ($r^2 > 0.9999$). Weighted linear regression analysis was also used to calculate r^2, slopes and intercepts (1/var, 1/x, $1/x^2$, $1/\sqrt{x}$, 1/y, $1/y^2$, $1/\sqrt{y}$) that showed best weighting factors as $1/y^2$ and 1/var for LSF and PTX respectively which have minimum percentage relative error (% Σ RE) although the difference observed was not significant from the un-weighted method (Supplementary data; Table S3). The observed mean back calculated concentrations for calibration standards with accuracy (% bias) and precision (% CV) are presented in Table 1. At LLOQ accuracy (% bias) was found to be −0.97 for LSF and −2.1% for PTX with precision of ≤10.25% for both the analytes. For S/N method, S/N ratio was found to be 4.16 and 14.28 respectively (acceptable limits ≥3 for LOD and ≥10 for LLOQ). LOD and LLOQ by S/N method and visual evaluation method were determined which were found to be 10 ng/mL and 50 ng/mL respectively for both analytes as shown in Fig. 3.

3.2.3. Precision and accuracy

As shown in Table 2, inter and intra-day precision at all QC level (LQC, MQC and HQC) and LLOQ were ≤4.19 for LSF and ≤7.25 for PTX. The % accuracy for both LSF and PTX was found in range of −4.43 to 5.01%. Thus the obtained values for accuracy and precision for both the analytes were found to be within the recommended range (± 15% except LLOQ ± 20%).

3.2.4. Recovery, carry over, dilution integrity

The mean absolute recovery values for LSF and PTX were found to be > 80% as shown in Table 3. The mean absolute recovery for I.S was found to be 78.87 ± 1.84% (n = 6). No carry over effect was observed as there was absence of any peaks of analytes and I.S in blank sample injected after ULOQ. Integrity of method upon dilution was also established by 10 times dilution of LSF and PTX containing plasma (25,000 ng/mL) demonstrated accuracy values as 99.90 ± 4.58 and 100.35 ± 1.74% respectively.

3.3. Stability studies

The stability studies of LSF and PTX in rat plasma as per procedure described in Section 2.6. Stability studies indicated that both the analytes were stable in aqueous solutions and in rat plasma under different storage conditions that may be encountered during routine study sample analysis (Table 4).

3.4. Pharmacokinetic study of LSF and PTX in rats

The suitability of the method was demonstrated in pharmacokinetic studies wherein, LSF and PTX were administered at a single dose of

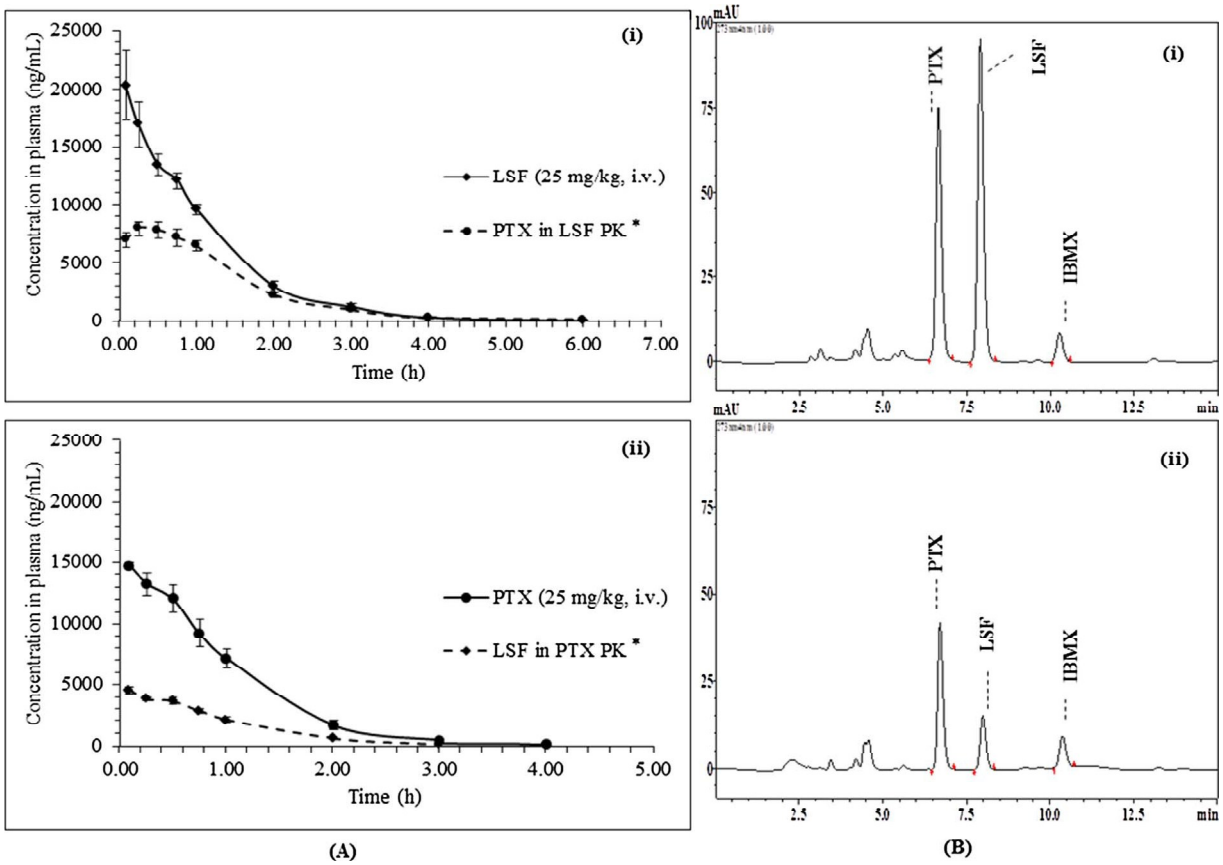

Fig. 4. Application of the developed method to pharmacokinetic study of LSF and PTX. (A) Plasma concentration-time profiles of (i) LSF and (ii) PTX (Mean ± SEM, n = 4) and, (B) Representative chromatograms of plasma samples obtained 2 h post drug administration for (i) LSF and (ii) PTX.
*In these studies, LSF and PTX were administered by i.v. bolus at a single dose of 25 mg/kg each in rat (n = 4).
*In both the chromatograms; a peak corresponding to the other analyte is also seen which is attributed to the interconversion of both these analytes *in vivo* [15].

Table 5
The non-compartmental pharmacokinetic parameters for LSF and PTX in rat plasma after i.v. bolus (25 mg/kg) administration to rat (n = 4).

Parameters	Mean ± SEM	
	LSF	PTX
C_0 (ng/mL)	22,295.204 ± 3691.39	15,835.204 ± 711.96
$t_{1/2}$ (h)	0.661 ± 0.03	0.539 ± 0.06
Ke (1/h)	1.056 ± 0.05	1.317 ± 0.13
$AUC_{0\text{-last}}$ (ng h/mL)	23,944.589 ± 992.83	17,092.707 ± 1008.34
$AUC_{0\text{-}\infty}$ (ng h/mL)	24,067.711 ± 995.38	17,198.155 ± 959.69
$AUMC_{0\text{-last}}$ (ng.h/mL)	22,441.435 ± 1592.68	13,198.186 ± 382.86
$AUMC_{0\text{-}\infty}$ (ng h/mL)	22,789.458 ± 1692.67	13,711.159 ± 502.03
MRT (h)	0.937 ± 0.07	0.778 ± 0.05
V_z (mL/kg)	997.077 ± 71.35	1152.149 ± 201.24
CL (mL/h/kg)	1044.124 ± 43.53	1463.108 ± 84.87

25 mg/kg (i.v.) individually in wistar rats. Fig. 4 shows representative chromatograms of pharmacokinetic study samples at 2 h and mean plasma concentration-time profiles of LSF and PTX. Different pharmacokinetic parameters were evaluated by non-compartmental model approach using Phoenix 2.1 WinNonlin software as shown in Table 5. The initial concentrations (C_0) were found to be 22295.20 ng/mL and 15835.20 ng/mL for LSF and PTX respectively. The half-life for LSF and PTX were found to be 0.66 and 0.54 h respectively which indicates rapid metabolism of both the analytes. The $AUC_{0\text{-last}}$ for LSF and PTX, calculated based on the trapezoidal rule were found to be 23944.59 and 17092.70 ng h/mL respectively. The V_z for LSF and PTX were found to be 997.07 and 1152.15 mL/kg where CL for LSF and PTX were 1044.12 and 1463.10 mL/h/kg respectively. In both the pharmacokinetic studies, peak of corresponding analyte (LSF or PTX) was obtained which is attributed to the interconversion of both analytes *in vivo* (Fig. 4).

4. Conclusion

The analytes quantified in the present study, LSF and PTX carry immense therapeutic potential. Considering this fact, the reported method has been developed and validated such that it could be extensively used for their routine analysis for understanding the *in vivo* drug–drug interactions and pharmacokinetic-pharmacodynamic (PK-PD) studies *etc.* Additionally the reported method is based upon use of a simple and rapid sample preparation process, shows freedom from matrix interference and requires a small plasma sample volume (200 μL). It can analyze the drugs in a wide concentration range (> 5000 ng/mL) with a short overall run time (15 min) without using any sophisticated instruments.

The study also highlighted complete stability of LSF and PTX in plasma when stored under different conditions; freezer storage (−80 °C), auto-sampler, bench top conditions and after three consecutive freeze-thaw cycles.

Declaration of interest

The authors report no conflict of interest.

Acknowledgement

The author would like to gratefully acknowledge the financial support from Science and Engineering Research Board (SERB), Department of Science and Technology (DST), India (YSS/2014/000551).

Appendix A. Supplementary data

Supplementary data associated with this article can be found, in the online version, at http://dx.doi.org/10.1016/j.jchromb.2017.06.043.

References

[1] J.S. Striffler, J.L. Nadler, Lisofylline, a novel anti-inflammatory agent, enhances glucose-stimulated insulin secretion in vivo and in vitro: studies in prediabetic and normal rats, Metabolism 53 (2004) 290–296.
[2] A.V. Furth, E.V. Seijmonsbergen, R.V. Furth, J. Langermans, Effect of lisofylline and pentoxifylline on the bacterial-stimulated production of TNF-α, IL-1β and IL-10 by human leucocytes, Immunology 91 (1997) 193–196.
[3] J.W. Singer, S.L. Rursten, G.C. Rice, W.P. Gordon, J.A. Bianco, Inhibitors of intracellular phosphatidic acid production: novel therapeutics with broad clinical applications, Expert Opin. Investig. Drugs 3 (1994) 631–644.
[4] G.C. Rice, J. Rosen, R. Weeks, J. Michnick, S. Bursten, J.A. Bianco, J.W. Singer, CT-1501R selectively inhibits induced inflammatory monokines in human whole blood ex vivo, Shock 1 (1994) 254–266.
[5] K. Waxman, K. Daughters, S. Aswani, G. Rice, Lisofylline decreases white cell adhesiveness and improves survival after experimental hemorrhagic shock, Crit. Care Med. 24 (1996) 1724–1728.
[6] E. Abraham, S. Bursten, R. Shenkar, J. Allbee, R. Tuder, P. Woodson, D.M. Guidot, G. Rice, J.W. Singer, J.E. Repine, Phosphatidic acid signaling mediates lung cytokine expression and lung inflammatory injury after hemorrhage in mice, J. Exp. Med. 181 (1995) 569–575.
[7] P. Masiello, C. Broca, R. Gross, M. Roye, M. Manteghetti, D. Hillaire-Buys, M. Novelli, G. Ribes, Experimental NIDDM: development of a new model in adult rats administered streptozotocin and nicotinamide, Diabetes 47 (1998) 224–229.
[8] J. Leahy, S. Bonner-Weir, G. Weir, Abnormal glucose regulation of insulin secretion in models of reduced B-cell mass, Diabetes 33 (1984) 667–673.
[9] S.L. Bursten, D. Federighi, J. Wald, B. Meengs, W. Spickler, E. Nudelman, Lisofylline causes rapid and prolonged suppression of serum levels of free fatty acids, J. Pharmacol. Exp. Ther. 284 (1998) 337–345.
[10] P. Cui, T.L. Macdonald, M. Chen, J.L. Nadler, Synthesis and biological evaluation of lisofylline (LSF) analogs as a potential treatment for Type 1 diabetes, Bioorg. Med. Chem. Lett. 16 (2006) 3401–3405.
[11] M. Chen, Z. Yang, R. Wu, J.L. Nadler, Lisofylline, a novel antiinflammatory agent, protects pancreatic β-cells from proinflammatory cytokine damage by promoting mitochondrial metabolism, Endocrinology 143 (2002) 2341–2348.
[12] Z.D. Yang, M. Chen, R. Wu, M. McDuffie, J.L. Nadler, The anti-inflammatory compound lisofylline prevents Type I diabetes in non-obese diabetic mice, Diabetologia 45 (2002) 1307–1314.
[13] National Institutes of Health, A Safety, Tolerability and Bioavailability Study of Lisofylline After Continuous Subcutaneous (12, (2012) http://clinicaltrials.gov/show/NCT01603121/ (Accessed 28 January 2017).
[14] R. Müller, Hemorheology and peripheral vascular diseases: a new therapeutic approach, J. Med. 12 (1981) 209–235.
[15] E. Wyska, E. Pękala, J. Szymura-Oleksiak, Interconversion and tissue distribution of pentoxifylline and lisofylline in mice, Chirality 18 (2006) 644–651.
[16] P. Noel, S. Nelson, R. Bokulic, G. Bagby, H. Lippton, G. Lipscomb, W. Summer, Pentoxifylline inhibits lipopolysaccharide-induced serum tumor necrosis factor and mortality, Life Sci. 47 (1990) 1023–1029.
[17] D. Chivers, D. Birkett, J. Miners, Simultaneous determination of pentoxifylline and its hydroxy metabolite in plasma by high-performance liquid chromatography, J. Chromatogr. 225 (1981) 261–265.
[18] D.M. Grasela, M.L. Rocci, High-performance liquid chromatographic analysis of pentoxifylline and 1-(5'-hydroxyhexyl)-3, 7-dimethylxanthine in whole blood, J. Chromatogr. 419 (1987) 368–374.
[19] P.B. Kyle, K.G. Adcock, R.E. Kramer, R.C. Baker, Use of liquid chromatography–tandem mass spectrometry for the analysis of pentoxifylline and lisofylline in plasma, Biomed. Chromatogr. 19 (2005) 231–236.
[20] E. Wyska, A. Świerczek, K. Pociecha, K.P. Pomierny, Physiologically based modeling of lisofylline pharmacokinetics following intravenous administration in mice, Eur. J. Drug Metab. Pharmacokinet. 41 (2016) 403–412.
[21] US Food Drug Administration, Guidance for Industry, Bioanalytical Methods Validation, (2013) https://www.fda.gov/downloads/Drugs/Guidances/ucm368107.pdf (Accessed 28 January 2017).
[22] S. Kollipara, G. Bende, N. Agarwal, B. Varshney, J. Paliwal, International guidelines for bioanalytical method validation: a comparison and discussion on current scenario, Chromatographia 73 (2011) 201–217.
[23] A.M. Almeida, M.M. Castel-Branco, A. Falcao, Linear regression for calibration lines revisited: weighting schemes for bioanalytical methods, J. Chromatogr. B Analyt. Technol. Biomed. Life Sci. 774 (2002) 215–222.
[24] T. Singtoroj, J. Tarning, A. Annerberg, M. Ashton, Y. Bergqvist, N. White, N. Lindegardh, N. Day, A new approach to evaluate regression models during validation of bioanalytical assays, J. Pharm. Biomed. Anal. 41 (2006) 219–227.

BASIC SCIENCE

Nanomedicine: Nanotechnology, Biology, and Medicine
15 (2019) 175–187

Original Article

nanomedjournal.com

Self-assembling lisofylline-fatty acid conjugate for effective treatment of diabetes mellitus

Kishan S Italiya, MS (Pharm)[a], Samrat Mazumdar, MS (Pharm)[a], Saurabh Sharma, M Pharm[a], Deepak Chitkara, PhD[a], Ram I. Mahato, PhD[b], Anupama Mittal, PhD[a,*]

[a]*Department of Pharmacy, Birla Institute of Technology and Science (BITS-PILANI), Pilani, Rajasthan, India*
[b]*Department of Pharmaceutical Sciences, University of Nebraska Medical Center, Omaha, United States*

Abstract

Lisofylline is an anti-inflammatory agent with proven anti-diabetic activity. Its high solubility and rapid metabolism results in poor bioavailability and short half-life, limiting its clinical utility. We have synthesized Lisofylline-Linoleic acid (LSF-LA) conjugate which self-assembled into micelles (156.9 nm; PDI 0.187; CMC 1 μg/mL; aggregation number 54) without any surfactant and showed enhanced cellular uptake. It protected MIN6 insulinoma cells from cytokine induced cell death and enhanced insulin production under inflammatory conditions. It also suppressed the proliferation of activated peripheral blood mononuclear cells and reduced the production of inflammatory cytokines, IFN-γ and TNF-α. LSF-LA micelles exhibited reduced protein binding, significantly higher half-life (5.7-fold) and higher apparent volume of distribution (5.3-fold) than free LSF. In T1D animals, reduced blood glucose levels were observed at a reduced dose (~15 mg/kg, once daily of LSF-LA micelles *vs.* 25 mg/kg, twice daily of free LSF) that was further confirmed by immunohistochemical analysis.

Key words: Lisofylline; Linoleic acid; Self-assembly; Pharmacokinetics; Diabetes

Type-1 diabetes (T1D) is a chronic metabolic autoimmune disease resulting in hyperglycemia due to the loss of insulin-producing β-cells in the endocrine part of the pancreas, the islets of Langerhans.[1–3] The discovery of small molecules that can protect β-cells against proinflammatory cytokines and preserve functional β-cell mass could potentially prevent life-long insulin therapy and complications in diabetic patients.[4,5] Lisofylline (LSF) is one such small synthetic molecule with anti-diabetic activity,[6] majorly attributed to its ability to a) inhibit the proinflammatory cytokine (IL-1β, TNF-α and IFN-γ) production[7–9] and, b) effective suppression of T-cell activation and differentiation *via* inhibition of the STAT4-mediated IL-12 signaling.[6,10–13] Most importantly, LSF can also maintain β-cell insulin secretory function in the presence of inflammatory cytokines and regulate immune cellular function to suppress autoimmunity.[7,13–15] Apart from T1D, LSF is effective in treatment for type 2 diabetes (T2D),[16] experimental sepsis-induced acute lung injury,[17,18] infectious sepsis,[19,20] endotoxic shock,[21] hemorrhagic shock[22] and autoimmune recurrence following islet transplantation,[13] mainly owing to its anti-inflammatory and immunomodulatory properties.

The broad spectrum of activities of LSF suggests its significant clinical potential but inspite of being a potent molecule it poses certain major challenges that limit its clinical development, including high aqueous solubility (~60 mg/mL in water) which hinders its encapsulation in any delivery system.[16] LSF is reported to be orally non-bioavailable and possesses an extremely short half- life[23–25] and is hence administered at a high dose of 25 mg/kg twice daily in T1D animals[12,16] and in clinical trials, at a single dose of 12 mg/kg by continuous subcutaneous (s.c.) or i.v. infusion over 24 hours. It also undergoes rapid metabolism to form metabolite pentoxifylline (PTX) and this LSF-PTX interconversion is mainly responsible for the high dose of LSF.[26]

In the present work, our objective was to overcome the physicochemical and pharmacokinetic limitations associated with LSF. For this purpose, we designed a LSF-fatty acid conjugate which could self-assemble into micelles in nano size range. This would enable hydrophobization of the drug, increase in its mean residence time in the body, and reduce LSF-PTX interconversion. As shown in **Fig. S1**, LSF-PTX interconversion is attributed to the presence of a secondary hydroxyl group in the side chain of LSF which oxidizes into ketone group and forms metabolite PTX. In this work, we protected the hydroxyl group by conjugating LSF with a

Acknowledgments/Funding Sources: Financial support from Science and Engineering Research Board (SERB), Department of Science and Technology (DST), Govt. of India [#YSS/2014/000551] and Ph.D. fellowship (K.S.I.) from DST-INSPIRE, Govt. of India [#IF160659] is gratefully acknowledged.

*Corresponding author at: Department of Pharmacy, Birla Institute of Technology and Science (BITS), Pilani, Pilani Campus, Pilani, Rajasthan, India, 333 031.
E-mail address: anupama.mittal@pilani.bits-pilani.ac.in. (A. Mittal)

https://doi.org/10.1016/j.nano.2018.09.014
1549-9634/

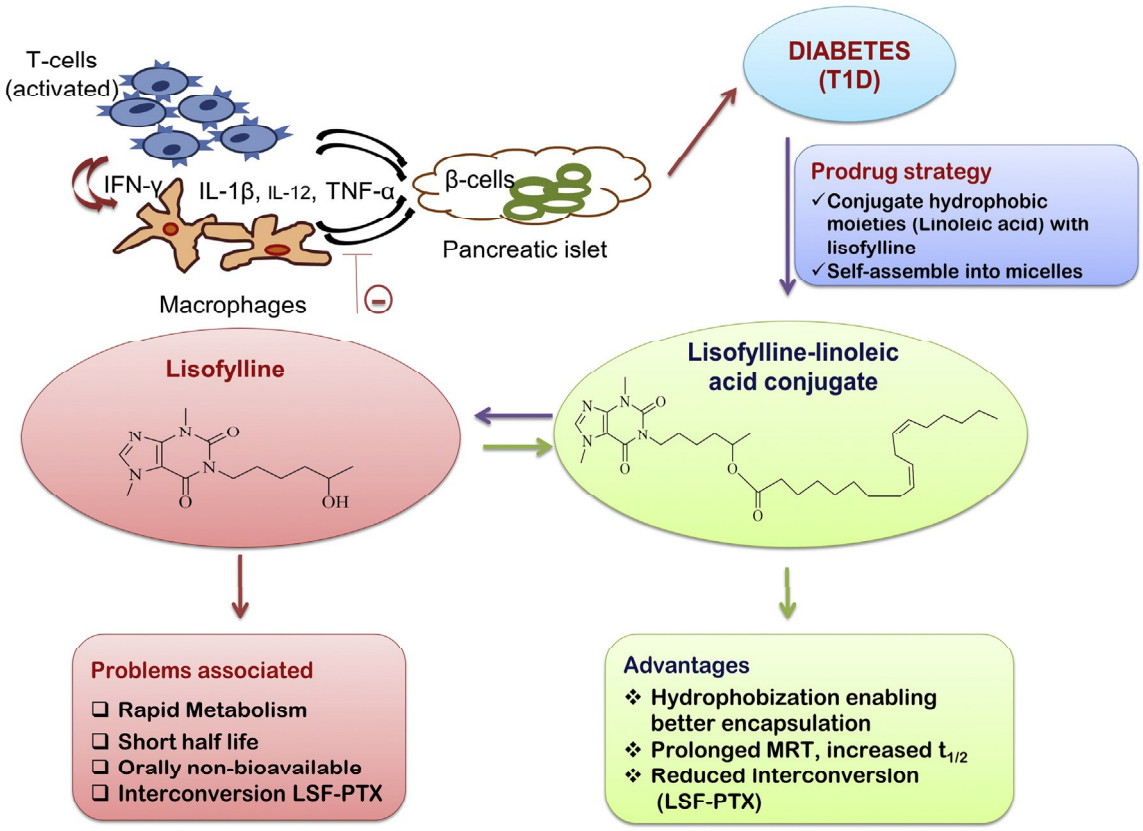

Figure 1. Mechanism of action of LSF in T1D, problems associated with LSF and our proposed strategy and its advantages.

fatty acid that is linoleic acid (LA) *via* ester bond formation. Using this approach there is a possibility that the resulting molecule (LSF-LA conjugate) would be amphiphilic in nature as LSF is hydrophilic and LA is hydrophobic and hence would self-assemble into micelles which would further improve the pharmacokinetics and therapeutic efficacy of LSF. This could also reduce the dose since micellar formulations are known to prolong the circulation time and significantly decrease the metabolism and renal clearance of the encapsulated drugs.[27] Figure 1 depicts the role of LSF in T1D, problems associated with it and our proposed strategy along with its advantages for drug delivery of LSF. To our knowledge, this is the first report on self-assembling nano-drug delivery system of LSF using the drug-fatty acid conjugation strategy.

Methods

Materials and reagents

LSF (purity ≥99%) was purchased from Cayman Chemicals Inc. (Michigan, USA). HPLC grade solvents, acetonitrile, methanol and methylene chloride were obtained from Merck (Mumbai, India). Dulbecco's Modified Eagle Medium (DMEM), Fetal Bovine Serum (FBS), TrypLE and recombinant proteins (TNF-α, IL-1β and IFN-γ) were obtained from Invitrogen (USA); Linoleic acid (purity ≥99%), Streptozotocin (STZ), 3-Isobutyl-1-methylxanthine (IBMX; ≥99%; Internal standard), 3-[4,5-dimethylthiazol-2-yl]-2,5-diphenyltetrazolium bromide (MTT) Cetylpyridinium chloride and D-glucose were purchased from Sigma Aldrich (USA). ELISA kits for TNF-α and IFN-γ (ELISA MAX™) were obtained from BioLegend (USA). Carboxyfluorescein succinimidyl ester (CFSE) staining assay kit (CellTrace™), Ficoll-Paque and Phytohaemagglutinin (PHA) were obtained from ThermoFisher (USA). N-(3-Dimethylaminopropyl)-N′-ethylcarbodiimide hydrochloride (EDC.HCl), Bovine serum albumin and 4-Dimethylaminopyridine (DMAP) were purchased from Spectrochem Ltd. (Mumbai, India). All other chemicals and reagents were of analytical grade and used as obtained. MIN-6 cells were procured from NCCS, Pune (INDIA).

Synthesis of lisofylline-linoleic acid conjugate (LSF-LA conjugate)

It was synthesized by carbodiimide coupling reaction using EDC.HCl and DMAP as shown Figure 2. Under N_2, LA (21.6 mmol, 1.2 eq) solution in anhydrous CH_2Cl_2 (DCM; 250 mL) was mixed with DMAP (21.6 mmol, 1.2 eq) for 15 min. EDC.HCl (27 mmol, 1.5 eq) solution in DCM was added and the reaction mixture was stirred for 1 h at 4 °C. Thereafter, LSF (19.8 mmol, 1.1 eq) was added and reaction was continued for 36 h at room temperature (RT) in dark conditions. Reaction was monitored by TLC. On completion of the reaction, reaction mixture was diluted with DCM, washed with water and brine solution and organic layer was dried on anhydrous $MgSO_4$ and evaporated under vacuum. The semi-solid crude product so obtained was purified using flash chromatography. This yielded the final product, LSF-LA conjugate; which appeared as a

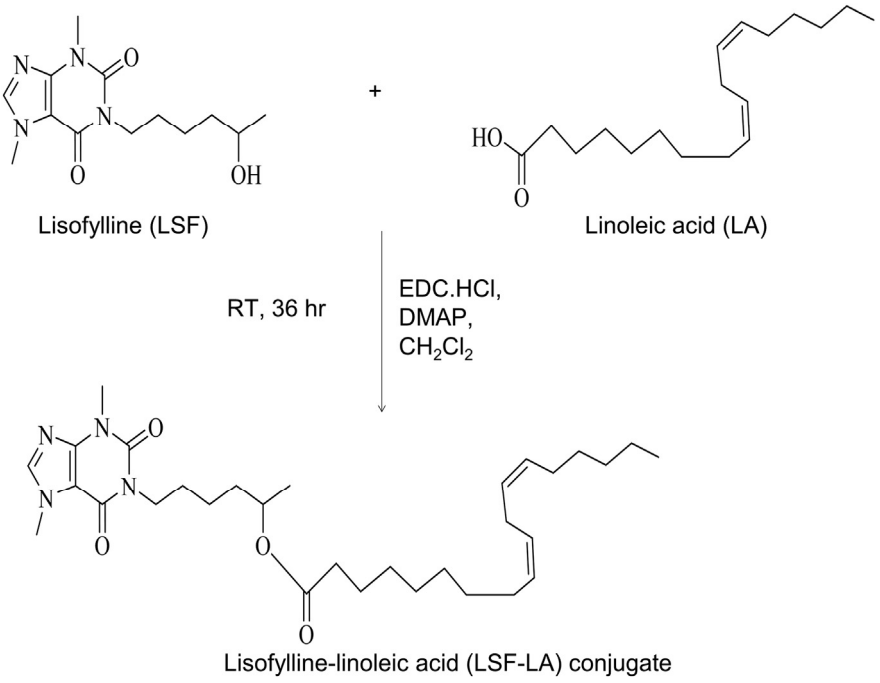

Figure 2. Synthetic scheme for LSF-LA conjugate.

transparent viscous colorless liquid. LSF-LA conjugate so obtained was characterized for its structure, molecular weight and purity by analytical techniques ^{1}H NMR, ^{13}C NMR, HR-MS, HPLC, FT-IR and DSC.

Stability of LSF-LA conjugate in plasma

LSF-LA conjugate (20 mg/mL in DMSO, 10 μL) was added to rat plasma (1 mL) and kept at 37 °C for 72 h. At pre-determined time points, 100 μL of sample was withdrawn to which 50 μL of internal standard (IBMX, 2 μg/mL) and 2 mL of DCM were added. The resulting mixture was centrifuged at 3500 rpm for 15 min at 4 °C, after which the supernatant was transferred into a fresh tube and evaporated to dryness under nitrogen. Dried samples were reconstituted in 100 μL of mobile phase and analyzed by HPLC (Shimadzu, Japan) using our previously reported method.[28]

Self-assembly of LSF-LA conjugate

The amphiphilic nature of LSF-LA conjugate indicates the possibility of its self-assembly into micelles. To explore this, LSF-LA conjugate in DCM was added dropwise into water, followed by stirring for 15 min and evaporation of DCM. Resulting micelle formulation was sonicated for 3 min under cold conditions. The size and zeta-potential of the micelles were measured using a Zetasizer Nano-ZS (Malvern, UK) with at scattering angle of 173°.

Critical micellar concentration (CMC) of LSF-LA conjugate

Formation of self-assembled micelles was confirmed by determination of CMC of LSF-LA conjugate in aqueous solution by fluorescence spectroscopy using pyrene. Self-assembled micelles of LSF-LA conjugate at concentrations ranging from 1.0×10^{-5} mg/ mL to 2.0 mg/mL were mixed with pyrene solution (6×10^{-7} M) and incubated for 24 h with shaking at RT. The fluorescence intensity of the solution was recorded using spectrofluorimeter (RF-5301 Shimadzu, Japan) at an excitation and emission wavelengths of 300 360 nm and 390 nm respectively. Plot was constructed between I_3/I_1 *versus* logarithm of LSF-LA micelles concentration wherein, the I_3 and I_1 values were determined from the shifting of peak intensities at the wavelengths of 337 and 333 nm.

Micelle aggregation number (N_{agg}) of LSF-LA conjugate

The micellar N_{agg} was determined by steady state fluorescence measurements based upon the theory of Turro and Yekta.[29] According to this theory, the relation between the steady state fluorescence intensities of the probe with and without quencher (F_Q and F_0 respectively) is determined by the micelle concentration (M) and the quencher concentration in the micelles (Q) according to:

$$\ln\left(\frac{F0}{FQ}\right) = \frac{Q}{M} \tag{1}$$

where,

$$M = \frac{C - CMC}{N_{agg}} \tag{2}$$

where, C = total surfactant concentration, CMC = critical micelle concentration, and N_{agg} = aggregation number.

In this experiment, pyrene and cetylpyridinium chloride (CPC) were used as probe and quencher, respectively. For

sample preparation, stock solutions of pyrene in LSF-LA micellar solution at 30 times the CMC (Solution I) and pyrene + CPC in LSF-LA micellar solution at 30 times the CMC (Solution II) were prepared. Solution-I was prepared by transferring 2 mL of pyrene in ethanol (10^{-4} M) into a 100 mL glass bottle followed by evaporation of the solvent with nitrogen. To this, 100 mL of the LSF-LA micellar solution at 30 times the CMC was added and stirred overnight. In solution-I, the final pyrene concentration was 2×10^{-6} M. For preparing Solution II, 220.01 mg of CPC was dissolved in 20 mL of Solution-I to obtain Solution-II having CPC concentration of 2.8×10^{-2} M. Appropriate volumes of these two solutions were then mixed to vary the CPC concentration from 0 to 1.54×10^{-3} M.

Fluorescence steady state measurements were carried out with a Shimadzu RF-5301 spectrofluorimeter at room temperature with an excitation wavelength at 318 nm, bandwidth 5 nm, and emission recorded from 320 nm to 450 nm. Each spectrum obtained with the instrument showed three vibronic peaks. The height (in arbitrary units) of the first vibronic peak at 376 nm was then taken as the fluorescence intensity generated by the above solutions.

Protein interaction studies with LSF-LA conjugate micelles

Interaction between LSF-LA micelles and bovine serum albumin (BSA) (as a model protein) was determined by fluorescence quenching method wherein, the change in emission fluorescence of BSA before and after incubation with LSF-LA micelles was studied. Binding constant as well as number of binding sites per BSA molecule were also determined using the Scatchard equation[30,31] (Eq. (3)) which represents binding of small molecules to a set of equivalent sites on another molecule.

$$\log\frac{F0-FQ}{FQ} = \log Kb + n.\log[Q] \quad (3)$$

where F_Q and F_0 represent the fluorescence intensity in the presence and absence of quencher respectively, K_b is the apparent binding constant and n is the number of binding sites per BSA molecule.

For this purpose, a series of different concentrations of LSF-LA micelles in water (0–100 μM) and BSA solution at 2 μM (constant) were incubated together for 30 min. Thereafter, fluorescence intensity of these solutions was measured at emission wavelength of 343 nm and excitation wavelength at 280 nm. Similar experiment was also performed using free LSF and BSA as a control. The fluorescence quenching data so obtained was plotted as log $(F_0\text{-}F_Q)/F_Q$ against log of quencher concentration (LSF-LA micelles or LSF; log [Q]) to determine the binding constant as well as number of binding sites per BSA molecule.

Further, the mechanism by which LSF quenches the fluorescence of BSA was also investigated by studying the change in the absorption spectra of BSA after binding of LSF-LA micelles.[32] The absorption spectra for this purpose were recorded using an ultraviolet–visible (UV–Vis) V-650 Jasco spectrophotometer equipped with a quartz cell with a 1-cm path length.

In vitro studies of LSF-LA conjugate

To evaluate the efficacy of LSF-LA micelles in diabetic conditions, mouse insulinoma cells, MIN-6 were used. Cells were maintained in RPMI media supplemented with 10% FBS and 1% antibiotic solution and incubated at 5% CO_2 and 37 °C.

Cell viability assay

MIN6 cells (5×10^3/well) were seeded in a 96 well cell culture plate and allowed to adhere for 24 h. Three different concentrations of LSF-LA conjugate ranging from 10 to 40 μM were added to the cells and incubated at 37 °C/5% CO_2. Untreated cells and cells treated with free LSF and LA at equivalent concentrations to LSF-LA conjugate were kept as controls. After 48 h, MTT assay was performed and the percentage cell inhibition was determined by comparison with untreated cells.

$$\%\text{Cell viability} = (\text{OD samples wells}/\text{OD control wells}) \times 100 \quad (4)$$

Protective effect rendered by LSF-LA conjugate micelles to cells under inflammatory conditions

MIN6 cells (5×10^3/well) were exposed to a cocktail of pro-inflammatory cytokines (TNF-α; 10 ng/mL, IL-1β; 5 ng/mL and IFN-γ; 100 ng/mL) to induce inflammation.[34] To these cells, along with cytokines, free LSF, free LA and LSF-LA conjugate were also added (~20 μM) and incubated for 48 h. Thereafter, the cells were evaluated for their viability by MTT assay and insulin secreting ability by a static incubation method using basal (3.33 mM) and stimulatory glucose (33.33 mM) concentrations prepared in Krebs-Ringer bicarbonate HEPES buffer (pH 7.4). After 1 h of incubation, supernatants were collected and analyzed for insulin using commercially available ELISA kit.

Suppression of PBMC proliferation and activation by LSF-LA conjugate

PBMCs were freshly isolated from mouse blood using Ficoll-Paque density gradient method. These cells were then exposed to PHA (1 μg/mL, mitogen activator) in the presence of LSF-LA conjugate keeping suitable controls as PBMCs with PHA alone, with PHA and free LSF and with PHA and free LA. After 48 h, the supernatants were evaluated for PBMCs proliferation using CFSC staining assay kit as per manufacturer's instructions using flow cytometry with a 488 nm excitation laser.[35] The extent of cell activation was also determined by measuring the level of inflammatory cytokines, TNF-α and IFN-γ in the conditioned medium of PBMCs using ELISA kits.

Cellular uptake studies for LSF-LA conjugate micelles

To evaluate the uptake of LSF after conjugation with LA in MIN6 cells, cellular uptake studies of LSF-LA self-assembled micelles was performed wherein, MIN6 cells were incubated with LSF-LA micelles (~20 μM LSF; n = 4) and free LSF (20 μM) for 6 h and untreated cells were kept as a control group. After 6 h, the media was withdrawn and centrifuged at 1000 rpm for 10 min to

remove any cells/debris. LSF-LA or LSF was then extracted from this media (0.5 mL) by adding 50 μL of I.S (IBMX) and 1.2 mL of DCM followed by centrifugation at 3500 rpm for 15 min; 1 mL of DCM layer was collected and dried. This was reconstituted in 100 μL of mobile phase out of which 80 μL of sample was injected in HPLC for LSF and LSF-LA analysis.

In vivo studies for LSF-LA conjugate

Experimental protocol was approved by IAEC, BITS-PILANI, Pilani and all the experiments were conducted as per CPCSEA guidelines. Rats were housed in well-ventilated cages under standard laboratory conditions with regular light/dark cycles for 12 h and fed with standard normal diet *ab libitum.*

Pharmacokinetics of LSF and LSF-LA conjugate

LSF and LSF-LA micelles were administered intravenously at the dose of 25 mg/kg and 50 mg/kg (~25 mg/kg of free LSF) respectively to Wistar rats (200–220 g) with maximum dosing volume of 250 μL per rat without fasting (n = 4). After i.v. dosing, blood samples were collected at pre-determined time points up to 36 h. Plasma concentration-time profiles were plotted and analyzed for various pharmacokinetic parameters by non-compartmental model using Phoenix 2.1 WinNonlin (Pharsight corporation, USA). Since LSF is known to interconvert to PTX, plasma levels of PTX were also assessed.

In vivo efficacy studies in STZ induced T1D model

Diabetes was induced in male Wistar rats (180–220 g) by injecting a single high dose of STZ (55 mg/kg, i.p.) dissolved in citrate buffer (0.01 M, pH 4.5) while the respective control rats received the vehicle, citrate buffer (pH 4.5). After 72 h of STZ injection, fasting glucose levels were measured, animals showing plasma glucose levels >250 mg/dl were considered diabetic. Animals were randomly divided into different groups, namely non-diabetic control (NC), diabetic control (DC), diabetic/treated with free LSF and diabetic/treated with self-assembled micelles of LSF-LA conjugate.

Treatment was started on 3rd day after confirming the diabetic conditions. For treatment, free LSF was administered as solution prepared in water for injection at two different doses, 25 mg/kg, i.p. twice daily and 15 mg/kg, i.p. once daily. LSF-LA conjugate was self-assembled into micelles using water for injection and administered at a dose of 30 mg/kg, (~ 15 mg/kg of free LSF) i. p. once daily. Treatment was continued for 1 week and fasting glucose levels were measured daily by tail bleeding method using Accu-Check active glucometer. After 7 days, the levels of insulin, TNF-α and IFN-γ in plasma were also measured using ELISA kits.

Histopathology and immunohistochemical analysis

After 1 week of treatment, animals were euthanized and pancreata were isolated, processed and stained with hematoxylin/eosin (H&E) to allow the assessment of pancreatic islet morphology. For immunohistochemical (IHC) analysis of insulin, standard protocol was followed using primary insulin rabbit antibody (dilution, 1:2000; Santa Cruz Biotechnology, USA), a secondary antibody (goat anti-rabbit IgG, dilution, 1:2000; Sigma) and peroxidase/anti-peroxidase method. After immunostaining, the sections were lightly counterstained with hematoxylin and observed under a light microscope. For determining % insulin staining area (brownish stain), six random pancreatic islets in each group were quantified by using ImageJ software (version 1.42q, NIH, USA).

Statistical analysis

Statistical analysis was performed using one way ANOVA followed by Tukey–Kramer multiple comparison post-test using graphpad prism software.

Results

Synthesis of LSF-LA conjugate

The ^{1}H NMR spectrum of LSF-LA conjugate showed a peak at 3.75 ppm (f) related to hydroxyl proton present in side chain of LSF (the only conjugation site available in LSF) which disappeared completely in LSF-LA conjugate. **Fig. S2(I)** indicating that –CH-OH group of LSF has been consumed for ester bond formation between LSF and LA. This was confirmed by presence of a new peak at 4.9 ppm (-CH-COO; f') in LSF-LA conjugate NMR spectrum. Since ^{1}H NMR was unable to confirm presence or absence of free LA in LSF-LA conjugate, additionally ^{13}C NMR was performed. ^{13}C NMR spectrum of LA exhibited the carbon signal at 180 ppm corresponding to its terminal -COOH which disappeared in LSF-LA conjugate as shown in **Fig. S2(II).** Moreover, LSF-LA conjugate showed the carbon signal at 174.06 ppm in the ^{13}C NMR spectrum corresponding to –COO- group.

The LSF-LA conjugate was also characterized by Fourier-transform infrared spectroscopy (FT-IR), and differential scanning calorimetry (DSC). In FTIR, LSF shows –CH-OH peak at 3400–3300 cm^{-1} (**Fig. S2 (III)**), which was absent in LSF-LA conjugate as free –CH-OH group of LSF participated in ester bond formation with –CH-COOH group of LA. Molecular weight of LSF-LA conjugate ($C_{13}H_{50}N_4O_4$; 542.3832 g/mol) was confirmed by HR-MS (**Fig. S3**). Further, DSC revealed a change in the melting point (**Fig. S4**) of LSF-LA conjugate (379.81 °C) as compared to LSF (124.45 °C). There was no melting peak corresponding to free LSF in LSF-LA conjugate thermogram.

HPLC analysis of LSF-LA conjugate and LSF revealed that the retention time of LSF-LA increased to 18.9 min as compared to LSF which eluted out at 3.1 min, indicating a significant increase in hydrophobicity of LSF upon attaching LA (Figure 3, *A*). Peak purity of LSF-LA conjugate was found to be >98%.

All the experimental results demonstrated that LSF-LA conjugate was synthesized successfully.

Stability of LSF-LA conjugate in plasma

As shown in Figure 3, *B*, LSF-LA conjugate gets slowly hydrolyzed in rat plasma. During the first 2 h, only 4.7% of free LSF is released followed by release of 42.73% LSF from LSF-LA within the next 72 h.

Self-assembly of LSF-LA conjugate

LSF-LA conjugate contains hydrophobic (LA) and hydrophilic (LSF) components in 1:1 proportion that provides it a characteristic

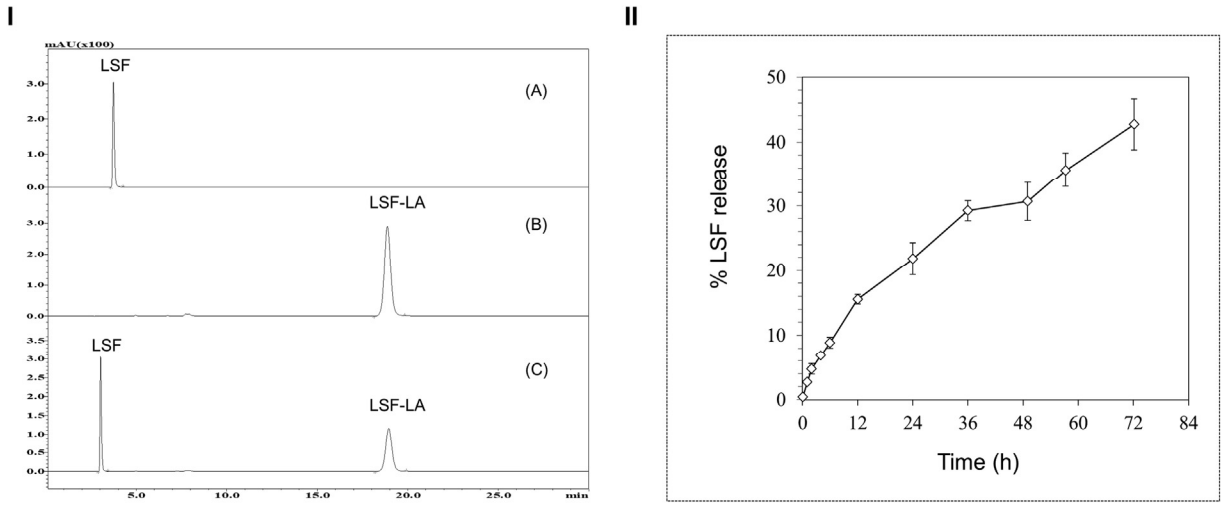

Figure 3. Characterization of LSF-LA conjugate by (A) HPLC analysis and, (B) hydrolysis of LSF-LA in rat plasma.

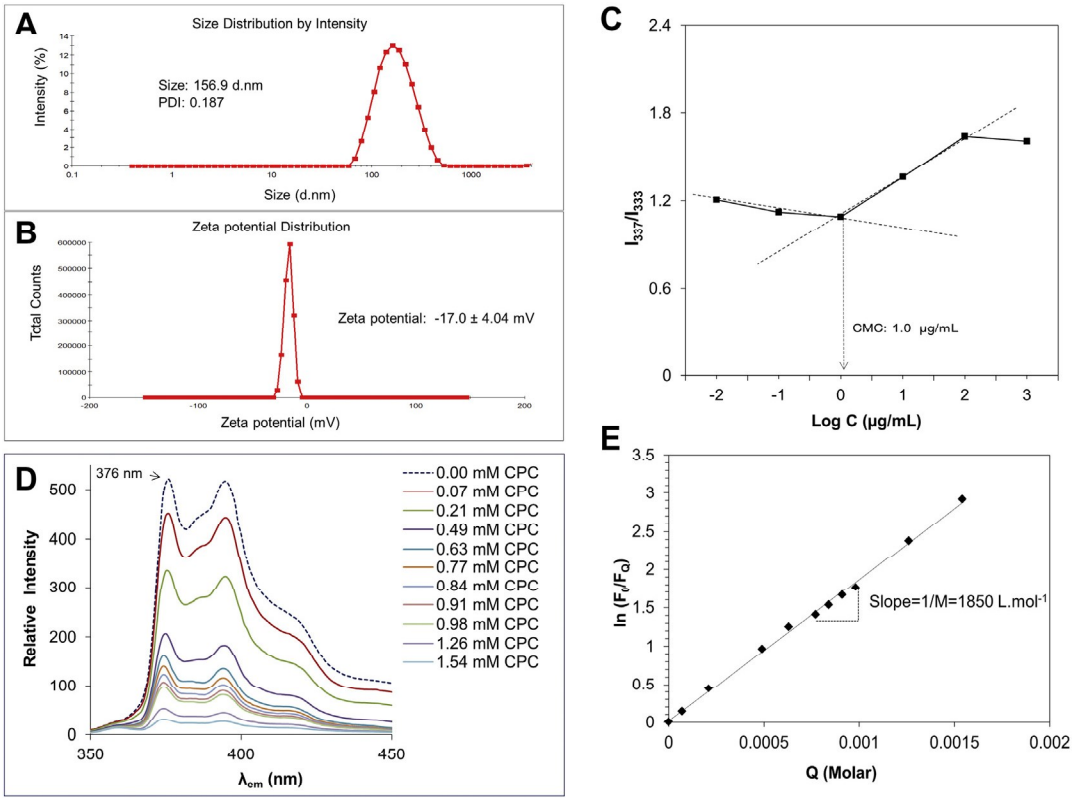

Figure 4. Self-assembled micelles of LSF-LA conjugate, (A) Particle size distribution, (B) Zeta-potential curve, (C) CMC determination and, (D) and (E) Micelle aggregation number wherein, (D) shows steady-state emission spectra of pyrene in LSF-LA micelles (at concentration 30 times the CMC) at different concentrations of CPC (see inserted legend) and, (E) plot of $\ln(F_0/F_Q)$ against quencher concentration (Q) at room temperature

ability to self-assemble into micelles in water. Figure 4, *A* and *B* gives the dynamic light scattering (DLS) curve of LSF-LA micelles in aqueous medium indicating the formation of micelles with a unimodal distribution and an average hydrodynamic diameter of 156.9 nm (polydispersity index: 0.187) and negative zeta potential (−17.0 ± 4.04 mV. CMC value for LSF-LA conjugate was 1 µg/mL indicating micelle formation and hence its ability to self-assemble (Figure 4, *C*).

Aggregation number of LSF-LA self-assembled micelles

The aggregation number of LSF-LA self-assembled micelles was obtained using the static fluorescence quenching method. Figure 4, *D* shows decrease in emission intensity of pyrene in the presence of different quencher (CPC) concentrations (as indicated in the graph) at 30 times the CMC of LSF-LA micelles. Figure 4, *E* shows plot of $\ln(F_0/F_Q)$ *vs.* Q as a straight

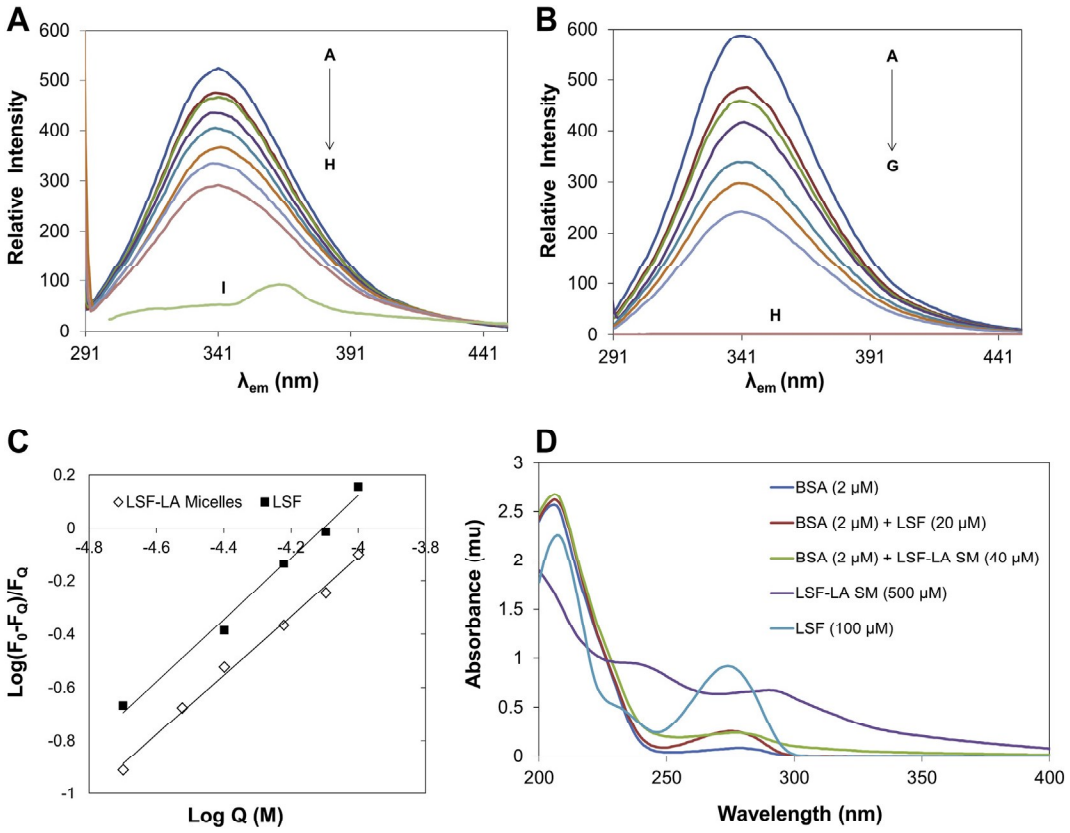

Figure 5. BSA-LSF interaction study: (A) Emission spectra of BSA (λ_{ex} = 280 nm) at 2.0 μM in the presence of different concentrations of LSF-LA micelles 0.0, 10, 20, 30, 40, 60, 80 and 100 μM, corresponding to curves A–H. Plot I corresponds to the emission spectrum of LSF-LA micelles only (500 μM). (B) Emission spectra of BSA at 2.0 μM in the presence of various concentrations of LSF 0.0, 20, 30, 40, 60, 80 and 100 μM, corresponding to curves A–G. Plot H corresponds to the emission spectrum of LSF alone (100 μM) (C) Plot of Log(F_0/F_Q) against log (Q) (LSF and LSF-LA micelles) at different concentrations at room temperature and, (D) UV–Vis absorption spectra of BSA in the presence of LSF-LA micelles and free LSF.

line passing through the origin. The inverse of the slope of this plot corresponds to the micellar concentration [M], and then the aggregation number for LSF-LA self-assembled micelles was calculated as 54 using Eq. (2).

Protein interaction studies of LSF-LA conjugate micelles

In this study, the interaction between BSA and LSF-LA micelles was investigated by fluorescence quenching. Figure 5, *A* and *B* show the emission spectra of BSA before and after interaction with LSF-LA micelles and free LSF respectively. LSF-LA micelles or LSF alone exhibited no fluorescence as seen in their respective graphs (Plot I for LSF-LA micelles in Figure 5, *A* and plot H for free LSF in Figure 5, *B*), however, a decrease in the fluorescence intensity of BSA was observed with increase in the concentration of LSF or LSF-LA micelles without any peak shifting, indicating that there were interactions between LSF or LSF-LA micelles and BSA. Based upon Eq. (3), a plot was constructed between log $(F_0\text{-}F_Q)/F_Q$ *vs.* log [Q] (Figure 5, *C*) and the values of K_b and *n* were determined from its intercept and slope respectively. K_b for LSF-LA micelles and LSF was found to be 2.14×10^4 and 6.11×10^4 $L.mol^{-1}$ respectively. The value of *n* for LSF-LA micelles and LSF was found to be similar (1.11 and 1.16 respectively per BSA molecule).

Further, UV–Vis absorption spectrum of BSA underwent a decrease in intensity at different wavelengths in the presence of LSF or LSF-LA micelles (Figure 5, *D*) indicating a static type quenching mechanism between BSA and LSF-LA/LSF.[32,36]

In vitro studies of LSF-LA conjugate

Cell viability assay

LSF-LA conjugate micelles were found to be non-toxic at all the tested concentrations (10, 20 and 40 μM) which indicated that the conjugate did not have any harmful effect on the cells (Figure 6, *A*).

Protective effect rendered by LSF-LA conjugate to cells under inflammatory conditions

As seen in Figure 6, *B*, cell viability under inflammatory conditions was reduced to ~42.92% however, presence of LSF and LSF-LA conjugate (20 μM) restored the viability to 73.55 and 83.90% respectively which was significantly higher than free LSF. However, no significant improvement was observed in β -cell viability upon increasing the concentration of LSF and LSF-LA conjugate from 20 μM to 40 μM.

Figure 6, *C* reveals that cells in the presence of cytokines showed decreased level of insulin production when compared to normal cells (without cytokines). However, in the presence of LSF and LSF-LA conjugate (20 μM), insulin secretion

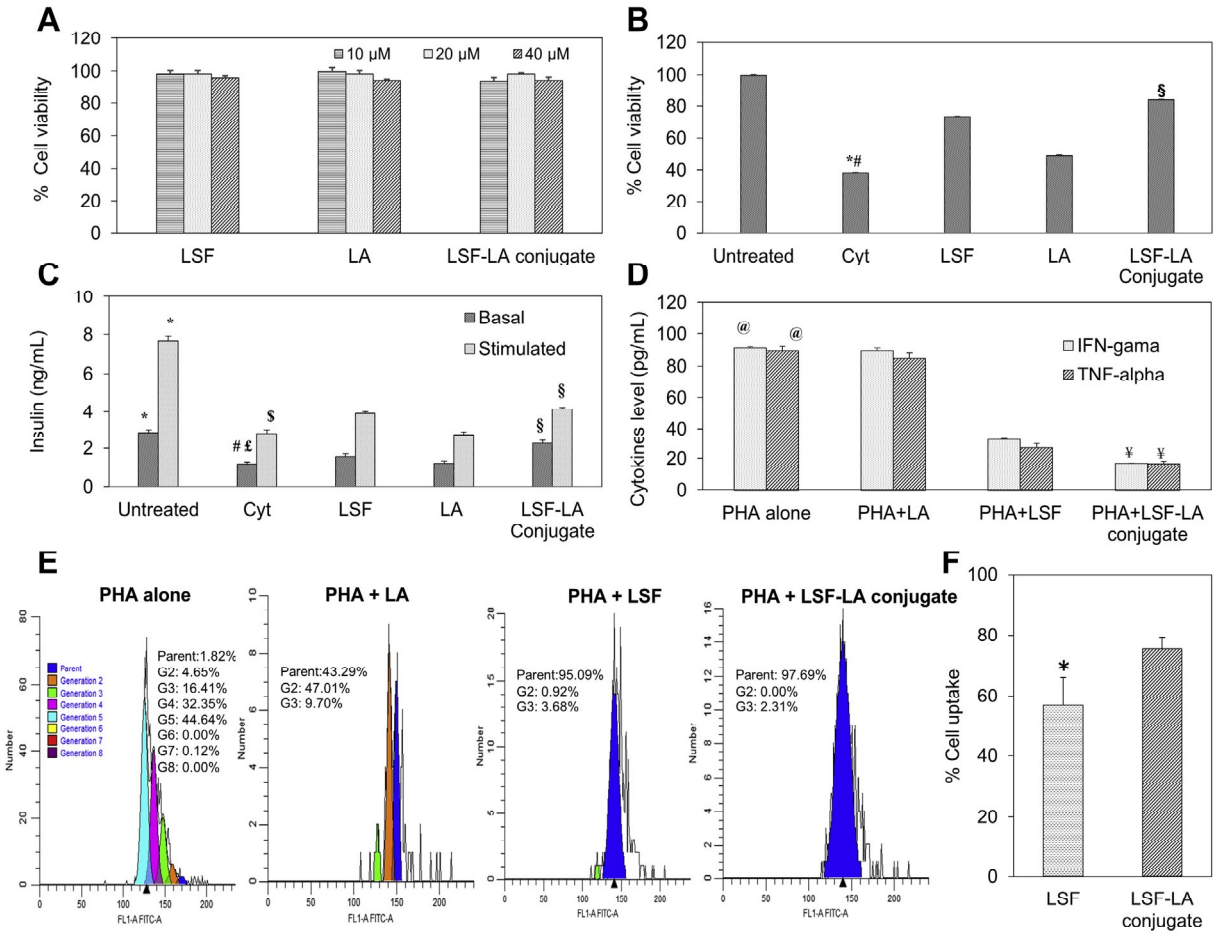

Figure 6. Cell culture studies of LSF-LA conjugate in insulin secreting MIN-6 cells, (A) Cytotoxicity of LSF-LA conjugate, (B) Anti-inflammatory activity of synthesized LSF-LA conjugate (20 μM) in the presence of cytokines (TNF-α, IL-1β and IFN-γ), (C) Basal and stimulated insulin levels after inflammatory challenge following treatment with LSF, LA and LSF-LA (20 μM), (D) IFN-γ and TNF-α level (pg/mL) in the conditioned media of PBMCs, (E) Effect of LSF-LA on activated PBMCs, cell proliferation by flow cytometry and (F) Cellular uptake study for LSF and LSF-LA SM (~20 μM) by HPLC. *LSF *vs.* LSF-LA SM (*$P < 0.05$). *Cyt *vs.* Untreated; #Cyt *vs.* all; §LSF-LA *vs.* LSF and LA (*#§$P < 0.001$) @PHA stimulated PBMCs *vs.* LSF and LSF-LA; ¥LSF-LA *vs.* LSF (@¥$P < 0.001$)

Table 1
The non-compartmental pharmacokinetic parameters for LSF and LSF-LA in rat plasma after i.v. bolus at dose of 25 mg/kg LSF and LSF-LA 50 mg/kg (25 mg/kg equivalent to LSF) administration to rat.

Parameters	Mean ± SEM	
	Free LSF (n = 4)	LSF in LSF-LA (n = 4)
C_o (ng/mL)	22,295.204 ± 3691.39	20,110.94 ± 2552.43
$t_{1/2}$ (h)	0.661 ± 0.03	3.82 ± 0.13
Ke (1/h)	1.056 ± 0.05	0.18 ± 0.01
$AUC_{0\text{-last}}$ (ng.h/mL)	23,944.589 ± 992.83	25,177.93 ± 1037.94
$AUC_{0\text{-}\infty}$ (ng.h/mL)	24,067.711 ± 995.38	26,245.08 ± 937.06
$AUMC_{0\text{-last}}$ (ng.h/mL)	22,441.435 ± 1592.68	93,378.84 ± 4459.30
$AUMC_{0\text{-}\infty}$ (ng.h/mL)	22,789.458 ± 1692.67	124,912.76 ± 6029.35
MRT (h)	0.937 ± 0.07	4.78 ± 0.367
V_z (mL/kg)	997.077 ± 71.35	5279.41 ± 377.18
CL (mL/h/kg)	1044.124 ± 43.53	955.08 ± 35.36

was significantly improved wherein, LSF-LA conjugate showed a significant increase in the levels of insulin in comparison to free LSF.

Suppression of PBMC proliferation and activation by LSF-LA conjugate

Figure 6, *E* shows the flow cytometric graphs of PBMC proliferation wherein, each peak represents a cell division or generation. Cells treated with PHA alone exhibit maximum proliferation (up to 7th generation) in contrast to the un-stimulated cells which do not proliferate beyond 1st generation (data not shown). In the presence of LSF and LSF-LA conjugate, a significant reduction in the proliferation of PBMCs is evident. This is further supported by the significant decrease in IFN- γ and TNF-α levels by LSF-LA micelles in comparison to free LSF treated cells ($p < 0.001$) (Figure 6, *D*). PHA stimulated cells and those treated with LA do not exhibit any significant difference in IFN-γ and TNF-α level.

Cellular uptake studies for LSF-LA conjugate micelles

Figure 6, *F* shows the relative cellular uptake of free LSF and LSF-LA micelles by MIN-6 cells after 6 h of incubation. LSF-LA micelles revealed a significantly higher uptake into the cells (75.48 ± 4.01) in comparison to the free LSF group (56.86 ± 9.26) because of its hydrophobicity and nanosize.

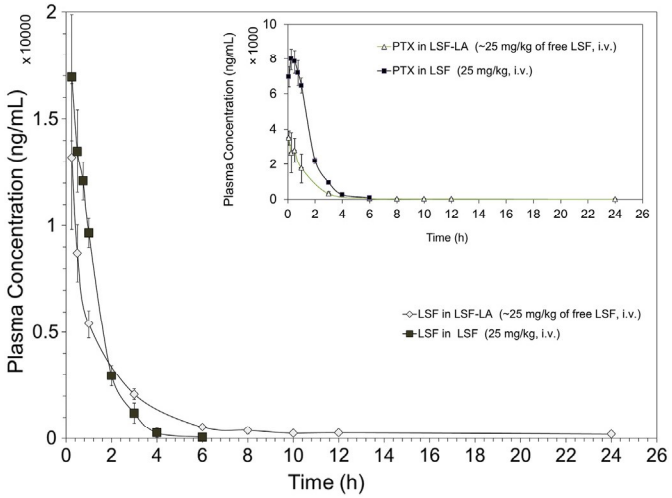

Figure 7. Pharmacokinetic studies of free LSF and LSF-LA conjugate after intravenous (i.v.) administration in rat. Due to interconversion of LSF to PTX, free PTX levels were also observed; PTX plasma concentration-time profiles obtained after administration of free LSF and LSF-LA conjugate are also shown. Each point represents mean (N = 4) ± SEM at dose ~25 mg/kg of free LSF.

In-vivo studies of LSF-LA conjugate

Pharmacokinetics of LSF and LSF-LA conjugate

As shown in Table 1, LSF-LA micelles significantly improved the PK profile of LSF. It increased the half-life to 3.82 ± 0.13 h which was 5.7-fold higher than that of free LSF (0.661 ± 0.03 h) and MRT (~5-fold). LSF-LA micelles showed 5 times higher apparent volume of distribution (5279.41 ± 377.18 mL/kg) compared to free LSF (997.077 ± 71.35 mL/kg) indicating that LSF-LA micelles were much more distributed to different tissues. Further, clearance of LSF-LA micelles was also reduced.

PTX was also detected in the plasma upon administration of both free LSF and LSF-LA conjugate due to the LSF-PTX *in vivo* interconversion.[26] Figure 7 reveals a significant decrease in PTX plasma level (~50%) in LSF-LA micelles PK in comparison to LSF PK which might be attributed to a decrease in LSF-PTX interconversion upon administering LSF as a self-assembling conjugate.

In vivo efficacy studies in STZ induced T1D model

LSF-LA micelles were tested in STZ induced T1D rat model over 1 week period at 15 mg/kg, once daily (LSF-LA-15) and compared with free LSF administered at two dose levels that is, 25 mg/kg, twice daily (LSF-25) and at 15 mg/kg, once daily (LSF-15; same dose as that of LSF-LA micelles). As shown in Figure 8, *A*, a decrease in the fasting glucose levels was seen after 7 days of LSF-LA micelles treatment. Since day 2 of treatment, glucose levels started to decrease and this trend was continued up to 7 days. LSF-15 lowered glucose levels in some rats but failed to maintain the reduced levels compared to LSF-25. LSF-25 stabilized blood glucose levels in some rats but did not correct the values to normal. However, upon treatment with LSF-LA micelles, blood glucose levels got stabilized as well as corrected to normal level in some animals. As shown in Figure 8, *B* and *D*, LSF-LA conjugate treated group showed significantly increased levels of insulin in comparison to free LSF treated groups along with a drastic reduction in TNF-α and IFN-γ.

Histopathology and immunohistochemical analysis

Rat pancreas of diabetic group showed a significant decrease in the number of β cells as compared to the normal control group (Figure 8, *C*). The damage or necrosis of β cells in diabetic control group is a hallmark of diabetes. In LSF-25 and LSF-LA-15 conjugate treated groups, more number of β-cells were observed as compared to the diabetic control group. Although the rats treated with LSF-25 showed better β cell protection compared to LSF-15, the distorted morphology of the islets in both the groups was similar to the diabetic group. Immunohistochemical analysis for insulin in the non-diabetic (normal control) rats revealed presence of abundant insulin (% insulin staining area, 17.85 ± 1.01) however, pancreatic sections from diabetic rats exhibited minimal/no apparent insulin staining (Figure 8, *E*; % insulin staining area, 2.88 ± 0.99) which is consistent with active islet β cell destruction as revealed by H&E staining of these sections and is in agreement with the decrease in cell viability and insulin secretion under the inflammatory stress as observed in the cell culture experiments (Figure 6, *C*). In rats treated with LSF-LA micelles, insulin-positive cell clusters were significant and widely distributed throughout the pancreas despite evidence of persistent insulitis compared to normal control ($P < 0.001$). Treatment with free LSF-25 increased insulin stained area as compared to LSF-15 which was not significantly different from diabetic group.

Discussion

LSF is a potent anti-inflammatory and immunomodulatory agent but possesses challenging physico-chemical properties like high solubility and pharmacokinetics showing a high rate of metabolism, poor bioavailability and rapid clearance, all necessitating a high dose and frequent dosing.[15,16,37] Due to

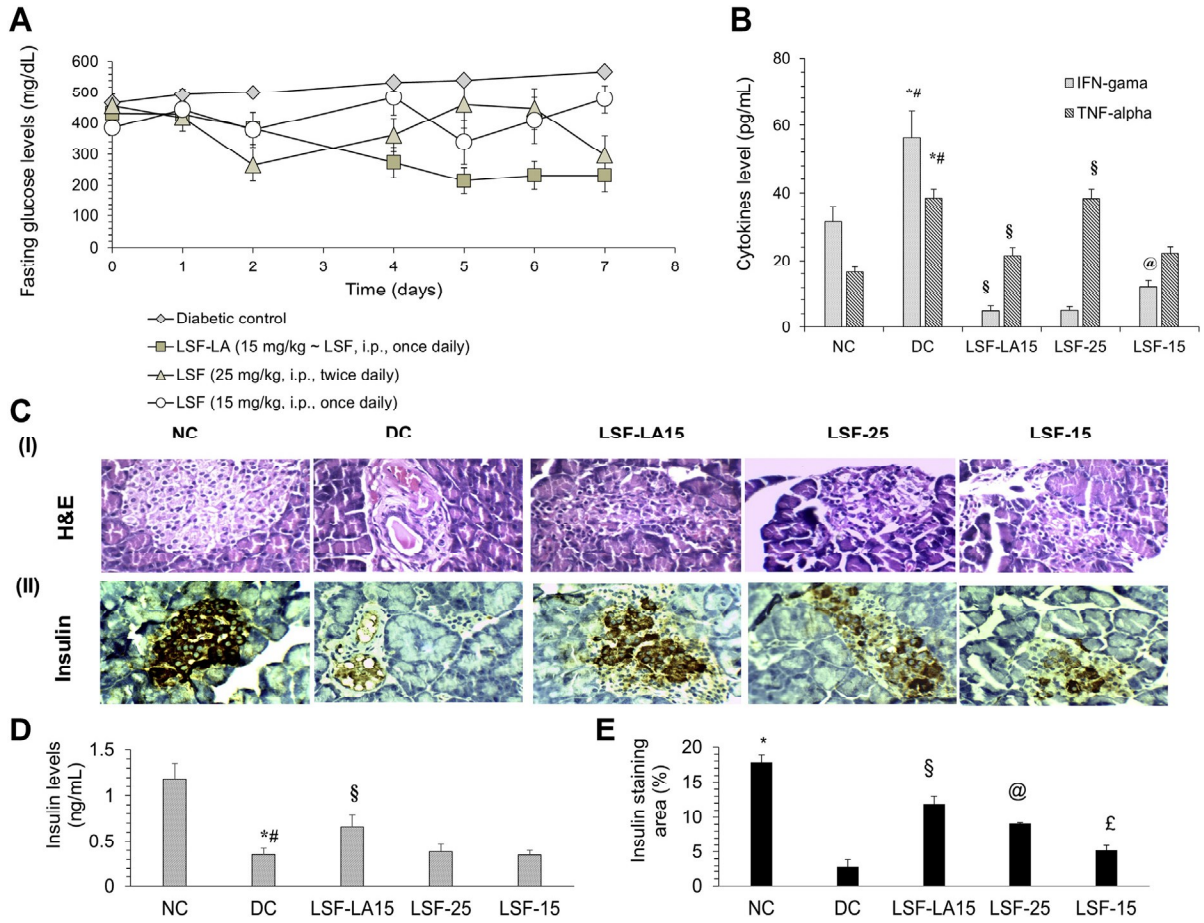

Figure 8. *In vivo* efficacy study of LSF-LA conjugate in STZ induced T1D animal model, (A) Fasting blood glucose levels in different groups, (B) IFN-γ and TNF-α levels in rat plasma after 1 week of treatment. *NC *vs.* DC; #DC *vs.* all groups; §LSF-LA15 *vs.* LSF-25 and LSF-15; @LSF-15 *vs.* LSF-LA15 and LSF-25 (*#§$P < 0.001; @ P < 0.05) and TNF-α levels in rat plasma after 1 week treatment. *NC *vs.* DC; #DC *vs.* LSF-LA15 and LSF-15; §LSF-LA15 *vs.* LSF-25; $LSF-25 *vs.* LSF-15 (*#§$P < 0.001) (C) Immunohistochemical (IHC) analysis of pancreatic tissues treated with various treatments (a) H&E (b) Insulin staining (Magnification ×400, scale: 50 μm) staining (D) Insulin levels in rat plasma after 1 week treatment. *NC *vs.* DC; #DC *vs.* LSF-LA15; §LSF-LA15 *vs.* LSF-15 (*P < 0.001; #§P < 0.05), (E) In IHC, % Insulin staining area analysis by ImageJ software.*NC *vs.* all groups; §LSF-LA15 *vs.* DC and LSF-15; @LSF-25 *vs.* LSF-LA15; £LSF-15 *vs.* LSF-25. (*#§$P < 0.001, @P < 0.01, £P < 0.05).

these concerns associated with LSF, it is very challenging to encapsulate it in a delivery system and that might be probable reason that no report is available on its formulation or delivery aspects in the literature. As the major shortcomings of LSF are attributed to its hydrophilic nature, in this paper, we attempted to initially reduce the hydrophilicity of LSF by conjugating a hydrophobic moiety LA to it. This approach served another fundamental purpose which was to overcome the rapid metabolism of LSF to PTX since LA was conjugated to the free secondary hydroxyl group in side chain of LSF thus protecting this group which is mainly responsible for its rapid metabolism and clearance.[13] Further, a nano-sized self-assembling system of LSF-LA conjugate was attempted to harness the advantages of a nano formulation without use of any external excipient. LA is an essential fatty acid (18:2, ω-6) which cannot be synthesized by the human body and is hence supplemented from external sources to reap its benefits.[38,39] Apart from its health benefits, LA was selected as the fatty acid of choice since it has similar molecular weight (280.3 g/mol) as LSF. Taking advantage of its hydrophobic properties, it was conjugated to LSF in 1:1 ratio to form an amphiphilic drug-fatty acid conjugate, which could self-assemble into micelles with hydrophobic core of LA with hydrophilic shell composed of LSF. This self-assembly provided various advantages of a nano delivery system including an altered uptake mechanism which bypasses the first pass metabolism of LSF, prolongs MRT in the body, reduces clearance due to escape from the RES and ease of handling and most importantly, no external surfactant/excipient was used for this purpose.

LSF-LA conjugate was synthesized and characterized by various analytical techniques, which confirmed the formation of LSF-LA conjugate, its molecular weight, enhanced hydrophobicity and its purity. LSF-LA micelles underwent slow hydrolysis in plasma indicating possibility of prolonged action and reduced rate of metabolism. It self-assembled into nano-sized micelles with a CMC of ≥1 μg/mL (1.84 μM) which is 10 times lower than CMC value of the low molecular weight amphiphile, tween 80 (18 μM) indicating that micelles would remain stable *in vivo*.[40] The aggregation number of the self-assembled micelles of LSF-LA was found to be 54 (at 30 times

CMC) which further increased upon increasing the concentration of LSF-LA. The significance of aggregation number could be understood from the fact that self-assembled aggregates or micelles do not absorb directly but must dissociate into unimers for their absorption.[41] An optimum N_{agg} is desirable to ensure effective solubilization since a very high value of N_{agg} warns of a smaller diffusion coefficient which could lower the rate of transport from air-water interfaces to the bulk of the medium thus hindering the solubilization of micelles.[29]

After systemic administration, nanomaterials are exposed to different physiological fluids including blood, wherein, several thousands of proteins present in the blood can bind or adsorb onto the nanoparticles (NPs) thus modifying their physicochemical properties such as size, surface charge, surface composition, and functionality. This gives a new biological identity to the NPs which represents its 'true identity' in the body and influences various biological responses such as fibrillation, cellular uptake, circulation time, bioavailability, and even toxicity.[42,43] The layers consisting of bound or adsorbed proteins around NPs is known as protein corona. In the present study, protein corona formation with LSF-LA self-assembled micelles was studied using BSA due to its high structural homology with human serum albumin, the major soluble protein constituent of the circulatory system.[33] It is also one of the most abundant proteins in humans and plays a dominant role in transport and disposition of a wide variety of different endogenous and exogenous compounds in blood.[44] Our primary goal was to assess the nature and extent of interaction of BSA (protein corona) with LSF-LA micelles in comparison to free LSF. LSF-LA micelles and free LSF showed non-covalent binding with BSA possibly by static mechanism. Further, LSF-LA micelles showed lower binding constant (~3 times) when compared to free LSF with similar number of binding sites per BSA (*n*; 1.11 *vs.* 1.16) signifying a lower binding affinity and hence weaker interaction of LSF-LA micelles than LSF.[45] This indicates lesser recognition by RES and hence prolonged circulation time in the body along with availability of more amount of unbound LSF-LA to elicit its therapeutic response in the body which was further corroborated by the results of the PK and PD studies.

In-vitro efficacy testing of LSF-LA micelles in MIN-6 insulin secreting cells revealed its non-toxicity to the cells. LSF has been reported to protect the pancreatic β -cells from cytokine-induced cell death by inhibiting the production of TNF-α, IL-1β, macrophage inflammatory protein (MIP)-lα, TGF-β and IFN-γ.[46,47] LSF-LA micelles also protected the β–cells from dying under inflammatory conditions and as compared to control and LSF alone showed ~40% and ~10% higher viability of cells. This enhanced viability of β–cells was also reflected in increased insulin secretion under inflammatory conditions in response to basal and stimulated levels of glucose. Further, after conjugation with LA and formation of micelles, the cellular uptake of LSF by MIN6 cells was significantly increased in comparison to free LSF. This could be attributed to the hydrophobicity of LA and self-assembly of LSF-LA into nano-sized micelles (156.9 nm) since cellular uptake is mainly influenced by size, shape, surface charge, and surface hydrophobicity.[48] Better uptake into the cells ensures more amount of LSF being available at the site of action for its therapeutic activity indicating possibility of dose reduction and hence lesser side effects.

T1D develops when one or more immunoregulatory mechanisms fail, allowing auto-reactive T cells (one of the PBMCs) directed against islet β-cells to become active, to expand clonally, and to entrain a cascade of immune/inflammatory processes in the islet (insulitis), culminating in β-cell destruction.[49,50] Thus, in T1D, spontaneous proliferation of PBMCs, as well as a high production of cytokines such as IFN-γ, TNF-α *etc.* are observed which cause direct β-cell cytotoxic effect in rodent islets.[51] In our study, proliferation of activated PBMCs was significantly suppressed by LSF-LA micelles along with decreased pro-inflammatory cytokines level in the conditioned media of PBMCs in comparison to free LSF treated cells signifying its ability to impair the activation of adaptive immune system in T1D.

Drug-lipid conjugation approach has demonstrated improvement in PK parameters and hence therapeutic action of hydrophilic drugs as observed in the case of gemcitabine prodrugs developed by Jin et al. through the conjugation of lipid derivatives which showed 3–6-fold higher cytotoxicity in five different human cancer cell lines than that of gemcitabine.[52–54] Similarly, lipidated irinotecan prodrug was developed by Liang et al. that demonstrated increased cytotoxicity in cancer cells.[55] In our study, LSF was conjugated to LA, which exhibited a marked improvement in the PK parameters such as $t_{1/2}$, MRT and Vz (~5 fold higher than free LSF). Furthermore, compared to free drug, LSF-LA conjugate showed a longer circulation time in the bloodstream due to escape from RES uptake. Similarly, in *in vivo* efficacy studies, LSF-LA micelles treated group exhibited significant decrease in fasting blood glucose and notable increase in insulin production compared to LSF treated group (even at high dose). Initially, 25 mg/kg, twice daily dose of LSF-LA micelles was administered to the diabetic animals however, at this dose of LSF-LA, severe hypoglycemia was produced in the animals. So, the dose of LSF-LA conjugate was reduced to 15 mg/kg, once daily. LSF-LA conjugate also drastically reduced the levels of TNF-α and IFN-γ in the plasma; these proinflammatory cytokines are known to cause β-cell destruction by activating both CD4+ and CD8+ T lymphocytes.[56] H&E staining and IHC analysis of pancreatic tissue revealed that LSF-LA micelles showed significant β-cell protection as well as enhanced insulin secretion as was indicated by *in vitro* studies in MIN-6 cells and insulin assay in plasma samples.

In a nutshell, our results have demonstrated that as compared to free LSF, LSF-LA micelles consisting of hydrophilic LSF and hydrophobic LA linked through an ester linkage exhibited a much better therapeutic effect in insulin secreting MIN-6 cells as well as in STZ induced T1D model. Apart from the conjugation approach, the improvement in the therapeutic effect of the LSF-LA conjugate can also be attributed to its ability to self-assemble into micelles with an average hydrodynamic diameter of 156.9 nm. Additionally, it also reduced the LSF-PTX interconversion thus showing efficacy at a reduced dose and dosing frequency, which would eliminate the high-dose requirement for effective treatment of T1D. Overall, we believe that this LSF prodrug strategy based on self-assembly of amphiphilic drug-fatty acid conjugate may open new avenues in treatment of T1D

and could also be further explored in treatment of other autoimmune diseases where LSF has demonstrated significant therapeutic efficacy.

Appendix A. Supplementary data

Supplementary data to this article can be found online at https://doi.org/10.1016/j.nano.2018.09.014.

References

1. Mathieu C, Gillard P, Benhalima K. Insulin analogues in type 1 diabetes mellitus: getting better all the time. *Nat Rev Endocrinol* 2017;**13**:385-99.
2. Atkinson MA, Eisenbarth GS, Michels AW. Type 1 diabetes. *Lancet* 2014;**383**:69-82.
3. Atkinson MA, Eisenbarth GS. Type 1 diabetes: new perspectives on disease pathogenesis and treatment. *Lancet* 2001;**358**:221-9.
4. Modi P. Diabetes beyond insulin: review of new drugs for treatment of diabetes mellitus. *Curr Drug Discov Technol* 2007;**4**:39-47.
5. Aghazadeh Y, Nostro MC. Cell therapy for type 1 diabetes: current and future strategies. *Curr Diab Rep* 2017;**17**:37.
6. Yang Z, Chen M, Nadler JL. Lisofylline: a potential lead for the treatment of diabetes. *Biochem Pharmacol* 2005;**69**:1-5.
7. Yang ZD, Chen M, Wu R, McDuffie M, Nadler JL. The anti-inflammatory compound lisofylline prevents type I diabetes in non-obese diabetic mice. *Diabetologia* 2002;**45**:1307-14.
8. Chen M, Yang Z, Wu R, Nadler JL. Lisofylline, a novel antiinflammatory agent, protects pancreatic β-cells from proinflammatory cytokine damage by promoting mitochondrial metabolism. *Endocrinology* 2002;**143**:2341-8.
9. Yang Z, Chen M, Fialkow LB, Ellett JD, Wu R, Nadler JL. Inhibition of STAT4 activation by lisofylline is associated with the protection of autoimmune diabetes. *Y Acad Sci* 2003;**1005**:409-11.
10. Coon ME, Diegel M, Leshinsky N, Klaus SJ. Selective pharmacologic inhibition of murine and human IL-12-dependent Th1 differentiation and IL-12 signaling. *J Immunol* 1999;**163**:6567-74.
11. Bright JJ, Du C, Coon M, Sriram S, Klaus SJ. Prevention of experimental allergic encephalomyelitis via inhibition of IL-12 signaling and IL-12-mediated Th1 differentiation: an effect of the novel anti-inflammatory drug lisofylline. *J Immunol* 1998;**161**:7015-22.
12. Yang Z, Chen M, Fialkow LB, Ellett JD, Wu R, Nadler JL. The novel anti-inflammatory compound, lisofylline, prevents diabetes in multiple low-dose streptozotocin-treated mice. *Pancreas* 2003;**26**:e99-e104.
13. Yang Z, Chen M, Ellett JD, Fialkow LB, Carter JD, Nadler JL. The novel anti-inflammatory agent lisofylline prevents autoimmune diabetic recurrence after islet transplantation1. *Transplantation* 2004;**77**:55-60.
14. Yang Z, Chen M, Carter JD, Nunemaker CS, Garmey JC, Kimble SD, et al. Combined treatment with lisofylline and exendin-4 reverses autoimmune diabetes. *Biochem Biophys Res Commun* 2006;**344**:1017-22.
15. Vieira A, Courtney M, Druelle N, Avolio F, Napolitano T, Hadzic B, et al. β-Cell replacement as a treatment for type 1 diabetes: an overview of possible cell sources and current axes of research. *Diabetes Obes Metab* 2016;**18**:137-43.
16. Striffler JS, Nadler JL. Lisofylline, a novel anti-inflammatory agent, enhances glucose-stimulated insulin secretion in vivo and in vitro: studies in prediabetic and normal rats. *Metabolism* 2004;**53**:290-6.
17. George CL, Fantuzzi G, Bursten S, Leer L, Abraham E. Effects of lisofylline on hyperoxia-induced lung injury. *Respir Crit Care Med* 1999;**276**:L776-85.
18. Network ACT. Randomized, placebo-controlled trial of lisofylline for early treatment of acute lung injury and acute respiratory distress syndrome. *Crit Care Med* 2002;**30**:1-6.
19. Oka Y, Hasegawa N, Nakayama M, Murphy GA, Sussman HH, Raffin TA. Selective downregulation of neutrophils by a phosphatidic acid generation inhibitor in a porcine sepsis model. *J Surg Res* 1999;**81**:147-55.
20. Hasegawa N, Oka Y, Nakayama M, Berry GJ, Bursten S, Rice G, et al. The effects of post-treatment with lisofylline, a phosphatidic acid generation inhibitor, on sepsis-induced acute lung injury in pigs. *Respir Crit Care Med* 1997;**155**:928-36.
21. Rice GC, Brown PA, Nelson RJ, Bianco JA, Singer JW, Bursten S. Protection from endotoxic shock in mice by pharmacologic inhibition of phosphatidic acid. *S A* 1994;**91**:3857-61.
22. Waxman K, Daughters K, Aswani S, Rice G. Lisofylline decreases white cell adhesiveness and improves survival after experimental hemorrhagic shock. *Crit Care Med* 1996;**24**:1724-8.
23. National Institutes of Health. A safety, tolerability and bioavailability study of lisofylline after continuous subcutaneous (12 mg/kg) and intravenous (12 mg/kg) administration in healthy subjects and in subjects with type 1 diabetes mellitus. http://clinicaltrials.gov/show/NCT01603121/2012.
24. Wyska E. Pharmacokinetic-pharmacodynamic modeling of methylxanthine derivatives in mice challenged with high-dose lipopolysaccharide. *Pharmacology* 2010;**85**:264-71.
25. Lillibridge JA, Kalhorn TF, Slattery JT. Metabolism of lisofylline and pentoxifylline in human liver microsomes and cytosol. *Drug Metab Dispos* 1996;**24**:1174-9.
26. Wyska E, Pękala E, Szymura-Oleksiak J. Interconversion and tissue distribution of pentoxifylline and lisofylline in mice. *Chirality* 2006;**18**:644-51.
27. Jeevanandam J, San Chan Y, Danquah MK. Nano-formulations of drugs: recent developments, impact and challenges. *Biochimie* 2016;**128**:99-112.
28. Italiya KS, Sharma S, Kothari I, Chitkara D, Mittal A. Simultaneous estimation of lisofylline and pentoxifylline in rat plasma by high performance liquid chromatography-photodiode array detector and its application to pharmacokinetics in rat. *Analyt Technol Biomed Life Sci* 2017;**1061**:49-56.
29. Tehrani-Bagha AR, Kärnbratt J, Löfroth J-E, Holmberg K. Cationic ester-containing gemini surfactants: determination of aggregation numbers by time-resolved fluorescence quenching. *J Colloid Interface Sci* 2012;**376**:126-32.
30. Gharagozlou M, Boghaei DM. Interaction of water-soluble amino acid Schiff base complexes with bovine serum albumin: fluorescence and circular dichroism studies. *Spectrochim Acta A* 2008;**71**:1617-22.
31. Zhang J, Chen L, Zeng B, Kang Q, Dai L. Study on the binding of chloroamphenicol with bovine serum albumin by fluorescence and UV–vis spectroscopy. *Spectrochim Acta A* 2013;**105**:74-9.
32. Zhang G, Wang A, Jiang T, Guo J. Interaction of the irisflorentin with bovine serum albumin: a fluorescence quenching study. *J Mol Struct* 2008;**891**:93-7.
33. Guo M, Zou J-W, Yi P-G, Shang Z-C, Hu G-X, Yu Q-S. Binding interaction of gatifloxacin with bovine serum albumin. *Anal Sci* 2004;**20**:465-70.
34. Cui P, Macdonald TL, Chen M, Nadler JL. Synthesis and biological evaluation of lisofylline (LSF) analogs as a potential treatment for type 1 diabetes. *Bioorg Med Chem Lett* 2006;**16**:3401-5.
35. Quah BJ, Warren HS, Parish CR. Monitoring lymphocyte proliferation in vitro and in vivo with the intracellular fluorescent dye carboxyfluorescein diacetate succinimidyl ester. *Nat Protoc* 2007;**2**:2049-56.
36. Rodríguez Galdón B, Pinto Corraliza C, Cestero Carrillo JJ, Macías Laso P. Spectroscopic study of the interaction between lycopene and bovine serum albumin. *Luminescence* 2013;**28**:765-70.
37. Wyska E, Świerczek A, Pociecha K, Przejczowska-Pomierny K. Physiologically based modeling of lisofylline pharmacokinetics following intravenous administration in mice. *Drug Metab Pharmacokinet* 2016;**41**:403-12.

38. Anand R, Kaithwas G. Anti-inflammatory potential of alpha-linolenic acid mediated through selective COX inhibition: computational and experimental data. *Inflammation* 2014;**37**:1297-306.
39. Johnson MM, Swan DD, Surette ME, Stegner J, Chilton T, Fonteh AN, et al. Dietary supplementation with γ-linolenic acid alters fatty acid content and eicosanoid production in healthy humans. *J Nutr* 1997;**127**:1435-44.
40. Uchegbu IF, editor. *Low molecular weight micelles*. Springer; 2013.
41. Fletcher PD. Self-assembly of micelles and microemulsions. *Curr Opin Colloid Interface Sci* 1996;**1**:101-6.
42. Lee YK, Choi E-J, Webster TJ, Kim S-H, Khang D. Effect of the protein corona on nanoparticles for modulating cytotoxicity and immunotoxicity. *Nanomedicine* 2015;**10**:97.
43. Nguyen Van Hong, B-JL. Protein corona: a new approach for nanomedicine design. *Nanomedicine* 2017;**12**:3137.
44. Mote U, Bhattar S, Patil S, Kolekar G. Interaction between felodipine and bovine serum albumin: fluorescence quenching study. *Luminescence* 2010;**25**:1-8.
45. Yu X, Liu R, Ji D, Yang F, Li X, Xie J, et al. Study on the synergism effect of lomefloxacin and ofloxacin for bovine serum albumin in solution by spectroscopic techniques. *J Solution Chem* 2011;**40**:521-31.
46. Du C, Cooper JC, Klaus SJ, Sriram S. Amelioration of CR-EAE with lisofylline: effects on mRNA levels of IL-12 and IFN-γ in the CNS. *J Neuroimmunol* 2000;**110**:13-9.
47. Van Furth A, Verhard S EM, Van Furth R, Langermans J. Effect of lisofylline and pentoxifylline on the bacterial stimulated production of TNF-α, IL-1β and IL-10 by human leucocytes. *Immunology* 1997;**91**:193-6.
48. Fröhlich E. The role of surface charge in cellular uptake and cytotoxicity of medical nanoparticles. *Nanomedicine* 2012;**7**:5577.
49. Herold KC, Vignali DA, Cooke A, Bluestone JA. Type 1 diabetes: translating mechanistic observations into effective clinical outcomes. *Nat Rev Immunol* 2013;**13**:243-56.
50. Kahanovitz L, Sluss PM, Russell SJ. Type 1 diabetes-a clinical perspective. *Point Care* 2017;**16**:37-40.
51. Rabinovitch A. Immunoregulatory and cytokine imbalances in the pathogenesis of IDDM: therapeutic intervention by immunostimulation? *Diabetes* 1994;**43**:613-21.
52. Jin Y, Lian Y, Du L, Wang S, Su C, Gao C. Self-assembled drug delivery systems. Part 6: in vitro/in vivo studies of anticancer N-octadecanoyl gemcitabine nanoassemblies. *Pharm* 2012;**430**:276-81.
53. Li M, Qi S, Jin Y, Dong J. Self-assembled drug delivery systems. Part 8: in vitro/in vivo studies of the nanoassemblies of cholesteryl-phosphonyl gemcitabine. *Pharm* 2015;**478**:124-30.
54. Chitkara D, Mittal A, Behrman SW, Kumar N, Mahato RI. Self-assembling, amphiphilic polymer–gemcitabine conjugate shows enhanced antitumor efficacy against human pancreatic adenocarcinoma. *Bioconjug Chem* 2013;**24**:1161-73.
55. Zhang C, Jin S, Xue X, Zhang T, Jiang Y, Wang PC, et al. Tunable self-assembly of irinotecan-fatty acid prodrugs with increased cytotoxicity to cancer cells *J Mater Chem B* 2016;**4**:3286-91.
56. Amrani A, Verdaguer J, Thiessen S, Bou S, Santamaria P. IL-1α, IL-1β, and IFN-γ mark β cells for Fas-dependent destruction by diabetogenic CD4+ T lymphocytes *J Clin Invest* 2000;**105**:459-68.

molecular pharmaceutics

Cite This: Mol. Pharmaceutics 2019, 16, 4954−4967

Article

pubs.acs.org/molecularpharmaceutics

Scalable Self-Assembling Micellar System for Enhanced Oral Bioavailability and Efficacy of Lisofylline for Treatment of Type-I Diabetes

Kishan S. Italiya, Moumita Basak, Samrat Mazumdar, Deepak K. Sahel, Richa Shrivastava, Deepak Chitkara, and Anupama Mittal*

Department of Pharmacy, Birla Institute of Technology and Science (BITS PILANI), Pilani, Rajasthan 333031, India

Supporting Information

ABSTRACT: The study summarizes the development of an orally active nanoformulation of a potent but one of the least explored molecules, lisofylline (LSF), in type 1 diabetes (T1D). LSF undergoes rapid metabolism, resulting in poor oral bioavailability and short half-life. In this work, to improve its pharmacokinetic (PK) properties, LSF was encapsulated in the form of its ester prodrug [LSF−linoleic acid (LA) prodrug] into biodegradable self-assembling polymeric micelles [LSF−LA PLM, size: 149.3 nm; polydispersity index: 0.209; critical micelle concentration (cmc); 5.95 μg/mL and N_{agg}: 14.82 at 10 cmc] of methoxypoly(ethylene glycol)-*b*-poly(carbonate-*co*-L-lactide) (mPEG-*b*-P(CB-*co*-LA)) block copolymer. LSF−LA PLM was found to be equally effective as the LSF−LA prodrug in cell culture studies in insulin-secreting MIN6 cells and showed excellent stability in simulating biological fluids and plasma. PK of LSF−LA PLM (10 mg/kg dose) revealed a significant improvement in oral bioavailability of LSF (74.86%; 3.3-fold increase in comparison to free LSF) and drastic reduction in the drug metabolism. Further, LSF−LA PLM showed a significant reduction in fasting glucose levels and increase in insulin levels by intraperitoneal as well oral routes in a streptozotocin (STZ)-induced T1D rat model. Production of inflammatory cytokines (TNF-α and IFN-γ) and different biochemical markers for liver and kidney functions were much reduced in diabetic animals after treatment with LSF−LA PLM. LSF−LA PLM-treated pancreatic sections showed minimal infiltration of CD4+ and CD8+ T-cells as indicated by hematoxylin/eosin staining and immunohistochemical analysis.

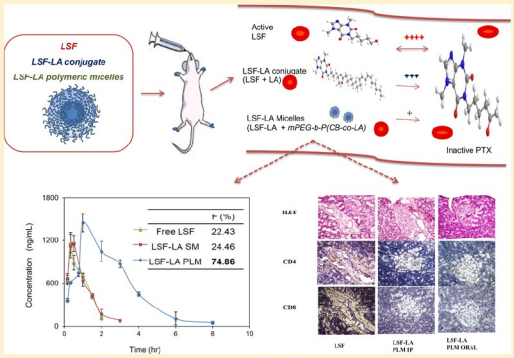

KEYWORDS: *lisofylline prodrug, self-assembly, scale up, type 1 diabetes, mPEG-b-P(CB-co-LA), oral delivery*

1. INTRODUCTION

Type 1 diabetes (T1D) is an inflammatory autoimmune disorder, caused by both specific and nonspecific inflammation induced by cytokines and cellular activation. Suppression of the inflammatory as well as autoimmune responses is crucial to any approach to treat T1D.[1,2] Lisofylline (LSF) is one such potent anti-inflammatory agent which suppresses the activation and proliferation of proinflammatory cytokines, resulting in hypoglycemic effect in T1D.[3] LSF improves insulin secretory function in isolated rat islets;[4] reduces inflammatory cytokine release in response to cancer[5,6] and hyperoxia-induced lung injury;[7,8] inhibits interleukin 12 (IL-12) signaling and IL-12 mediated Th1-type T cell differentiation in T1D;[9,10] prevents the development of autoimmune allergic encephalomyelitis in mouse models;[11] and reduces transforming growth factor β release from bone marrow cells in diabetic nephropathy.[12] In addition, LSF can maintain adenosine triphosphate levels, normalize the mitochondrial membrane potential, and block apoptosis induced by inflammatory cytokines.[13] It can block formation of lipid peroxide and generation of reactive oxygen species because of its antioxidant and free radical scavenging properties.[14] In spite of its multiple therapeutic benefits, delivery of LSF is a major challenge owing to its high solubility, low encapsulation efficiency in any delivery system, quick metabolism, and rapid clearance resulting in poor oral bioavailability. In humans, the oral bioavailability of LSF is reported to be 5.9%, whereas, in mice, it is merely 16%.[15,16]

It undergoes rapid interconversion into pentoxifylline (PTX), necessitating a high dose and frequent dosing for its therapeutic action.[16] Nadler et al. have reported the antidiabetic potential of LSF in streptozotocin (STZ)-induced diabetic models at a dose of 25 mg/kg, intraperitoneally (ip), twice daily.[4] Similarly, Yang et al. reported the role of LSF in diabetes prevention in multiple low-dose STZ-induced mice models at a dose of 25 mg/kg, ip, twice daily for 14 consecutive days.[17] Combination delivery of LSF and β-cell growth factor, exendin-4 has been explored for reversal of autoimmune diabetes in NOD mice, wherein LSF

Received: August 3, 2019
Revised: October 21, 2019
Accepted: October 24, 2019
Published: October 24, 2019

DOI: 10.1021/acs.molpharmaceut.9b00833
Mol. Pharmaceutics 2019, 16, 4954−4967

was administered at 27 mg/kg/day by s.c. route using osmotic mini pump for 28 days.[18] In clinical trials of LSF in T1D, LSF has been administered at a single dose of 9 mg/kg by continuous intravenous (iv) infusion or at 12 mg/kg by continuous subcutaneous infusion over a 10 h period.[19] Apart from T1D, in other ongoing clinical trials of LSF for treatment of allogeneic bone marrow transplants,[20] acute lung injury, and acute respiratory distress syndrome, the drug is administered at a dose of 3 mg/kg with a maximum of 300 mg iv every 6 h.[21] These studies and reports bring forth the immense therapeutic potential of LSF but also illustrate a difficult and patient noncompliant dosage regimen of LSF attributed to its short half-life (0.75−1.17 h after iv infusions in humans at doses of 1−3 mg/kg) and rapid clearance. Thus, orally active formulation of the drug if available could provide a major relief to several patients of autoimmune and inflammatory diseases.

In literature, very few attempts have been made to overcome the problems associated with LSF. One of first attempts was to synthesize its analogues, wherein, 32 LSF analogues were synthesized by varying the xanthine core substructure of LSF. Among these, only two lead compounds were identified as active as these protected β-cells from cytokine-induced injury and maintained insulin secretory capability in in vitro studies in INS-1 cells; however, no further progress/in vivo studies on these active analogues have been reported.[22] Our group designed and reported hydrophobic prodrugs of LSF by chemically coupling fatty acids like linoleic acid (LA) to the drug molecule LSF. This LSF−LA prodrug self-assembled into micelles (LSF−LA SM), which showed a drastic improvement in the physicochemical properties as well as the pharmacokinetic (PK) profile of LSF along with a significant decrease in conversion rate to the inactive metabolite, PTX, as compared to the free drug.[23] In addition to this, the prodrug exhibited improved efficacy in animal models of T1D at a reduced dose (15 mg/kg, once daily) in comparison to the free drug at 25 mg/kg, twice daily. Nevertheless, LSF−LA SM failed to exhibit oral bioavailability because of easily cleavable ester linkage between LSF and LA, which undergoes rapid cleavage in GIT before it reaches the systemic circulation. As an alternate to this, to enhance the oral bioavailability of LSF and to decrease its interconversion into PTX, we developed its polymeric micellar formulation, which could protect the LSF−LA ester linkage from degradation in the GIT environment and provide sustained release of LSF.

In light of the abovementioned facts, in the present work, our objective was to develop an orally active polymeric nanoformulation of LSF−LA prodrug and reduce interconversion of LSF to PTX. The LSF−LA prodrug was encapsulated into micelles of an in-house synthesized amphiphilic polymer methoxypoly(ethylene glycol)-*b*-poly(carbonate-*co*-D,L-lactide) block copolymer (mPEG-*b*-P(CB-*co*-LA)) and formulation batches were scaled up. The polymeric micelles of LSF−LA were tested for their stability and ability to release free LSF in plasma and further evaluated in cell culture studies in rat insulinoma cells, MIN-6 for their cytotoxicity, β-cell protective effect, and insulin secretory ability under inflammatory conditions, PBMCs proliferation, and cellular uptake. This formulation exhibited a drastic improvement in the oral PK profile of LSF along with a significant decrease in its conversion to the inactive metabolite, PTX, as compared to the free drug, resulting in significantly improved oral bioavailability (oral bioavailability of free LSF vs LSF−LA SM vs LSF−LA mPEG-*b*-P(CB-*co*-LA) micelles (LSF−LA PLM) was found to be 22.43, 24.46, and 74.86%, respectively, in rats). Apart from improvement in the oral PK profile, LSF−LA PLM formulation by oral route also demonstrated therapeutic efficacy equivalent to that administered by parenteral route (ip) in STZ-induced T1D rat models, which was further supported by a study of various biochemical parameters and confirmed by histopathological and immunohistochemical (IHC) analysis of rat pancreatic tissues.

2. MATERIALS AND METHODS

2.1. Materials, Reagents, and Experimental Animals. LSF [purity ≥ 99%, high-performance liquid chromatography (HPLC)] was purchased from Cayman Chemicals Inc. (Michigan, USA). LA (purity ≥ 99%, HPLC) was obtained from Hi-Media Laboratories (Mumbai, India). Streptozotocin (STZ), 3-isobutyl-1-methylxanthine (IBMX; ≥99%, HPLC; internal standard), 3-[4,5-dimethylthiazol-2-yl]-2,5-diphenyltetrazolium bromide (MTT), D-glucose, stannous 2-ethylhexanoate ($Sn(Oct)_2$), 2,2-methoxy poly(ethylene glycol) (mPEG, M_n 5000), and DL-lactide purchased from Sigma-Aldrich (St. Louis, MO). Dulbecco's modified Eagle medium, fetal bovine serum (FBS), and TrypLE were obtained from Invitrogen (USA); bovine serum albumin (BSA), dimethyl sulfoxide (Molecular Biology Grade), and phosphate buffered saline (PBS), pH 7.4, were purchased from Hi-Media Laboratories. ELISA kits for TNF-α and IFN-γ (ELISA MAX) were obtained from BioLegend (USA). Recombinant TNF-α, IL-1β, and IFN-γ were obtained from Invitrogen (MD, USA). Carboxyfluorescein succinimidyl ester (CFSE) staining assay kit (CellTrace), Ficoll-Paque, and phytohaemagglutinin (PHA) were obtained from Thermo Fisher (USA). Accucheck Active Glucometer was purchased from Roche Diabetes Care India Pvt. Ltd. (Mumbai, India). All the kits for determination of biochemical parameters were purchased from Coral Clinical Systems (India). MIN-6 cell line was procured from NCCS, Pune (India). Wistar rats (male; 8−10 weeks, 200−220 g) were procured from Central Animal Facility, BITS-Pilani (Pilani, India). All animal experiments were performed as per CPCSEA guidelines and according to protocols approved by the Institutional Animal Ethics committee (IAEC) (animal testing protocol no. IAEC/RES/23/26; Central Animal Facility (CAF), BITS-Pilani). All other chemicals and reagents were of analytical grade and used as obtained. Antibodies used in immunohistochemistry including CD4 Rabbit mAb (cat no. 25229); signal stain IHC boost reagent (antirabbit; cat no. 8114), and antimouse IgG (H + L) antibody (cat no. 7076) were purchased form Cell Signaling Technologies and CD8a Mouse mAb (OX-8 Cat no. 550298) was procured from BD Pharmingen.

2.1.1. LSF−LA Prodrug and LSF−LA SM. The LSF−LA prodrug was synthesized in-house by carbodiimide coupling reaction as reported earlier.[24] The product was successfully purified by flash chromatography and characterized for its structure, molecular weight, purity, and self-assembly into micelles (LSF−LA SM) of size 156.9 nm with a narrow polydispersity index (PDI) of 0.187.

2.2. Synthesis and Characterization of mPEG-Poly(carbonate-*co*-lactide) [mPEG-*b*-P(CB-*co*-LA)]. To improve the delivery, PK, and stability of the LSF−LA prodrug in comparison to free LSF and LSF−LA SM, amphiphilic polymer with carbonate blocks (5-methyl-5-benzyloxycarbonyl-1,3-dioxane-2-one; MBC) was synthesized as reported earlier by our group with modification in the preparation method. Instead of the previously reported method (130 °C for 24 h), a microwave synthesizer (Monowave 300; Anton Paar GmbH, Austria) was employed to facilitate the polymerization reaction

DOI: 10.1021/acs.molpharmaceut.9b00833
Mol. Pharmaceutics 2019, 16, 4954−4967

and the reaction time was reduced from 24 h to 45 min along with improved yield of polymer.

For synthesis of $mPEG_{114}$-*b*-P(CB_{25}-*co*-LA_{50}), first, the MBC monomer was synthesized and purified as reported earlier[25,26] followed by ring-opening polymerization reaction of mPEG, DL-lactide, and MBC using stannous 2-ethylhexanoate (10 mol % relative to mPEG) as a catalyst at 130 °C for 45 min in a microwave synthesizer. The copolymer so obtained was dissolved in chloroform and purified using cold isopropyl alcohol (twice) and diethyl ether (once). Characterization of the synthesized polymer was done using ^{1}H NMR and gel permeation chromatography (GPC) to obtain number-average molecular weight and the units of lactic acid and MBC attached in the final polymer.

2.2.1. Critical Micelle Concentration. Critical micelle concentration (cmc) determination was carried out to ascertain the self-assembling nature of the polymer mPEG-*b*-P(CB-*co*-LA) using pyrene as a fluorescent extrinsic probe. mPEG-*b*-P(CB-*co*-LA) at various dilutions (5.0×10^{-5} to 1.0 mg/mL) was mixed with pyrene (6×10^{-7} M) in different test tubes and incubated at room temperature (RT) for 48 h to ensure the solubilization of pyrene in the aqueous phase. The emission spectra of the solution were recorded from 320 to 450 nm and emission wavelength of 390 nm. A plot was constructed between I_3/I_1 ratio versus logarithm of mPEG-*b*-P(CB-*co*-LA) concentration, wherein the I_3 and I_1 values were determined from the peak intensities at the wavelengths of 337 and 333 nm. The cmc value of mPEG-*b*-P(CB-*co*-LA) was determined from the intersection of the best-fit lines.

2.2.2. Aggregation Number (N_{agg}) Determination. The Stern−Volmer equation (eq 1) was employed to determine the aggregation number of the LSF−LA PLM[27,28]

$$\ln\left(\frac{F_0}{F_Q}\right) = \frac{Q \times N_{agg}}{(C - \text{cmc})} \tag{1}$$

where F_0 and F_Q are intensities of the probe without and with a quencher, Q is the total quencher concentration, C is the total surfactant concentration, and N_{agg} refers to the mean aggregation number.

The steady-state fluorescence quenching method was used to determine the mean aggregation number in polymeric micelles by using a fluorescence spectrophotometer (Shimadzu RF-5301). Pyrene and cetylpyridinium chloride (CPC) were used as probe and quencher, respectively. For fluorescence measurements, stock solutions of pyrene (2×10^{-6} M) in PLM at 10 times the cmc value and pyrene + CPC (2.8×10^{-2} M) in PLM micellar solution at 10 times the cmc value were prepared. Appropriate volumes of these two solutions were then mixed to vary the CPC concentration from 0 to 1.54×10^{-3} M. By exciting the samples at 318 nm, emission spectra of pyrene were obtained and the emission was measured in the range of 320−450 nm. The emission peak at 376 nm was considered for calculating the micellar aggregation number.

2.3. Formulation Development, Scale Up, and Characterization of the LSF−LA Prodrug-Loaded PLM. LSF−LA PLM was prepared by the thin-film hydration method. Dichloromethane solution of the LSF−LA prodrug (20 mg) and polymer (180 mg) was transferred into a round bottom flask; the thin film was prepared by solvent evaporation under vacuum, followed by reconstitution of the film with water with stirring for 30 min. The resulting micellar formulation was sonicated for 1 min under cold conditions and characterized for size, zeta potential, encapsulation, and loading efficiency. Blank PLM (BLK) formulation was also prepared by a similar method without the LSF−LA prodrug.

2.3.1. Scale-Up of the LSF−LA PLM Formulation. Scale-up studies of LSF−LA PLM were carried out in three different batch sizes of 0.5, 2, and 4 gm. All the batches were prepared using the initially optimized conditions with minor changes in film preparation and reconstitution time. For scale-up batches of the formulation, thin films were prepared in 500 mL round bottom flasks and dried overnight. These films were reconstituted with water aided by bath sonication for 2 min followed by stirring for 1 h. Theoretical drug loading (DL) was increased up to 12.5% w/w.

2.3.2. Particle Size, Zeta Potential, and Morphology Determination. The measurement was performed using a Zetasizer Nano-ZS (Malvern Instrument Ltd., UK) with a helium laser at 633 nm and the scattering angle was fixed at 173°. The morphology of the developed formulation was studied using high-resolution transmission electron microscopy (HR-TEM; JEM 2100, Jeol Ltd., Japan).

2.3.3. DL and Entrapment Efficiency. DL and entrapment efficiency (EE) of the LSF−LA prodrug in LSF−LA PLM was estimated using a previously reported HPLC-PDA method.[29] For DL calculation, the formulation was lyophilized and drug content was analyzed by HPLC. Practical DL (eq 2) and EE were calculated using following formulae (eq 3)

$$\text{Drug loading (\% DL)} = \frac{W_0}{W_t} \times 100 \tag{2}$$

$$\text{Encapsulation efficiency (\% EE)} = \frac{W_0}{W_1} \times 100 \tag{3}$$

where W_0 is the weight of the drug entrapped in micelles, W_t is the weight of lyophilized micelles, and W_1 is the amount of drug initially added in the system.

2.4. Lyophilization of LSF−LA PLM Formulations. PEG 2000 was selected as the lyoprotectant and dissolved in freshly prepared LSF−LA PLM formulation to obtain a concentration of 5% w/v of lyoprotectant and loaded into a bench top lyophilizer (FreeZone Triad Freeze Dry System (Labconco, USA)). The lyophilization cycle was carried out in three sequential steps, namely, freezing, primary drying, and secondary drying for a total duration of 56 h (Table 1). During the lyophilization process, the temperature of the product was monitored using active vials probed with thermocouples.

2.5. Stability of the LSF−LA PLM Formulation. *2.5.1. In Simulated Biological Fluids.* The stability of drugs/dosage forms in simulated biological fluids indicates the likelihood of oral bioavailability. The stability of different formulations (LSF−LA PLM and LSF−LA SM) was determined in simulated gastric fluid (SGF, pH 1.2), simulated intestinal fluid (SIF, pH 6.8), and PBS (pH 7.4). SGF and SIF without enzymes were prepared as per USP. A stock solution of LSF−LA SM/LSF−LA PLM (500 μg/mL) was added to the SGF, SIF, and PBS ($n = 3$) separately and incubated at 37 °C and 100 rpm in a shaking water bath. An aliquot of the sample (200 μL; without replacement of media) was collected at each time point (0, 10, 20, 30, 45, 60, 90, and 120 min for SGF; 0, 10, 20, 30, 45, 60, 90, 120, 180, and 240 min for SIF and 0, 10, 20, 30, 45 min, 1, 2, 4, 6, 8,12, and 24 h for PBS) followed by quenching of the sample with ice cold acetonitrile (800 μL), vortexing, and centrifugation; then, the supernatant was collected and the LSF−LA

DOI: 10.1021/acs.molpharmaceut.9b00833
Mol. Pharmaceutics 2019, 16, 4954−4967

Table 1. Lyophilization Cycles Used in the Lyophilization Process of LSF−LA PLM

segment/step	temperature (°C)	hold time (h)	RAMP (°C/min)
Thermal Treatment: Freezing (Vacuum: OFF)			
1	10	0.5	5
2	0	2.0	2
3	−10	1.0	1
4	−30	3.0	1
5	−55	10.0	0.25
Primary Drying (Vacuum: 200 mTorr)			
1	−55	6.0	0.25
2	−20	6.0	0.25
3	−10	5.0	0.25
4	4	5.0	0.25
5	20	5.0	0.25
Secondary Drying (Vacuum: 100 mTorr)			
1	25	12	0.25

prodrug in the samples was analyzed by HPLC. The graph between % LSF−LA remaining intact in the medium and time was plotted considering LSF−LA at the initial time point (0 min) as 100%.

2.5.2. At Different Storage Temperatures. The Stability of LSF−LA PLM in water was assessed at two different storage temperatures: (a) at RT (25 °C) and, (b) at 4 °C for a period of 30 days by determining the particle size and PDI of the LSF−LA PLM at a time interval of 3 days up to 30 days.

2.6. Ex Vivo Release Study of LSF−LA PLM in Rat Plasma. The objective of this study was to determine the rate of release of LSF−LA from LSF−LA PLM followed by its hydrolysis in plasma by cleavage of the ester bond to release free LSF. Plasma was separated from fresh blood collected from male wistar rats. For this study, LSF−LA PLM (10 mg) containing the LSF−LA prodrug (∼1 mg equivalent of LSF) was spiked into fresh rat plasma and incubated in a shaker at 37 °C for 72 h. An aliquot of plasma (200 μL; without replacement of media) was withdrawn at different time intervals, 5 and 15 min, 1, 2, 4, 6, 12, 24, 36, 48, 60, and 72 h into 5 mL glass tubes, followed by the addition of 50 μL of internal standard (IBMX, 2 μg/mL) solution. Samples were mixed by vortexing for 1 min followed by addition of 2 mL of methylene chloride as extracting solvent. The samples were vortexed for 5 min and centrifuged at 3500 rpm for 15 min at 4 °C. The lower organic layer was collected and evaporated. The residue was reconstituted with 100 μL of mobile phase (methanol/water: 1:1) and vortexed for 30 s. For quantitation of LSF, 80 μL of this sample was injected into HPLC.

2.7. Cell Culture-Based Studies for LSF−LA PLM. To evaluate the efficacy of the LSF−LA PLM prodrug in hyperglycemic/diabetic conditions, mouse insulinoma cells, MIN-6, were used. The cells were grown in RPMI media supplemented with 10% FBS and 1% antibiotic solution and grown at 37 °C in a humidified atmosphere containing 5% CO_2.

2.7.1. Inflammation-Mediated β-Cell Death and Decrease in Insulin Secretion. MIN6 cells (5×10^3/well) were allowed to attach for 24 h in 96-well cell culture plates. To mimic the in vivo inflammatory conditions as seen in diabetes, MIN6 cells were treated with recombinant proinflammatory cytokines, TNF-α (10 ng/mL), IL-1β (5 ng/mL), and IFN-γ (100 ng/mL); the concentrations of cytokines were selected to mimic the pathological levels of cytokines as observed during the development of diabetes. Simultaneously, cells were also treated with LSF−LA PLM and controls (free LSF, LA, LSF−LA SM, BLK) at ∼20 μM in the presence of cytokines. After 48 h of treatment period, MTT assay was performed to evaluate cytotoxicity and absorbance was recorded at 560 and 630 nm. Untreated cells and cells treated with free LSF, free LA, LSF−LA SM formulation (all at equivalent concentrations) and blank PLM (BLK) were kept as controls. The cell viability was calculated by comparison with untreated cells by the following equation (eq 4).

$$\text{Cell viability (\%)} = (\text{absorbance of test sample}/\text{absorbance of control}) \times 100 \quad (4)$$

Cytotoxicity assay for all treatment groups (at ∼20 μM) is also performed in MIN6 cells without cytokines to check the toxicity of the formulation in the absence of inflammatory conditions. Thereafter, the cells were evaluated for their insulin production ability using a static incubation method, wherein MIN6 cells were sequentially incubated in the media containing basal (3.33 mM) and stimulatory glucose (33.33 mM) levels at 37 °C for 1 h each. Supernatants were collected and analyzed for insulin release using the commercially available ELISA kit (Crystal Chem, USA).

2.7.2. PBMC Proliferation and Activation. PBMCs (freshly isolated from mice blood using the Ficoll Paque density gradient method) were stained with CFSC (5 μM) using the manufacturer's protocol. CFSC-stained PBMCs were further activated using PHA (3 μg/mL, mitogen activator) followed by treatment with LSF−LA PLM (∼20 μM) and controls-free LSF, LA, LSF−LA SM (all at ∼20 μM), and BLK. After 96 h of incubation, PBMC proliferation was evaluated by flow cytometry with a 488 nm excitation laser. The extent of cell activation was also studied by measuring the level of inflammatory cytokines (IFN-γ and TNF-α) in the culture supernatants after 48 h using ELISA kits (ELISA MAX, BioLegend, USA).

2.7.3. Cellular Uptake of LSF−LA PLM. MIN6 cells were incubated with LSF−LA PLM and LSF−LA SM (∼20 μM to LSF) for 6 h keeping LSF (20 μM) and untreated cells as controls. After 6 h of incubation, LSF−LA and free LSF were quantified in culture supernatants using a previously reported HPLC method.[29]

2.8. PKs of Free LSF, LSF−LA SM, and LSF−LA PLM. The PK studies of LSF, LSF−LA SM, and LSF−LA PLM were performed on Wistar rats (200−220 g). LSF (solution in water), LSF−LA SM, and LSF−LA PLM were administered orally at the dose of 10 mg/kg (∼LSF) with maximum dosing volume of 1 mL to each rat with overnight fasting (n = 4). For oral bioavailability determination of LSF in comparison to LSF−LA, these were also administered iv at 10 mg/kg dose. After dosing, blood samples were collected at each preset time point of 10, 20, 30 min, 1, 1.5, 2, 3, 4, 6, 8, 12, and 24 h. Plasma concentration−time profiles of LSF released from LSF−LA SM and LSF−LA PLM were plotted and analyzed by the noncompartmental model approach using Phoenix 2.1 WinNonlin (Pharsight Corporation, USA) to determine various PK parameters. In vivo LSF shows interconversion into PTX by oxidation−reduction reaction. LSF−PTX interconversion is a major hurdle in effectiveness of LSF therapy. Hence, PTX plasma concentration−time profiles were also generated in all the PK studies of LSF and its formulations to understand the rate and extent of interconversion of LSF to PTX.

DOI: 10.1021/acs.molpharmaceut.9b00833
Mol. Pharmaceutics 2019, 16, 4954−4967

2.9. In Vivo Efficacy Studies in the T1D Model. Diabetes was induced in male wistar rats weighing 180−220 g. The animals were maintained under standard environmental conditions and provided with feed and water ad libitum. Initially, for 1 week (prior to the experimentation), all the animals were fed on normal pellet diet. The animals were injected with a single high dose of STZ (45 mg/kg, ip) dissolved in sodium citrate buffer (0.01 M, pH 4.5), whereas the respective control rats received the vehicle citrate buffer (pH 4.5) only. After 72 h of STZ injection, fasting glucose levels were measured. The animals showing plasma glucose levels >250 mg/dL were considered diabetic. Thereafter, glucose and insulin levels of the experimental animals were checked throughout the study by the tail bleeding method.

2.9.1. Experimental Design. The animals were randomly divided into eight different groups as shown in Table 2.

Table 2. Experimental Groups for Efficacy Studies in the STZ-Induced T1D Model

s. no.	experimental groups
1	normal control (NC)
2	diabetic control (DC)
3	PLM blank formulation (BLK)
4	free lisofylline (LSF)
5	free linoleic acid (LA)
6	LSF−LA SM via ip route (LSF−LA SM ip)
7	LSF−LA PLM via ip route
8	LSF−LA PLM via oral route

Treatment was started on the third day after confirming the diabetic conditions. For treatment, LSF and LA (in 0.5 % w/v tween 80) were administered as solutions prepared in water for injection at a dose of 15 mg/kg, once daily. LSF−LA SM ip (by intraperitoneal route), LSF−LA PLM ip (by intraperitoneal route), and LSF−LA PLM ORAL (by oral route) were given at a dose equivalent to 15 mg/kg of LSF (~30 mg/kg of LSF−LA) once daily. Treatment was continued for 3 weeks and fasting glucose levels were measured twice weekly by the tail bleeding method using an AccuChek active glucometer. After 3 weeks, the levels of insulin and inflammatory cytokines, TNF-α, and IFN-γ were measured in serum using commercially available ELISA kits.

2.9.2. Evaluation of Blood and Serum Biochemical Parameters. In diabetes, there are significant changes in serum protein and lipid profile as well as liver and kidney functions before and after treatment with hypoglycemic agents. To assess the effect of LSF−LA PLM on lipid and protein profile of the animals, serum protein, cholesterol, and triglyceride levels were measured. For liver and kidney function, SGPT, SGOT, serum urea, uric acid were also measured. All biochemical parameters were measured after 3 weeks of study period using commercially available kits (Coral Diagnostics, India).

2.9.3. Histopathology and IHC Analysis. After 3 weeks of treatment, the animals were euthanized and pancreata were isolated and fixed in 4% paraformaldehyde solution. Tissues were then processed for paraffin embedding, subsequent serial sectioning, and staining with hematoxylin/eosin (H&E) to allow the assessment of pancreatic islet morphology in the studied groups. IHC analysis was also performed in pancreas for expression of CD4+ and CD8+ T-cells as per the standard

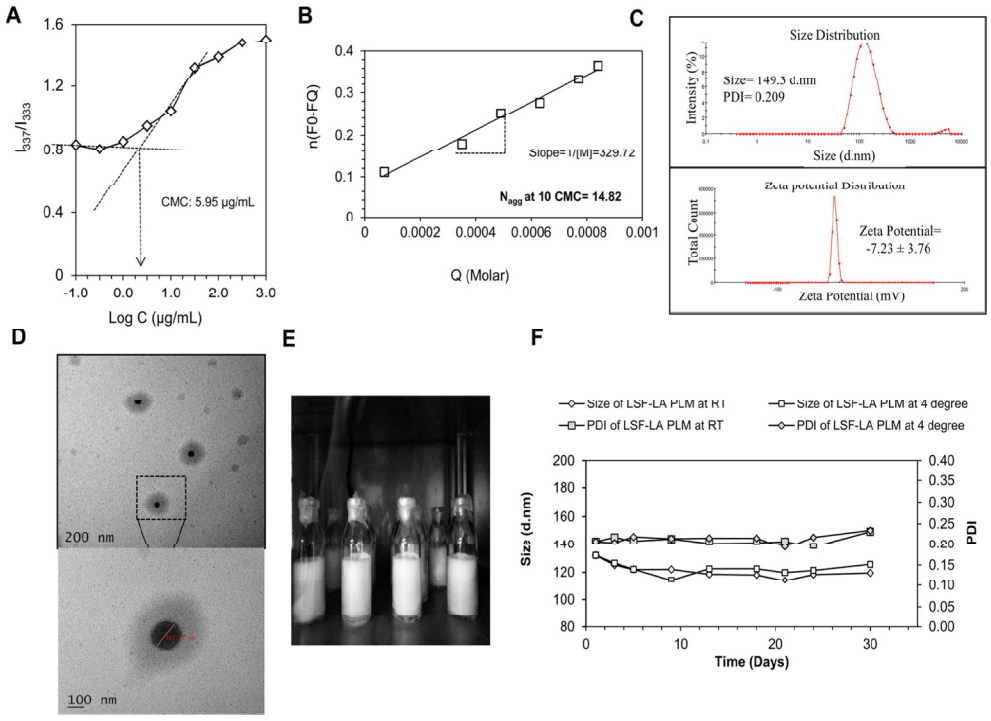

Figure 1. Characterization of blank and LSF−LA-loaded mPEG-*b*-P(CB-*co*-LA) micelles (PLM) (A) cmc of PLM determined by fluorescence spectroscopy using pyrene as a fluorescent probe (cmc: 5.95 μg/mL); (B) micellar aggregation number of PLM at 10× cmc value determined by pyrene as a fluorescent probe and CPC as a quencher (N_{agg}: 14.82); (C) particle size and zeta potential distribution of LSF−LA PLM; (D) particle size morphology of LSF−LA PLM by HR-TEM analysis; (E) intact and fluffy cake of lyophilized LSF−LA PLM using trehalose (5% w/v) as the lyoprotectant; and (F) LSF−LA PLM stability at RT and 4 °C for 30 days: particle size and PDI analysis.

DOI: 10.1021/acs.molpharmaceut.9b00833
Mol. Pharmaceutics 2019, 16, 4954−4967

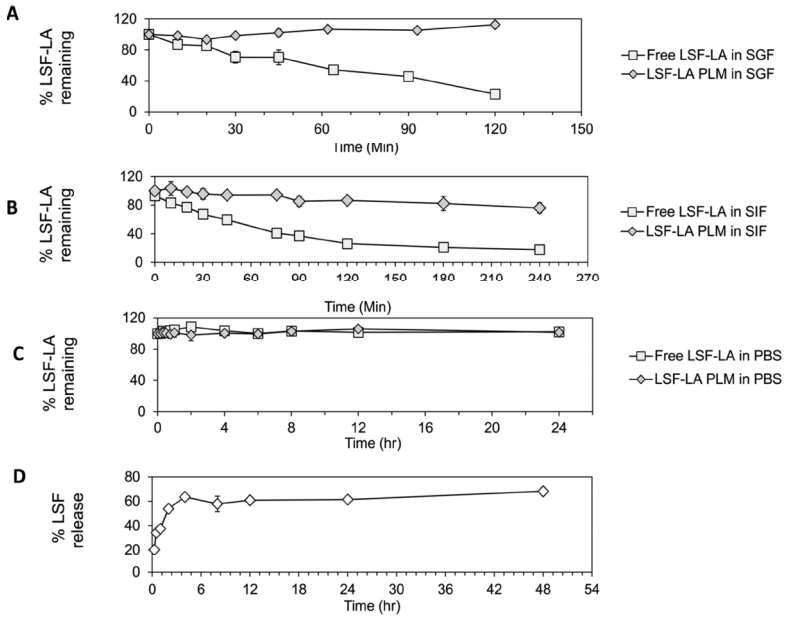

Figure 2. Stability of LSF–LA PLM in comparison to the free LSF–LA prodrug in different simulating biological fluids: (A) SGF (pH 1.2); (B) SIF (pH 6.8); (C) PBS (pH 7.4) and, (D) ex vivo release of LSF from LSF–LA PLM in rat plasma.

protocol. After immunostaining, the sections were lightly counterstained with hematoxylin and observed under a light microscope. Primary antibodies, CD4 Rabbit mAb, and CD8a Mouse mAb were optimized at dilutions of 1:400 and 1:20, respectively. Signal stain IHC boost reagent and antimouse IgG (H + L) antibody were used as secondary antibody at a dilution of 1:1 (3–4 drops) and 1:500, respectively.

3. RESULTS

3.1. Characterization of the mPEG-*b*-P(CB-*co*-LA) Polymer. To deliver the LSF–LA prodrug, the mPEG-*b*-P(CB-*co*-LA) copolymer was synthesized and characterized using ^{1}H NMR and GPC (Figure S1). ^{1}H NMR showed the presence of 26 units of the MBC monomer and 50 units of lactic acid in the copolymer with an overall molecular weight of 15 168 Da and the molecular weight determined by GPC was found to be 15 014 Da. As shown in Figure 1A,B, synthesized polymer showed a cmc of 5.95 μg/mL and an aggregation number (N_{agg}) of 14.92 at 10 times the cmc value.

3.2. Formulation Characterization and Scale-Up. LSF–LA prodrug-loaded polymeric micelles prepared by the thin-film hydration method exhibited self-assembly, demonstrating a particle size and zeta potential of 149.3 nm (PDI: 0.209) and −7.23 + 3.76 mV, respectively (Figure 1C). The EE of LSF–LA in PLM was found to be 75 ± 4.12% with a practical DL of 9.29 ± 1.16%. Figure 1D shows the TEM image of LSF–LA PLM, confirming the spherical morphology of the micelles.

Similar parameters were also seen in scale-up batches of LSF–LA PLM with an average particle size of 145.45 ± 7.64 nm (PDI: 0.138 ± 0.07) and zeta potential value of −8.72 ± 3.69. % EE was marginally increased in scale-up batches and was determined to be 78.45 + 6.65%.

3.3. Lyophilization of LSF–LA PLM. In the present study, PEG 2000 showed an intact cake of LSF–LA PLM with a good appearance (Figure 1E). After the cake formation, when lyophilized micelles were reconstituted in water, the cake got re-dispersed immediately (within 30 s upon addition of water), and the re-dispersity index was found to be 1.16.

3.4. Stability Study of LSF–LA PLM. Stability studies of LSF–LA PLM at 4 and 25 °C (RT) revealed no significant change in size and PDI of LSF–LA PLM at both the temperatures (Figure 1F). As shown in Figure 2A–C, the LSF–LA prodrug (free) was not found to be stable in SGF and SIF (even in the absence of enzyme) and exhibited a half-life of 1.3 and 1.12 h for SGF and SIF, respectively, but was found to be stable in PBS (102.29 + 4.20% of LSF–LA was found to be intact even after 24 h). However, LSF–LA PLM showed stability in all the media, including SGF, SIF, and PBS, wherein 112.61 ± 4.26% of the LSF–LA prodrug could be detected intact in case of PLM after 2 h of incubation in SGF; 76.05 ± 7.13% after 4 h of incubation in SIF; and 101.61 ± 5.15% after 24 h in PBS. These data clearly indicated the feasibility of administering LSF–LA PLM by the oral route.

3.5. Ex Vivo Release Study of LSF–LA PLM in Rat Plasma. As shown in Figure 2D, LSF LA PLM released the LSF–LA prodrug into the plasma, which further underwent hydrolysis to release free LSF, which is then available to elicit its therapeutic effect. After 48 h of incubation in plasma, 68.17 ± 1.63% of free LSF was released from LSF–LA PLM. Mass balance studies were carried out to detect the remaining amount of unhydrolyzed LSF–LA prodrug in PLM under alkaline conditions; however, owing to the degradation of LSF under alkaline conditions, the remaining LSF could not be detected.

3.6. Cell Culture-Based Evaluation of LSF–LA PLM. The major objective of these experiments was to evaluate if the activity/potency of the LSF–LA prodrug remains intact after encapsulation into the PLM, that is, if the processes and excipients used during formulation development have affected the antidiabetic activity of the prodrug in any way.

3.6.1. Inflammation-Mediated β-Cell Death and Decrease in Insulin Secretion. It is well known that release of proinflammatory cytokines during diabetes causes death of β-cells and thus severely compromises both basal as well as postprandial insulin levels. Cytotoxicity assay of LSF–LA PLM

DOI: 10.1021/acs.molpharmaceut.9b00833
Mol. Pharmaceutics 2019, 16, 4954–4967

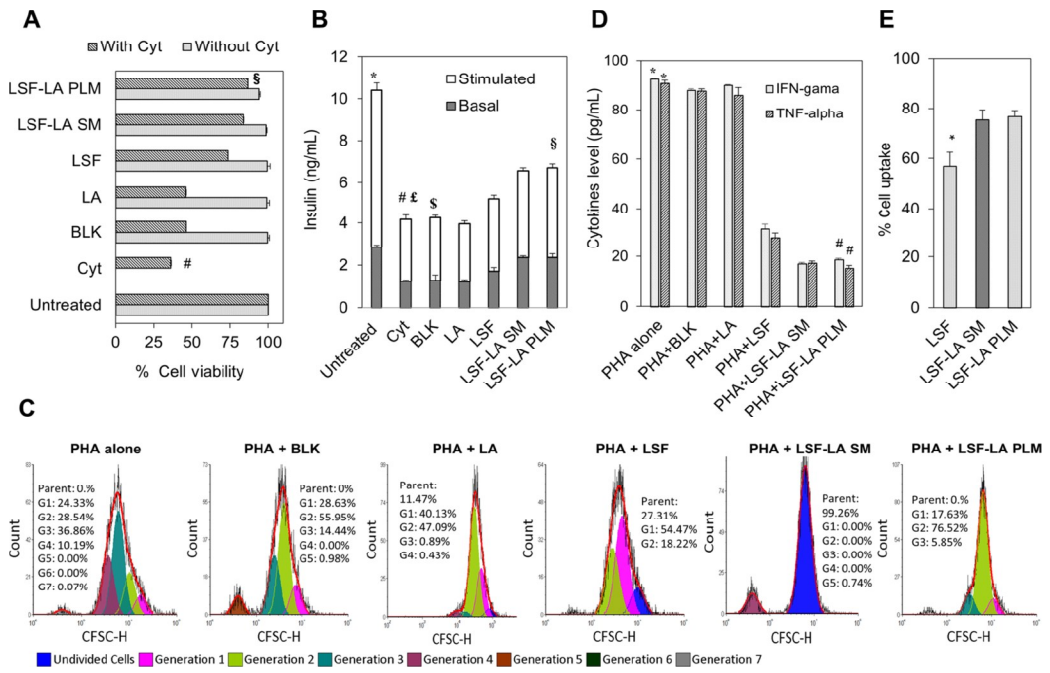

Figure 3. In vitro cell culture evaluation of LSF−LA PLM in MIN6 cells (A) cytotoxicity evaluation (MTT assay) of LSF−LA PLM (~20 μM) in the presence and absence of cytokines (TNF-α, IL-1β, and IFN-γ). $^{\#}$Cyt vs all; $^{\$}$LSF−LA PLM vs LSF and LA ($^{\#\$}P < 0.001$); (B) basal and stimulated insulin levels in MIN6 cells after inflammatory challenge following treatment with LSF, LA, LSF−LA SM, and LSF−LA PLM (~20 μM) *untreated vs all: $^{\#}$Cyt vs LSF, LSF−LA SM, and LSF−LA PLM; $^{\$}$BLK vs LSF−LA SM and LSF−LA PLM: $^{\$}$LSF−LA PLM vs LSF and LA ($^{*\#\$}P < 0.001$); (C) spontaneous proliferation of PBMCs (after stimulation with PHA) studied by CFSE staining and analyzed by FCS Express software; (D) IFN-γ and TNF-α (pg/mL) levels in the conditioned media of PBMCs stimulated with PHA. *PHA-stimulated PBMCs vs LSF and LSF−LA SM and PLM; $^{\#}$LSF−LA PLM vs LSF ($^{*\#}P < 0.001$); and (E) cell uptake study using HPLC. *LSF vs both ($^{*}P < 0.05$).

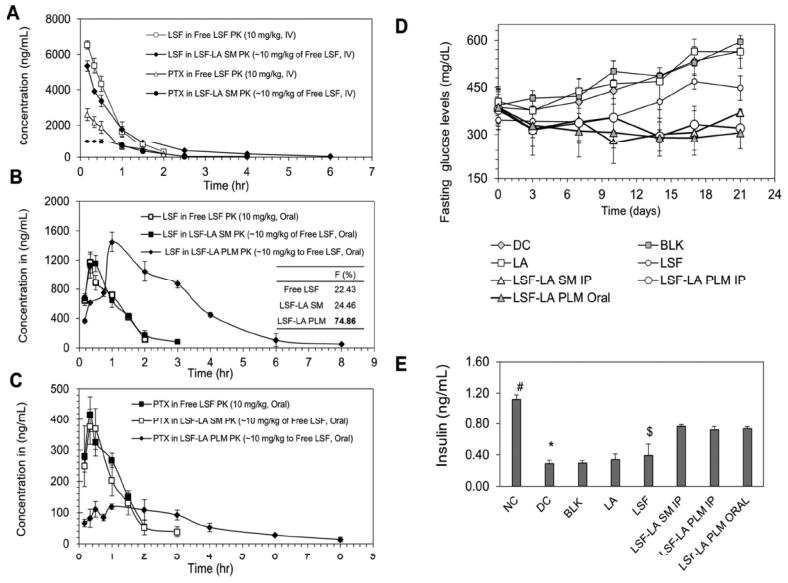

Figure 4. In vivo PK and PD studies of LSF−LA PLM: PK studies in normal rats at ~10 mg/kg dose (A) LSF and PTX plasma concentration−time profiles obtained from free LSF and LSF−LA SM after iv administration (mean ± SEM, $N = 4$); (B) LSF plasma concentration−time profiles obtained from free LSF, LSF−LA SM, and LSF−LA PLM after oral administration (mean ± SEM, $N = 4$). F: oral bioavailability; (C) PTX plasma concentration−time profiles obtained from free LSF, LSF−LA SM, and LSF−LA PLM after oral administration at ~10 mg/kg dose in rats (mean ± SEM, $N = 4$). Antidiabetic effect of LSF−LA PLM in an STZ-induced T1D model: (D,E) fasting blood glucose levels and serum insulin levels respectively in STZ-induced diabetic rats after 3 weeks of treatment with LSF−LA PLM via ip and oral route where NC, DC, BLK, LA, LSF, and LSF−LA SM ip are studied as controls. $^{\#}$NC vs all groups; *DC vs LSF−LA groups; $^{\$}$LSF vs LSF−LA groups; $^{\#*\$}P < 0.001$.

and BLK micelles revealed that these were nontoxic toward insulin-secreting pancreatic beta cells, MIN-6, in the absence of cytokines. This was also observed in the present study, wherein, in the presence of a cocktail of cytokines (TNF-α, IL-1β, and IFN-γ), cell viability was reduced to ~36.28% (Figure 3A) along with a drastic reduction in the level of insulin when compared to

DOI: 10.1021/acs.molpharmaceut.9b00833
Mol. Pharmaceutics 2019, 16, 4954−4967

Table 3. (A) Non-Compartmental PK Parameters for Free LSF and LSF−LA SM (iv) PK; (B) Noncompartmental PK Parameters for Free LSF (Oral) PK; (C) Noncompartmental PK Parameters for LSF−LA SM and LSF−LA PLM (Oral) PK

A

	free LSF; iv (mean ± SEM)		LSF−LA SM; iv (mean ± SEM)	
parameters	LSF	PTX	LSF	PTX
C_o (ng/mL)	7781.23 ± 434.35	4881.70 ± 929.97	7354.68 ± 532.15	1060.68 ± 87.73
$t_{1/2}$ (h)	0.39 ± 0.03	0.48 ± 0.04	0.96 ± 0.01	0.70 ± 0.08
AUC_{0-last} (ng·h/mL)	5289.77 ± 332.91	2510.72 ± 179.52	5680.53 ± 461.19	1438.40 ± 228.66
$AUC_{0-\infty}$ (ng·h/mL)	5450.27 ± 366.96	2632.88 ± 158.85	5794.56 ± 471.25	1492.91 ± 253.14
$AUMC_{0-last}$(ng·h/mL)	2663.41 ± 278.63	1312.27 ± 67.94	5718.25 ± 513.71	1266.88 ± 288.85
$AUMC_{0-\infty}$ (ng·h/mL)	3080.74 ± 400.24	1645.22 ± 19.99	6560.78 ± 587.14	1547.63 ± 417.61
MRT (h)	0.50 ± 0.03	0.53 ± 0.02	1.00 ± 0.01	0.85 ± 0.07

B

	free LSF; oral (mean ± SEM)	
parameters	LSF	PTX
C_{max} (ng/mL)	1138.64 ± 134.72	504.36 ± 38.44
$t_{1/2}$ (h)	0.61 ± 0.06	0.69 ± 0.07
K_e (1/h)	0.94 ± 0.06	1.04 ± 0.11
AUC_{0-last} (ng·h/mL)	1186.75 ± 70.40	491.12 ± 22.86
$AUC_{0-\infty}$ (ng·h/mL)	1321.69 ± 63.34	547.20 ± 18.29
$AUMC_{0-last}$ (ng·h/mL)	962.17 ± 35.82	379.06 ± 8.68
$AUMC_{0-\infty}$ (ng·h/mL)	1379.63 ± 27.71	549.76 ± 37.80
MRT (h)	0.81 ± 0.02	0.77 ± 0.02

C

	LSF−LA SM; oral (mean ± SEM)		LSF−LA PLM; oral (mean ± SEM)	
parameters	LSF	PTX	LSF	PTX
C_{max} (ng/mL)	1168.40 ± 89.73	409.55 ± 50.92	1449.39 ± 119.09	121.12 ± 12.30
$t_{1/2}$ (h)	0.72 ± 0.03	0.67 ± 0.09	2.09 ± 0.05	2.96 ± 0.35
K_e (1/h)	0.96 ± 0.04	1.12 ± 0.18	0.33 ± 0.01	0.24 ± 0.03
AUC_{0-last} (ng·h/mL)	1389.73 ± 111.51	406.33 ± 71.28	4252.69 ± 125.07	440.16 ± 30.75
$AUC_{0-\infty}$ (ng·h/mL)	1473.64 ± 124.12	471.32 ± 100.42	4409.34 ± 132.71	492.49 ± 28.78
$AUMC_{0-last}$ (ng·h/mL)	1273.34 ± 122.10	303.23 ± 64.17	10264.00 ± 531.25	1195.61 ± 82.78
$AUMC_{0-\infty}$ (ng·h/mL)	1614.18 ± 176.66	508.83 ± 167.07	11993.57 ± 568.57	1851.07 ± 172.48
MRT (h)	0.91 ± 0.02	0.72 ± 0.05	2.41 ± 0.07	2.72 ± 0.09

normal cells (without cytokines) (Figure 3B). However, upon treatment of the cells under inflammatory stress with free LSF, LSF−LA SM, and LSF−LA PLM (~20 μM), a sharp increase in cell viability up to 73.21, 82.63, and 86.68%, respectively, was observed. Further, the basal insulin level, which dropped to 1.12 ng/mL in the presence of cytokines, showed an increase to 1.58, 2.27, and 2.34 ng/mL in the presence of LSF, LSF−LA SM, and LSF−LA PLM, respectively. LSF−LA PLM showed a statistically significant increase in the viability of β-cells and insulin levels in comparison to free LSF but similar to that of LSF−LA SM, indicating a similar in vitro therapeutic efficacy of LSF−LA after formulating into PLM.

3.6.2. PBMC Proliferation and Activation. The presence of LSF and LSF−LA SM/PLM in the growth medium (RPMI 1640) of PBMCs caused a significant reduction in the proliferation of PBMCs even in the presence of a mitogen stimulator (Figure 3C), which otherwise exhibited spontaneous proliferation for up to seven generations in the presence of PHA alone. Levels of inflammatory cytokines, IFN-γ and TNF-α were also determined in the conditioned media of PBMCs under stimulation with PHA. As shown in Figure 3D, LA and BLK treated cells did not exhibit any significant difference in IFN-γ and TNF-α level as compared to PHA only stimulated cells. However, LSF−LA SM and LSF−LA PLM treatment revealed a significant reduction in the levels of cytokines in PHA stimulated cultures ($P < 0.001$) signifying retention of therapeutic efficacy of LSF during/after formulation development and also the ability of LSF−LA PLM to impair the activation of adaptive immune system in T1D.

3.6.3. Cellular Uptake Studies for LSF−LA PLM. LSF−LA PLM revealed a significantly higher uptake into the cells (76.78 ± 2.46%) after incubation for 6 h in comparison to the free LSF group (56.86 ± 9.26%) but not statistically significant from LSF−LA SM (75.48 ± 4.01%) (Figure 3E).

3.7. PK Studies. Interconversion of LSF to PTX was confirmed when PTX was found in the plasma upon iv administration of LSF or its formulations (Figure 4A). As shown in Table 3, LSF−LA PLM significantly improved the oral PK parameters of LSF. Upon oral administration, LSF−LA PLM showed a half-life of 2.08 + 0.05 h, which was 3.4-fold higher than that of free LSF (0.61 ± 0.06 h). Thus, LSF−LA PLM increased the MRT of LSF (from 0.81 to 2.41 h). Further, AUC_{0-t} for LSF−LA PLM was found to be 4252.69 ng·h/mL, which is three times higher than AUC_{0-t} observed in LSF−LA SM (1389.33 ng·h/mL) after oral administration. Interestingly, whereas LSF−LA SM exhibited a low oral bioavailability of 24.46%, it got significantly improved to 74.86% upon administration of LSF−LA PLM (Figure 4B). This hinted at the possibility of designing an orally viable system for delivery of LSF, which otherwise has a negligible oral bioavailability.

DOI: 10.1021/acs.molpharmaceut.9b00833
Mol. Pharmaceutics 2019, 16, 4954−4967

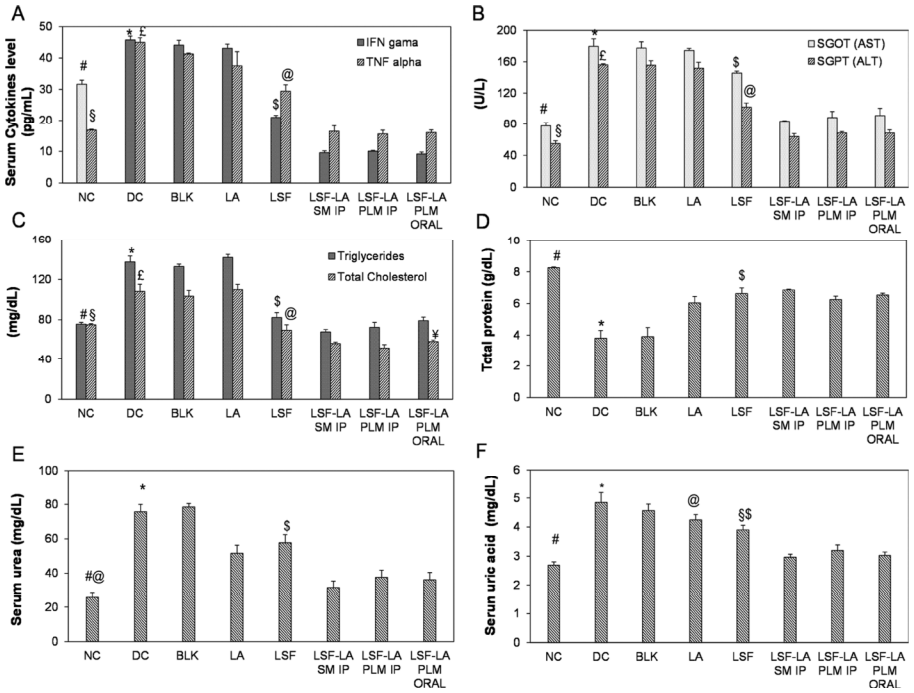

Figure 5. Effect of LSF−LA PLM on different biochemical parameters in the STZ-induced T1D model after 21 days of treatment (A) serum cytokines levels (IFN-γ and TNF-α), $^{\#}$NC vs all groups for IFN-γ and $^{\$}$NC vs DC, BLK, LA, LSF for TNF-α; $^{*£}$DC vs LSF, LSF−LA groups; $^{\$@}$LSF vs LSF−LA groups; $^{\#*\$\$£@}P < 0.001$, (B) SGOT (AST) and SGPT (ALT), $^{\#\$}$NC vs DC, BLK, LA, LSF; $^{*£}$DC vs LSF, LSF−LA groups; $^{\$@}$LSF vs LSF−LA groups; $^{\#*\$\$£@}P < 0.001$ (C) triglycerides and total cholesterol, $^{\#}$NC vs DC, BLK, LA for triglycerides and $^{\$}$NC vs DC, BLK, LA, LSF−LA groups for total cholesterol; $^{*£}$DC vs LSF, LSF−LA groups; $^{\$@}$LSF vs LSF−LA SM ip and SM PLM ip; $^{¥}$LSF−LA PLM oral vs LSF; $^{\#*\$\$£@}P < 0.001$, $^{¥}P < 0.05$ (D) total protein, $^{\#}$NC vs all groups; *DC vs LSF, LA, LSF−LA groups; $^{\$}$LSF vs BLK, LA; $^{\#*\$}P < 0.001$ (E) serum urea, $^{\#}$NC vs DC, BLK, LA, LSF; $^{@}$NC vs LSF−LA groups; *DC vs LSF, LA, LSF−LA groups; $^{\$}$LSF vs LSF−LA groups; $^{\#*\$}P < 0.001$, $^{@}P < 0.05$ and, (F) serum uric acid level, $^{\#}$NC vs DC, BLK, LA, LSF; $^{@}$LA vs LSF−LA groups; *DC vs LSF, LSF−LA groups; $^{\$}$LSF vs LSF−LA PLM ip; $^{\$}$LSF vs LSF−LA SM ip, LSF−LA PLM oral $^{\#*\$@}P < 0.001$, $^{\$}P < 0.05$.

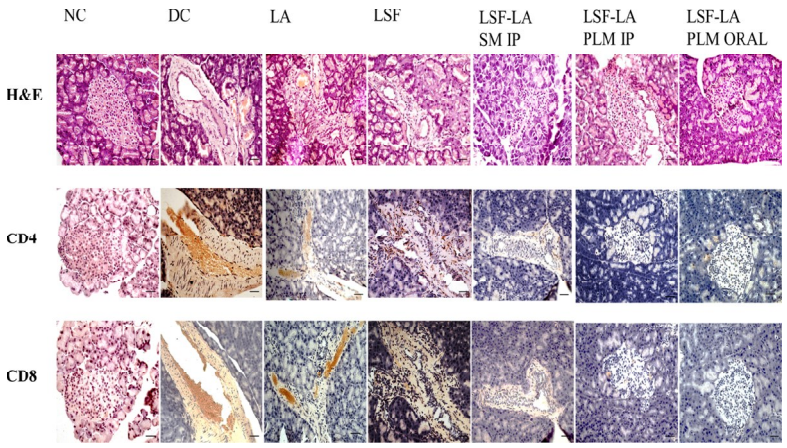

Figure 6. Histological and IHC analysis of pancreatic sections after 21 days of treatment: H&E staining and expression of CD4+ and CD8+ T-cells. *Magnification 400× and scale bar 20 μm.

PTX was also detected in the PK studies of both free LSF and LSF−LA nanoformulations because of the well-proved LSF−PTX in vivo interconversion. As shown in Figure 4, plasma concentration of PTX was much lower upon administration of LSF−LA PLM in comparison to LSF and LSF−LA SM PK (Figure 4A,C), which indicated that there was a significant decrease in the rate and extent of LSF−PTX in vivo interconversion upon administering LSF as a self-assembling prodrug, LSF−LA, which was further reduced upon encapsulating the LSF−LA prodrug in self-assembling polymeric micelles, LSF−LA PLM.

3.8. In Vivo Efficacy Studies in the STZ-Induced T1D Model. LSF−LA PLM was tested by ip and oral routes of administration in an STZ-induced T1D rat model over a 3 week time period at 15 mg/kg dose (equivalent to free LSF), once daily, keeping free LSF-, LA-, LSF−LA SM-, and BLK-treated diabetic animals as controls (~15 mg/kg, once daily).

As shown in Figure 4D, a decrease in the fasting glucose levels was observed throughout the treatment period after LSF−LA

DOI: 10.1021/acs.molpharmaceut.9b00833
Mol. Pharmaceutics 2019, 16, 4954−4967

PLM administration beginning from day 3 of treatment. LSF lowered glucose levels in some rats but was unable to maintain the reduced levels compared to LSF−LA SM ip, LSF−LA PLM ip, and LSF−LA PLM oral. LSF−LA PLM ip and LSF−LA PLM oral exhibited lowered as well as stabilized blood glucose levels as compared to diabetic animals. As shown in Figure 4E, the LSF−LA PLM-treated group showed significantly increased levels of insulin in comparison to control groups along with a drastic reduction in TNF-α and IFN-γ levels (Figure 5A). LSF−LA PLM delivered by the oral route exhibited similar levels of insulin and TNF-α and IFN-γ as that LSF−LA SM ip and LSF−LA PLM ip, implying a similar efficacy of oral route of administration to that of ip route when LSF−LA PLM was administered by both the routes.

Regarding the biochemical parameters, a change in the levels of serum cholesterol, triglycerides, SGPT (ALT), SGOT (AST), urea, uric acid, and total protein was observed in the diabetic animals as compared to the normal animals. LSF−LA SM and LSF−LA PLM (by both the routes) significantly decreased the levels of serum cholesterol, triglycerides, SGPT, SGOT, urea, and uric acid, whereas these treatments significantly increased the serum level of protein in comparison to NC-, DC-, LA-, LSF-, and BLK-treated groups (Figure 5).

3.8.1. In Vivo Histology and IHC Analysis. Histological examination of the H&E-stained sections of rat pancreas of the diabetic group showed a significant decrease in the number of β cells of the islets of Langerhans in comparison to the control group (normal animals), wherein the islets showed a large number of β cells (seen as hematoxylin-stained blue cells) distributed throughout the islet (Figure 6). The damage or necrosis of β cells in the diabetic control group is a hallmark of diabetes. In LSF−LA micelle-treated groups (LSF−LA SM and LSF−LA PLM), more number of β cells were observed along with reduced β cell fibrosis and inflammatory cell infiltration as compared to the diabetic control and LA-treated groups. This also explains the higher plasma insulin levels observed at the terminal end point (21 days) in LSF−LA micelle-treated group in comparison to the control groups (Figure 4E) and a similar observation in in vitro cell culture experiments, which revealed an increase in cell viability and insulin secretion under the inflammatory conditions upon treatment with LSF−LA micelles (Figure 3C). Further, as shown in Figure 6, expression of CD4+ and CD8+ inflammatory T-cells was carried out in pancreatic sections of the experimental animals. The high numbers of CD4+ and CD8+ stained T cells in DC and LA groups were consistent with active islet β-cell destruction as revealed by H&E staining in these groups. In rats treated with LSF−LA prodrug micelles (LSF−LA SM and PLM), CD4+ and CD8+ positive cell clusters were less prominent throughout the pancreas. Treatment with free LSF showed higher number of CD4+ and CD8+ inflammatory cells in comparison to LSF−LA micelle-treated groups. Among the LSF−LA micelle-treated groups, LSF−LA PLM (both by oral and ip route) showed minimal inflammatory T cells in comparison to LSF−LA SM.

4. DISCUSSION

Designing a patient-compliant and effective delivery system for a therapeutic molecule is a challenging task given the limitations regarding its solubility, stability, targeted release profile,, and PKs.[30] One such difficult to deliver but potent molecule is LSF which possesses anti-inflammatory and immunomodulatory activities and has shown potential in several clinical indications including diabetes, islet transplantation, acute lung injury, and acute respiratory distress syndrome.[31] However, the potency of LSF is far from being realized owing to its weak delivery prospects particularly, a very high aqueous solubility (~60 mg/mL; poor encapsulation in any drug delivery system)[4] and poor PK performance (poor oral bioavailability of 5.9, 1 and 22.4% in human,[15] mice[32] and rats, respectively). Presystemic metabolism of LSF is high and may be because of the presence of a free hydroxyl group in its side chain resulting in its low oral bioavailability. Major sites for this interconversion are erythrocytes (carbonyl reductase) in blood, lung clara cells (pulmonary carbonyl reductase), and liver microsomes; LSF−PTX interconversion is more pronounced in case of parenteral route of administration in comparison to oral route as LSF comes in direct contact with the blood.[16] These limitations associated with LSF make the delivery of the molecule quite complicated and hence it remains a poorly explored drug. As an attempt to resolve these limitations of LSF, our group first reported a drug-fatty acid prodrug of LSF with fatty acid LA, which showed self-assembly into micelles (LSF−LA SM) and exhibited potent activity and efficacy in in vitro and in vivo experiments at a reduced dose and dosage mainly attributed to reduced interconversion of LSF to its inactive metabolite PTX by blocking free hydroxyl group in side chain of LSF. LSF−LA SM is the first reported injectable nanoformulation of LSF, which made its sustained delivery possible for a variety of autoimmune disorders.[23] Considering that T1D is a chronic ailment which requires multiple injections of the antidiabetic agent every day, the parenteral route of administration is certainly not a patient-friendly alternative.[33,34] LSF−LA SM, when tested by oral route of administration, showed a very low bioavailability (24.46% in rat) because of the ease of cleavage of ester linkage between LSF and LA in the GIT before reaching the systemic circulation.

As LSF−LA SM was unable to show appreciable oral bioavailability, we designed a nanodrug delivery system of the synthesized LSF−LA prodrug, which could exhibit oral bioavailability and thus enhance the potential for its clinical translation. Shielding the ester bond between LSF and LA against cleavage in GIT by encapsulating it in a polymeric carrier not only demonstrated equivalent therapeutic activity by oral and parenteral routes but also decreased the interconversion of LSF to PTX substantially (Figure 3C).

For this purpose, the LSF−LA prodrug was encapsulated into an in-house designed self-assembling amphiphilic polymeric carrier. Among the different types of nanoparticulate formulations available, we selected polymeric micelles owing to their self-assembling nature, high encapsulation efficiency, controlled release, small size, biocompatibility, and biodegradability.[35−37] Additionally, polymeric micelles show enhanced stability and resistance to drug leakage under normal physiological conditions.[38] To develop polymeric micelles of the LSF−LA prodrug, we screened several polymers which could self-assemble and provide high payload. Literature suggests that a hydrophilic fraction of 0.25−0.4 ($f_{\text{hydrophilic}}$) in amphiphilic copolymers enables their self-assembly or aggregation into lamellar, micellar, or vesicular systems in aqueous solutions.[39,40] Primarily, we synthesized the polymeric carrier with a hydrophilic fraction of 0.3 or 30% comprising PEG_{114} (M_n—5000), whereas 70% of the weight fraction was composed of hydrophobic segments consisting of lactide and MBC, wherein 50 units of lactide and 25 units of MBC were attached. Previously, Danquah et al. synthesized a PEG-*b*-polyester/polycarbonate copolymer system [poly(ethylene glycol)-*b*-

DOI: 10.1021/acs.molpharmaceut.9b00833
Mol. Pharmaceutics 2019, 16, 4954−4967

poly(carbonate-*co*-lactide)] using a conventional technique which normally requires 130 °C for 24 h for synthesis.[26] We modified the technique to a microwave synthesizer-based technique, which reduced the reaction time from 24 h to 45 min. As our objective was to obtain a high DL, we varied the ratios of lactide and MBC in the final polymer without changing the weight fraction of hydrophilic and hydrophobic segments and the copolymer containing 25 units of MBC monomer and 50 units of lactic acid was selected for further studies. The self-assembling nature of the polymer was confirmed by determination of the cmc value (5.95 μg/mL) and aggregation number (14.82 at 10 cmc). The LSF−LA prodrug was encapsulated into the polymer [$mPEG_{114}$-*b*-P(CB_{25}-*co*-LA_{50})] by a simple film hydration method and formation of spherical micelles was confirmed by TEM (Figure 1D). Scaling up of the formulation is essential for clinical use but is often considered a major challenge for nanoformulations. The methodology designed for formulation of LSF−LA PLM was amenable to scale-up as observed by preparation of larger batch sizes of LSF−LA PLM. Lyophilization of the fresh micellar formulation was optimized using PEG 2000 (5% w/v) as a lyoprotectant (Table 1) to improve its stability, handling during transportation, and to improve its commercial viability. Since use of sugars as a lyoprotectant is generally not recommended in antidiabetic formulations, PEG 2000 was selected as the lyoprotectant of choice.

To ensure oral bioavailability of any molecule, its stability in the lumen of the GIT is important, which is often compromised because of chemical (pH-dependent) instability and/or enzymatic degradation of the molecule in the upper gut.[41,42] This might be the reason for low oral bioavailability of our previously designed LSF−LA SM. Hence, the stability of LSF−LA PLM in the GI tract was important to assess to ensure its oral bioavailability. Unlike LSF−LA which underwent substantial degradation in SGF and SIF (Figure 2A,B), LSF−LA PLM remained stable in all the simulating biological fluids (SGF, SIF, and PBS). This might be attributed to the higher stability of the micellar structure of LSF−LA PLM in the acidic pH of the SGF (pH 1.2). It has been reported that the strength of the hydrogen bonds is much higher under acidic conditions, which play a key role in enabling self-assembly of the amphiphilic polymers into micelles.[43,44] However, as the pH becomes alkaline in SIF (pH 6.8), the hydrogen bonding gets weakened, thus favoring the disassembly of micelles, resulting in minor release of LSF−LA from LSF−LA PLM (Figure 2B). These results provided a preliminary indication that the prepared $mPEG_{114}$-*b*-P(CB_{25}-*co*-LA_{50}) polymer could remain stable in the hostile environment of the GIT and, being nanosized, could be easily absorbed into the systemic circulation. Once into the systemic circulation, it would be able to release free LSF as revealed by the hydrolysis study of LSF−LA PLM in plasma (Figure 2D), wherein slow and sustained release of free LSF (68.17 + 1.63%) was observed from the nanoformulation within 48 h. A slow rate of hydrolysis of the prodrug also indicated the possibility of prolonged action and reduced rate of metabolism in vivo, in turn reflecting the possibility of reduced dose and dosage. These results indicated that the designed system has the potential of proving itself to be a good carrier for oral delivery of LSF, which was later validated by PK and pharmacodynamic studies. However, before proceeding to in vivo experiments, it was necessary to ensure that the potency and efficacy of LSF in LSF−LA PLM remains similar as was seen in LSF−LA SM. To meet this objective, cell culture-based evaluation was carried out, which revealed that LSF−LA PLM was nontoxic to MIN-6 cells. In fact, LSF−LA PLM protected these insulin secreting cells from death under cytokine-induced inflammatory conditions and boosted their insulin release (Figure 3B) similar to that of LSF−LA SM. Cytokines (TNF-α, IL-1β, and IFN-γ) are responsible for direct β-cell cytotoxic action in rodent islets, which could ultimately result in pathogenesis of T1D. PBMC proliferation and cellular uptake studies also indicated significantly enhanced activity of the LSF−LA PLM formulation as compared with free LSF. It was evident from these results that the activity of LSF−LA PLM was intact and similar to that of the LSF−LA prodrug. Although LSF−LA PLM exhibited a significant improvement in PK parameters over the LSF−LA prodrug, which was clearly reflected during the pharmacodynamic studies in diabetic animals, cell culture studies carried out in a controlled and static environment cannot explore these advantages of LSF−LA PLM.

To prove the oral efficacy of the formulation, PK studies were conducted, wherein, upon oral administration of LSF−LA SM, ester linkages present in the prodrug got directly exposed to hydrolase enzymes present in the GIT, resulting in the cleavage of the ester bond. Therefore, PK parameters of orally administered LSF−LA SM did not show any significant improvement in comparison to free LSF for example, LSF−LA SM showed a half-life of 0.72 h in comparison to free LSF (0.61 h). AUC was also found to be 1389.73 and 1186.75 ng·h/mL, respectively, for LSF−LA SM and free LSF. Hence, based on oral PK data of LSF−LA SM, we did not further evaluate the antidiabetic effect of LSF−LA SM by oral route as it showed low oral bioavailability and hence would also require a higher dose. Contrary to this, the LSF−LA PLM formulation upon oral administration showed excellent oral bioavailability of 74.86%, which may be attributed to protection of the ester bond in the GIT and reduction in its interconversion LSF to PTX (Figure 4B). This might result because of shielding of the entrapped drug molecules from direct interaction with the surrounding healthy tissues by the nanocarrier and thus protecting LSF against early activation and degradation processes. The hydrophilic part of the LSF−LA PLM that is, PEG, is important because of its brush-like architecture, which allows the hydrophilic part to protect the hydrophobic part from the harsh environment of the GIT and also minimizes protein adsorption onto its surface.[45] Owing to these reasons, LSF−LA SM undergoes much faster metabolism than LSF−LA PLM as revealed by the half-life values of LSF from the two systems (Table 3). Along with oral bioavailability, the LSF−LA PLM formulation in aqueous medium also exhibited stability at 4 °C for 1 month, making it a commercially viable and patient-compliant alternative.

The LSF−LA PLM formulation was further tested in the STZ-induced T1D model. The glycemic level in the DC group was significantly higher compared with the normal control group. This difference in glucose homeostasis under diabetic conditions is mostly attributed to low glucose intake by peripheral tissues and high hepatic glycogenolysis and gluconeogenesis.[46,47] Diabetic rats treated with LSF and LSF−LA prodrug formulations (LSF−LA SM and LSF−LA PLM) showed decreased fasting glucose levels, when compared with the DC group. Improved glycemic levels can be the result of improved insulin secretion and increase in β cell resistance to apoptosis caused by inflammatory cytokines.[23,31] Improvement was also seen in serum insulin levels after 3 weeks of treatment with LSF and LSF−LA prodrug formulations as also previously indicated by the in vitro cell culture studies. Interestingly, LSF−

DOI: 10.1021/acs.molpharmaceut.9b00833
Mol. Pharmaceutics 2019, 16, 4954−4967

LA PLM showed equivalent therapeutic efficacy by both oral and ip routes of administration at the same dose of LSF possibly because of reduction in interconversion of LSF to PTX, which enhanced the oral bioavailability of LSF as observed in PK studies (Figure 4). LSF and its formulations significantly reduced serum cytokines levels (Figure 5A), which also correlates well with our in vitro results (Figure 3E). The liver plays a vital role in regulating glucose levels in physiological and pathological states such as T1D.[48] Moreover, T1D is also associated with oxidative stress, leading to liver injury, which could be assessed by confirming the elevated levels of serum ALT and AST.[49,50] Treatment with LSF and LSF−LA PLM/SM reduced the levels of serum ALT and AST in comparison to DC- and LA-treated groups (Figure 5B), which indicated that the treatment exhibited appreciable protection from STZ-induced hepatic dysfunction. Increased plasma triglyceride, high low-density lipoprotein levels, and decreased high-density lipoprotein levels are common characteristics of dyslipidemia and can be observed in diabetic conditions because of insulin resistance-related lipolysis, which results in increase in the circulating fatty acids that are taken up by the liver as an energy source.[48,51,52] LSF as a strong anti-inflammatory agent modulates stress-associated changes in lipid metabolism and suppresses serum free fatty acids.[15] Upon treatment with LSF and LSF−LA prodrug PLM/SM, serum triglycerides and total cholesterol levels were decreased, whereas the total protein levels were increased (Figure 5C,D). Persistent hyperglycemia causes elevation in serum urea levels, which is considered as one of the significant markers of renal dysfunction.[52−54] Serum urea levels also decreased in diabetic groups after treating with LSF and LSF−LA PLM/SM. Few studies have examined the association between elevated serum uric acid and diabetes mellitus. The high-normal values of serum uric acid may be associated with diminished renal function in T1D for which underlying mechanisms are not clear.[55,56] LSF also reduced serum uric acid levels.

Destruction of β-cells by activated T cells (CD4+ and CD8+) and macrophages of the immune system mainly causes T1D, but unfortunately, preventing β-cell destruction has proven challenging.[57,58] To understand the protection rendered by any antidiabetic treatment to β-cells, measurement of β-cell function along with assessment of T-cell infiltration is required. CD4+ T cells are probably responsible for stimulation of islet-resident macrophages, and for activation and propagation of CD8+ T cells, which mainly infiltrate the islets of pancreas.[59] These T cells also stimulate cytokines production which further catalyzes the differentiation of native Th cells, leading to overall β-cell destruction.[24,60,61] To assess the therapeutic potential of LSF−LA PLM in immunomodulation, we first confirmed the role of the LSF−LA PLM formulation in proliferation and activation of PBMCs, wherein LSF−LA PLM suppressed the proliferation of PBMCs to a greater extent than free LSF. Diminished PBMC activation was confirmed by measurement of cytokines production, which showed significant decrease in the presence of LSF−LA PLM (Figure 3D,E). Literature shows that LSF is an inhibitor of IL-12 signaling and it inactivates functions of IL-12 in T cells as well as in macrophages. This IL-12 is one of the major immunoregulatory cytokines that promotes Th1 cell differentiation, cell-mediated immune responses, and induces proinflammatory cytokine production.[9,62] Further, presence of CD4+ and CD8+ T cells was confirmed in PD studies by IHC analysis of rat pancreatic sections after 3 weeks of treatment. CD4+ and CD8+ T cells were prominent in case of diabetic animals (Figure 5), whereas upon treatment with LSF−LA PLM, T cells levels were significantly decreased, which was possibly because of the immunomodulatory action of the drug. A similar observation was also made earlier in cell culture studies, wherein LSF prevented β-cell death in the presence of cytokines (Figure 3E) and prevented PBMC proliferation. Overall, this study presents the first report on a biodegradable polymeric micellar formulation of LSF that provides excellent oral bioavailability and efficacy of LSF in diabetic animals.

5. CONCLUSIONS

In this study, we demonstrated the first facile biodegradable polymeric micellar formulation of LSF that rendered excellent oral bioavailability to LSF by reducing its metabolism. First, LSF−LA PLM was prepared using an in-house-synthesized mPEG-*b*-P(CB-*co*-LA) polymer and the formulation was optimized, scaled up, and lyophilized. The optimized formulation was found to be stable during storage and in different simulating biological fluids as well as in rat plasma. Further, LSF−LA PLM improved insulin secretion capability of insulinoma cells, suppressed PBMC proliferation, and exhibited enhanced cellular uptake, which confirmed that there was no compromise in the potency of native LSF because of formulation development. LSF−LA PLM showed similar hypoglycemic activity by both ip and oral route in the STZ-induced T1D rat model. Protection of β-cells was evident in the histology of pancreatic sections after 3 weeks of treatment with LSF−LA PLM formulation, which was confirmed by CD4+ and CD8+ staining of pancreata demonstrating significant reduction in the T-cell population. In a nutshell, our results could set the ground for a number of potential clinical applications of LSF by oral route using LSF prodrug polymeric nanoformulation.

■ ASSOCIATED CONTENT

Supporting Information

The Supporting Information is available free of charge on the ACS Publications website at DOI: 10.1021/acs.molpharmaceut.9b00833.

mPEG-*b*-P(CB-*co*-LA) polymer characterization; ^{1}H NMR of MBC monomer and mPEG-poly(carbonate-*co*-lactide) polymer respectively; and GPC analysis of mPEG-poly(carbonate-*co*-lactide) (PDF)

■ AUTHOR INFORMATION

Corresponding Author

*E-mail: anupama.mittal@pilani.bits-pilani.ac.in. Phone: +91 1596 255708, +91 9660876009

ORCID

Deepak Chitkara: 0000-0003-4174-7664

Anupama Mittal: 0000-0003-3344-9579

Author Contributions

A.M., D.C., and K.S.I. contributed to the conception and design of the experiments. K.S.I. carried out the experiments and contributed to the formulation optimization and characterization. S.M. and K.S.I contributed to cell culture experiments. K.S.I and D.K.S. contributed to polymer synthesis and characterization. K.S.I, M.B., D.K.S., and R.S. contributed to in vivo experiments and analysis of data. K.S.I., A.M., and D.C. contributed to the drafting and revising of the paper including the figures and tables.

DOI: 10.1021/acs.molpharmaceut.9b00833
Mol. Pharmaceutics 2019, 16, 4954−4967

Notes

The authors declare no competing financial interest.

■ ACKNOWLEDGMENTS

This research work was supported by the Science and Engineering Research Board (SERB), Department of Science and Technology (DST), Govt. of India [#YSS/2014/000551] and Ph.D. fellowship for K.S.I. was provided by DST-INSPIRE, Govt. of India [#IF160659]. The authors also acknowledge the Sophisticated Test & Instrumentation Centre (SAIF), Kochi, Kerala, India, for the HR-TEM facility.

■ REFERENCES

(1) Bluestone, J. A.; Herold, K.; Eisenbarth, G. Genetics, pathogenesis and clinical interventions in type 1 diabetes. *Nature* **2010**, *464*, 1293−1300.
(2) Clark, M.; Kroger, C. J.; Tisch, R. M. Type 1 diabetes: a chronic anti-self-inflammatory response. *Front. Immunol.* **2017**, *8*, 1898.
(3) Tersey, S. A.; et al. Amelioration of type 1 diabetes following treatment of non-obese diabetic mice with INGAP and lisofylline. *J. Diabetes Mellitus* **2012**, *2*, 251−257.
(4) Striffler, J. S.; Nadler, J. L. Lisofylline, a novel anti-inflammatory agent, enhances glucose-stimulated insulin secretion in vivo and in vitro: studies in prediabetic and normal rats. *Metabolism* **2004**, *53*, 290−296.
(5) De Vries, P.; Singer, J. W. Lisofylline suppresses ex vivo release by murine spleen cells of hematopoietic inhibitors induced by cancer chemotherapeutic agents. *Exp. Hematol.* **2000**, *28*, 916−923.
(6) Husain, A.; Rosales, N.; Schwartz, G. K.; Spriggs, D. R. Lisofylline Sensitizes p53 Mutant Human Ovarian Carcinoma Cells to the Cytotoxic Effects ofcis-Diamminedichloroplatinum(II). *Gynecol. Oncol.* **1998**, *70*, 17−22.
(7) George, C. L. S.; Fantuzzi, G.; Bursten, S.; Leer, L.; Abraham, E. Effects of lisofylline on hyperoxia-induced lung injury. *Am. J. Physiol.: Lung Cell. Mol. Physiol.* **1999**, *276*, L776−L785.
(8) Hasegawa, N.; et al. The effects of post-treatment with lisofylline, a phosphatidic acid generation inhibitor, on sepsis-induced acute lung injury in pigs. *Am. J. Respir. Crit. Care Med.* **1997**, *155*, 928−936.
(9) Yang, Z.; et al. Inhibition of STAT4 activation by lisofylline is associated with the protection of autoimmune diabetes. *Ann. N. Y. Acad. Sci.* **2003**, *1005*, 409−411.
(10) Coon, M. E.; Diegel, M.; Leshinsky, N.; Klaus, S. J. Selective pharmacologic inhibition of murine and human IL-12-dependent Th1 differentiation and IL-12 signaling. *J. Immunol.* **1999**, *163*, 6567−6574.
(11) Bright, J. J.; Du, C.; Coon, M.; Sriram, S.; Klaus, S. J. Prevention of experimental allergic encephalomyelitis via inhibition of IL-12 signaling and IL-12-mediated Th1 differentiation: an effect of the novel anti-inflammatory drug lisofylline. *J. Immunol.* **1998**, *161*, 7015−7022.
(12) McLennan, S.; et al. The role of the mesangial cell and its matrix in the pathogenesis of diabetic nephropathy. *Cell. Mol. Biol.* **1999**, *45*, 123−135.
(13) Chen, M.; Yang, Z.; Wu, R.; Nadler, J. L. Lisofylline, a Novel Antiinflammatory Agent, Protects Pancreatic β-Cells from Proinflammatory Cytokine Damage by Promoting Mitochondrial Metabolism. *Endocrinology* **2002**, *143*, 2341−2348.
(14) Bolick, D. T.; Hatley, M. E.; Srinivasan, S.; Hedrick, C. C.; Nadler, J. L. Lisofylline, a Novel Antiinflammatory Compound, Protects Mesangial Cells from Hyperglycemia- and Angiotensin II-Mediated Extracellular Matrix Deposition. *Endocrinology* **2003**, *144*, 5227−5231.
(15) Bursten, S. L.; et al. Lisofylline causes rapid and prolonged suppression of serum levels of free fatty acids. *J. Pharmacol. Exp. Ther.* **1998**, *284*, 337−345.
(16) Wyska, E.; Pękala, E.; Szymura-Oleksiak, J. Interconversion and tissue distribution of pentoxifylline and lisofylline in mice. *Chirality* **2006**, *18*, 644−651.
(17) Yang, Z.; et al. The novel anti-inflammatory compound, lisofylline, prevents diabetes in multiple low-dose streptozotocin-treated mice. *Pancreas* **2003**, *26*, e99−e104.
(18) Yang, Z.; et al. Combined treatment with lisofylline and exendin-4 reverses autoimmune diabetes. *Biochem. Biophys. Res. Commun.* **2006**, *344*, 1017−1022.
(19) National Institutes of Health. *A Safety, Tolerability and Bioavailability Study of Lisofylline after Continuous Subcutaneous (12 mg/kg) and Intravenous (9 mg/kg) Administration in Subjects with Type 1 Diabetes Mellitus*. https://clinicaltrials.gov/ct2/show/NCT01603121, 2012 (accessed 25 April 2019).
(20) List, A.; et al. A randomized placebo-controlled trial of lisofylline in HLA-identical, sibling-donor, allogeneic bone marrow transplant recipients. *Bone Marrow Transplant.* **2000**, *25*, 283−291.
(21) Wiedemann, H. P.; et al. Randomized, placebo-controlled trial of lisofylline for early treatment of acute lung injury and acute respiratory distress syndrome. *Crit. Care Med.* **2002**, *30*, 1−6.
(22) Cui, P.; Macdonald, T. L.; Chen, M.; Nadler, J. L. Synthesis and biological evaluation of lisofylline (LSF) analogs as a potential treatment for Type 1 diabetes. *Bioorg. Med. Chem. Lett.* **2006**, *16*, 3401−3405.
(23) Italiya, K. S.; et al. Self-assembling lisofylline-fatty acid conjugate for effective treatment of diabetes mellitus. *Nanomedicine* **2019**, *15*, 175−187.
(24) Davidson, T. S.; Longnecker, D. S.; Hickey, W. F. An experimental model of autoimmune pancreatitis in the rat. *Am. J. Pathol.* **2005**, *166*, 729−736.
(25) Chitkara, D.; et al. Micellar delivery of cyclopamine and gefitinib for treating pancreatic cancer. *Mol. Pharm.* **2012**, *9*, 2350−2357.
(26) Danquah, M.; Fujiwara, T.; Mahato, R. I. Self-assembling methoxypoly(ethylene glycol)-b-poly(carbonate-co-l-lactide) block copolymers for drug delivery. *Biomaterials* **2010**, *31*, 2358−2370.
(27) Chakraborty, S.; Chakraborty, A.; Saha, S. K. Tuning of physicochemical characteristics of charged micelles by controlling head group interactions via hydrophobically and sterically modified counter ions. *RSC Adv.* **2014**, *4*, 32579−32587.
(28) Eismin, R. J.; et al. Evolution of aggregate structure in solutions of anionic monorhamnolipids: Experimental and computational results. *Langmuir* **2017**, *33*, 7412−7424.
(29) Italiya, K. S.; Sharma, S.; Kothari, I.; Chitkara, D.; Mittal, A. Simultaneous estimation of lisofylline and pentoxifylline in rat plasma by high performance liquid chromatography-photodiode array detector and its application to pharmacokinetics in rat. *J. Chromatogr. B: Anal. Technol. Biomed. Life Sci.* **2017**, *1061−1062*, 49−56.
(30) Anselmo, A. C.; Mitragotri, S. An overview of clinical and commercial impact of drug delivery systems. *J. Controlled Release* **2014**, *190*, 15−28.
(31) Yang, Z.; Chen, M.; Nadler, J. L. Lisofylline: a potential lead for the treatment of diabetes. *Biochem. Pharmacol.* **2005**, *69*, 1−5.
(32) Wyska, E.; Świerczek, A.; Pociecha, K.; Przejczowska-Pomierny, K. Physiologically based modeling of lisofylline pharmacokinetics following intravenous administration in mice. *Eur. J. Drug Metab. Pharmacokinet.* **2016**, *41*, 403−412.
(33) Wen, H.; Jung, H.; Li, X. Drug delivery approaches in addressing clinical pharmacology-related issues: opportunities and challenges. *AAPS J.* **2015**, *17*, 1327−1340.
(34) Banerjee, A.; et al. Ionic liquids for oral insulin delivery. *Proc. Natl. Acad. Sci. U.S.A.* **2018**, *115*, 7296−7301.
(35) Lu, Y.; Park, K. Polymeric micelles and alternative nanonized delivery vehicles for poorly soluble drugs. *Int. J. Pharm.* **2013**, *453*, 198−214.
(36) Xu, W.; Ling, P.; Zhang, T. Polymeric micelles, a promising drug delivery system to enhance bioavailability of poorly water-soluble drugs. *J. Drug Delivery* **2013**, *2013*, 1−15.
(37) Ahmad, Z.; Shah, A.; Siddiq, M.; Kraatz, H.-B. Polymeric micelles as drug delivery vehicles. *RSC Adv.* **2014**, *4*, 17028−17038.
(38) Owen, S. C.; Chan, D. P. Y.; Shoichet, M. S. Polymeric micelle stability. *Nano Today* **2012**, *7*, 53−65.

DOI: 10.1021/acs.molpharmaceut.9b00833
Mol. Pharmaceutics 2019, 16, 4954−4967

(39) Chen, Z.; et al. Micelle structure of novel diblock polyethers in water and two protic ionic liquids (EAN and PAN). *Macromolecules* **2015**, *48*, 1843−1851.
(40) Apolinário, A.; Magoń, M.; Pessoa, A., Jr.; Rangel-Yagui, C. Challenges for the Self-Assembly of Poly(Ethylene Glycol)-Poly(Lactic Acid) (PEG-PLA) into Polymersomes: Beyond the Theoretical Paradigms. *Nanomaterials* **2018**, *8*, 373.
(41) Date, A. A.; Hanes, J.; Ensign, L. M. Nanoparticles for oral delivery: Design, evaluation and state-of-the-art. *J. Controlled Release* **2016**, *240*, 504−526.
(42) Karavolos, M.; Holban, A. Nanosized drug delivery systems in gastrointestinal targeting: Interactions with microbiota. *Pharmaceuticals* **2016**, *9*, 62.
(43) Gilli, P.; Pretto, L.; Bertolasi, V.; Gilli, G. Predicting Hydrogen-Bond Strengths from Acid−Base Molecular Properties. The p K a Slide Rule: Toward the Solution of a Long-Lasting Problem. *Acc. Chem. Res.* **2008**, *42*, 33−44.
(44) Zhang, J.; et al. Facile fabrication of an amentoflavone-loaded micelle system for oral delivery to improve bioavailability and hypoglycemic effects in KKAy mice. *ACS Appl. Mater. Interfaces* **2019**, *11*, 12904−12913.
(45) Szymusiak, M.; et al. Core-Shell Structure and Aggregation Number of Micelles Composed of Amphiphilic Block Copolymers and Amphiphilic Heterografted Polymer Brushes Determined by Small-Angle X-ray Scattering. *ACS Macro Lett.* **2017**, 6, 1005−1012.
(46) Oliveira, G. O.; Braga, C. P.; Fernandes, A. A. H. Improvement of biochemical parameters in type 1 diabetic rats after the roots aqueous extract of yacon [Smallanthus sonchifolius (Poepp.& Endl.)] treatment. *Food Chem. Toxicol.* **2013**, *59*, 256−260.
(47) Petersen, M. C.; Vatner, D. F.; Shulman, G. I. Regulation of hepatic glucose metabolism in health and disease. *Nat. Rev. Endocrinol.* **2017**, *13*, 572.
(48) Mohamed, J.; Nafizah, A. N. H.; Zariyantey, A. H.; Budin, S. B. Mechanisms of diabetes-induced liver damage: the role of oxidative stress and inflammation. *Sultan Qaboos Univ. Med. J.* **2016**, *16*, e132−e141.
(49) Yu, Y. M.; Howard, C. P. Improper insulin compliance may lead to hepatomegaly and elevated hepatic enzymes in type 1 diabetic patients. *Diabetes Care* **2004**, *27*, 619−620.
(50) Aldahmash, B. A.; El-Nagar, D. M.; Ibrahim, K. E. Attenuation of hepatotoxicity and oxidative stress in diabetes STZ-induced type 1 by biotin in Swiss albino mice. *Saudi J. Biol. Sci.* **2016**, *23*, 311−317.
(51) Shoelson, S. E.; Lee, J.; Goldfine, A. B. Inflammation and insulin resistance. *J. Clin. Invest.* **2006**, *116*, 1793−1801.
(52) Jamshidi, M.; et al. The effect of insulin-loaded trimethylchitosan nanoparticles on rats with diabetes type I. *Biomed. Pharmacother.* **2018**, *97*, 729−735.
(53) Saeed, M. K.; Deng, Y.; Dai, R. Attenuation of biochemical parameters in streptozotocin-induced diabetic rats by oral administration of extracts and fractions of Cephalotaxus sinensis. *J. Clin. Biochem. Nutr.* **2008**, *42*, 21−28.
(54) Jaiswal, Y. S.; Tatke, P. A.; Gabhe, S. Y.; Vaidya, A. B. Antidiabetic activity of extracts of Anacardium occidentale Linn. leaves on n -streptozotocin diabetic rats. *J. Tradit. Complement. Med.* **2017**, 7, 421−427.
(55) Rosolowsky, E. T.; et al. High-normal serum uric acid is associated with impaired glomerular filtration rate in nonproteinuric patients with type 1 diabetes. *Clin. J. Am. Soc. Nephrol.* **2008**, *3*, 706−713.
(56) Bandaru, P.; Shankar, A. Association between serum uric acid levels and diabetes mellitus. *Int. J. Endocrinol.* **2011**, *2011*, 1−6.
(57) Walker, L. S. K.; von Herrath, M. CD4 T cell differentiation in type 1 diabetes. *Clin. Exp. Immunol.* **2016**, *183*, 16−29.
(58) Phillips, J. M.; et al. Type 1 diabetes development requires both CD4+ and CD8+ T cells and can be reversed by non-depleting antibodies targeting both T cell populations. *Rev. Diabet. Stud.* **2009**, *6*, 97−103.
(59) Burrack, A. L.; Martinov, T.; Fife, B. T. T cell-mediated beta cell destruction: autoimmunity and alloimmunity in the context of type 1 diabetes. *Front. Endocrinol.* **2017**, *8*, 343.
(60) Espinosa-Carrasco, G.; et al. CD4+ T helper cells play a key role in maintaining diabetogenic CD8+ T cell function in the pancreas. *Front. Immunol.* **2018**, *8*, 2001.
(61) Tiittanen, M.; Huupponen, J. T.; Knip, M.; Vaarala, O. Insulin treatment in patients with type 1 diabetes induces upregulation of regulatory T-cell markers in peripheral blood mononuclear cells stimulated with insulin in vitro. *Diabetes* **2006**, 55, 3446−3454.
(62) Yang, Z.; et al. The novel anti-inflammatory agent lisofylline prevents autoimmune diabetic recurrence after islet transplantation1. *Transplantation* **2004**, *77*, 55−60.

DOI: 10.1021/acs.molpharmaceut.9b00833
Mol. Pharmaceutics 2019, 16, 4954−4967